Title

Investigation of Groundwater Flow in Foothill and Mountain regions using Heat Flow measurements

Authors

Fogg, Graham E.
Trask, James C

Publication Date

2009-08-01

Investigation of Groundwater Flow in Foothill and Mountain regions using Heat Flow measurements

[1]Graham E. Fogg
[2]James C. Trask
Hydrologic Sciences Program
Land, Air, and Water Resources Dept.
UC Davis

[1]*gefogg@ucdavis.edu*
phone: (530) 752-6810

[2]*jctrask@ucdavis.edu*
phone: (530) 752-1372

UC Water Resources Center
Technical Completion Report Project No. WR-1006
Submitted April 2009

Table of Contents

Tables

Figures

Appendices

Abstract

A field and model investigation has been performed to assess the potential of subsurface temperature (T) measurements for tracing groundwater flow in montane areas. Field measurements included monitoring of soil T at numerous sites and measurement of T-profiles in many wells and boreholes. Field data collection for thermal tracing of groundwater flow is inexpensive and easy to perform relative to standard geophysical techniques for groundwater flow characterization, given wells that are accessible for T-profile measurement. Modeling investigations include development of a novel, conceptually simple 'black box' subsurface thermal energy balance approach. This robust model approach can be used together with T-profile data to bracket the rate of mountain-front groundwater recharge.

Results of the soil T monitoring investigation show a wide range in summer and mean annual soil T between different soil sites. Factors governing the observed inter-site differences in soil T were identified. A model for spatial variability in mean soil T was developed, showing the feasibility of creating maps of mean surface T in the Sierra Nevada using standard GIS land surface attributes. Accurate knowledge of surface T is needed in modeling subsurface heat and water flow, to distinguish spatial changes in T due to groundwater flow from those due to heterogeneity in surface T. T-profiles measured in the Tahoe Basin region indicate that there are substantial areal differences in the rate of high elevation deep bedrock groundwater recharge, and in valley bedrock discharge. Surface T and T-profile measurements together are shown to be useful in defining valley basin-fill aquifer recharge sources. Subsurface heat flow patterns are altered in distinct ways, as reflected in T-profiles, by recharge into the top (soil percolation down to water table), sides (mountain-front recharge) and bottom (mountain-block recharge) of montane valley basin-fill aquifers.

1: Introduction and Problem Statement

Continuing expansion of the human population in foothill and montane areas of California has been accompanied by increased use of groundwater resources in these areas, both for water supply and waste disposal. In many foothill and montane areas , a large proportion of domestic water wells have been contaminated (SWRCB, 2005). Groundwater flow patterns in most montane areas are not well known, due to expense and challenges inherent to hydraulic approaches alone in characterizing groundwater flow in hardrock areas. Consequently, estimation of groundwater recharge rates and sustainable yields as well as development of groundwater management strategies for both quantity and quality are sufficiently difficult that they seldom are performed in these areas.

This investigation addresses the ongoing challenge of developing inexpensive approaches to improve characterization of groundwater flow in basin-fill and bedrock aquifers in the rapidly developing foothill and montane areas of California. A recent report by the State Water Resources Control Board documented 30% of domestic water wells tested in foothill and montane areas of El Dorado county are contaminated above MCL limits by septic tank systems, agricultural byproducts, and other sources (SWRCB, 2005). Unlike alluvial aquifer systems, which are typically stratified by fine and coarse sediment layers into semi-confined systems that are substantially hydraulically isolated from overlying unconfined systems, and thus somewhat protected from contamination by overlying surface sources, bedrock aquifer systems are typically not so easily delineated into 'protected' zones. Fractures that are oriented sub-vertical can provide relatively direct pathways between nearby surface sources (e.g., septic tanks, fertilizer) and fracture zones tapped by wells. Preferential flow paths thru fracture zones have the potential to rapidly transport contaminated water both laterally and vertically. Natural and perturbed rates of vertical recharge are difficult and/or expensive to measure using standard hydraulic approaches. The amount and depth of recharge into bedrock is largely unknown in most foothill and montane areas, as is the recharge from mountain-front and bedrock areas into adjacent basin-fill aquifers.

2: Objectives

Our research objective in this investigation has been to use soil and borehole temperatures that we have previously measured in the Tahoe Basin region, as constraints on models of groundwater flow. This investigation complements and advances results from a former project, funded by AB303 thru DWR, involving groundwater flow modeling of the South Tahoe basin area, as part of an aquifer source protection management plan (Bergsohn et al, 2007). A major objective of this prior investigation was identification of valley aquifer recharge sources. T-profiles indicate significant mountain-block and mountain-front recharge of valley basin-fill aquifers, consistent with isotopic and hydraulic data. High elevation bedrock well T-profiles and hydraulic data indicate substantial areal heterogeneity in recharge to depth in bedrock. Aspects of our heat flow investigation warranted further research, beyond what was performed for the South Tahoe PUD (STPUD) project:

(1) Development of a 'black box' conceptual model of the thermal energy balance in the subsurface for cool mountain-front recharge of adjacent valley aquifers. This novel energy balance is conceptually simple, and the general modeling approach is proposed to be useful in estimating the magnitude of recharge sources into montane valley aquifers.

(2) Thorough presentation of results of a soil T monitoring survey. Soil T was monitored for more than a year at over 90 sites in the South Tahoe Basin, and for as much as three years at some sites. This may be the largest such collection of shallow soil T data for a montane area. This data was collected for the STPUD project, but we had not performed a thorough synthesis and evaluation of this large data set. Here, we present a rigorous analysis and synthesis of the shallow soil T data, and the relationship of mean annual soil T to surface radiation exchange, vegetative cover, soil moisture, and elevation. Accurate knowledge of the spatial variation of mean annual surface T is needed in order to accurately specify top surface thermal boundary conditions in modeling of subsurface heat and groundwater flow.

(3) Presentation of results of subsurface T measurements and analyses within the Tahoe Basin region but outside of the STPUD study area (Clear Ck. and Mt. Pluto).

(4) Dissemination of current and closely related prior results in this report and in peer-reviewed literature. Some of those results of the STPUD investigation that had been performed by Trask and Fogg and documented in Bergsohn et al (2007) are reproduced here with little modification, to aid in dissemination and as a reference source for future publications. We are currently revising a publication draft (appendix 9) for submission to a peer-reviewed journal.

3: Study Area

The study area for this investigation is the Tahoe Basin of CA and NV, with most data and analyses for the South Tahoe area.

3.1 Location and Physical Geography: Figure 3-1 shows the location of the Tahoe Basin, east of the Sierra Nevada crest and straddling the states of California and Nevada. The physical geography of the Tahoe Basin has been described previously (Crippen and Pavelka, 1970). Briefly, Tahoe is a montane basin, with elevations ranging from ~ 6225 ft at Lake Tahoe to 10,880 ft at Freel Peak (Fig 3-2). Watershed soils are generally thin and topography steep, with about half the land area having slope>20% (Crippen and Pavelka, 1970). Most of the watershed is vegetated with forest, chaparral, meadow, and wetland, typical of the diversity found in montane to subalpine regions of the Sierra Nevada. There are also sparsely vegetated high elevation exposed bedrock areas and a few low elevation commercial areas. 63 streams, most perennial, drain into Lake Tahoe from watershed sub-basins.

3.2 Hydrogeology: The Tahoe Basin is an active structural basin, with Lake Tahoe occupying a graben formed 2-3 million years ago by downward block faulting. Lake Tahoe is one of the deepest lakes in the world, with mean depth ~1000 ft. Figure 3-3 shows the rock types in the Tahoe Basin. Exposed bedrock (including decomposed granitic rock) covers 71% of the Tahoe Basin surface area (Thodal, 1997), the remaining 29% being covered with basin-fill sediments. Most of the bedrock is granitic; the surface exposure of plutonic intrusions of the Sierra Nevada batholith. The northwest corner of the basin is dominated by tertiary and quaternary volcanics.

The western side of the Tahoe Basin has undergone extensive Pleistocene glacial advances and retreats. Glacial scouring has left large areas of exposed bedrock that has been little altered by subsequent weathering (Burnett, 1968), with scant or no soil development. In dense hardrock, including granitic bedrock, groundwater flow is confined to fractures (faults, joints). Shallow (<100 -200 ft bgs) bedrock, which is typically more permeable than deep bedrock, contributes to stream recharge and valley aquifer recharge in mountain-front areas, which border most of the upgradient study area. Detailed investigation of the Fallen Leaf Lake Quadrangle (Loomis, 1981) identified three intersecting planes of jointing in granitic rocks. Various strikes and dips of joints are also indicated in the Freel Peak Quadrangle (Armin and John, 1983).

Many normal faults in the Tahoe Basin have been mapped in exposed bedrock areas, as well as some in areas of deep basin-fill sediment (Bonham and Burnett, 1976, Loomis, 1981, and Armin and John, 1983). A recent fault survey for the Tahoe Basin has been published by Schweickert et al (2000). In areas of high relief, faults can provide a path for water to depths of many thousands of feet (see appendix 1).

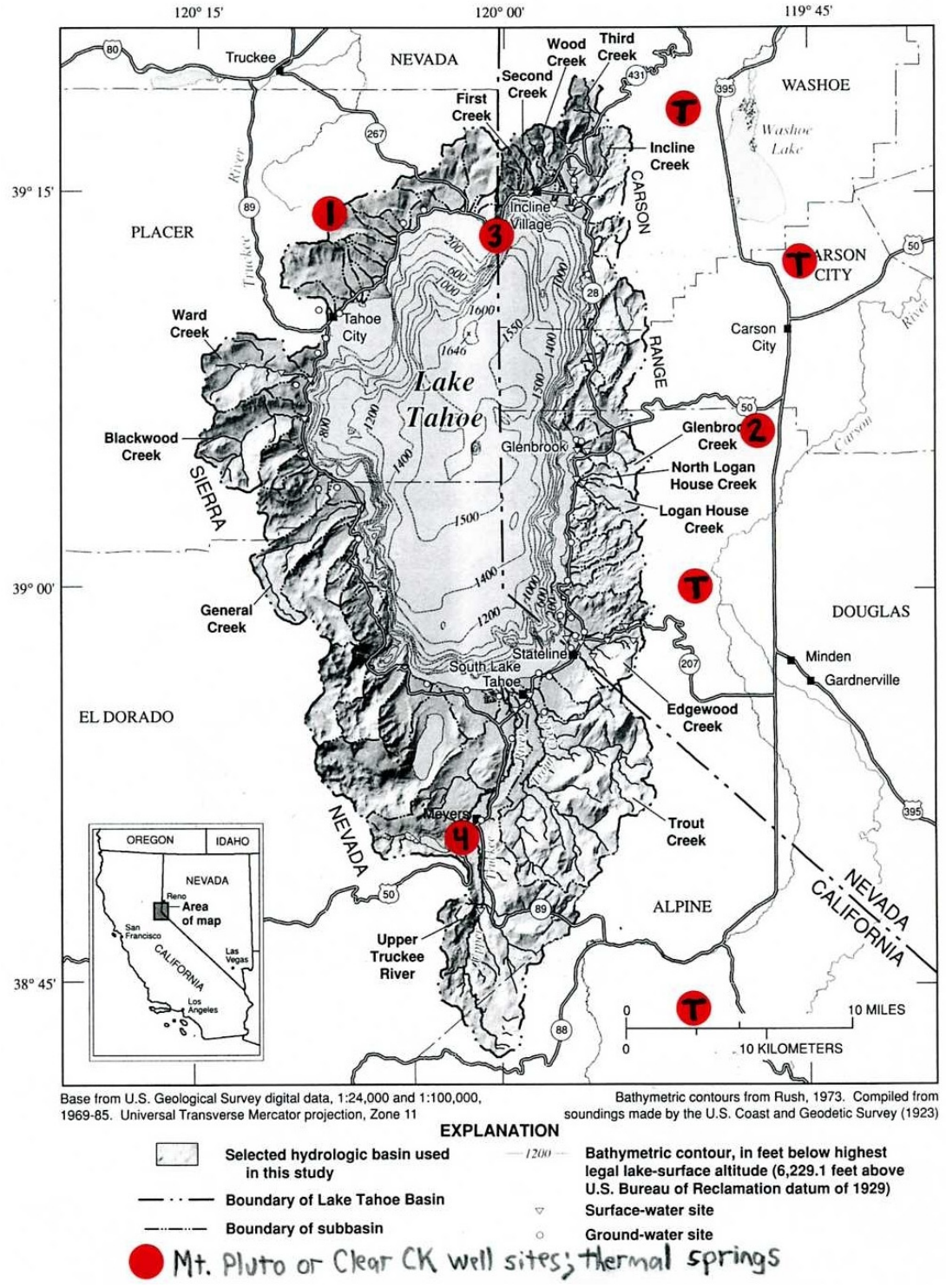

Figure 3-1. Tahoe Basin, CA and NV (location inset lower left). Large dots show locations of two profiled well sites and six thermal springs: 1-Mt. Pluto (well site); 2-Clear Ck (well site); 3-Brockway Hot Springs; 4-Meyers Warm Springs; T-thermal hot springs near eastern base of Carson Range; from north to south-Bowers Mansion, Carson, Walleys, Grovers. Map modified from USGS (Boughton et al,1997).

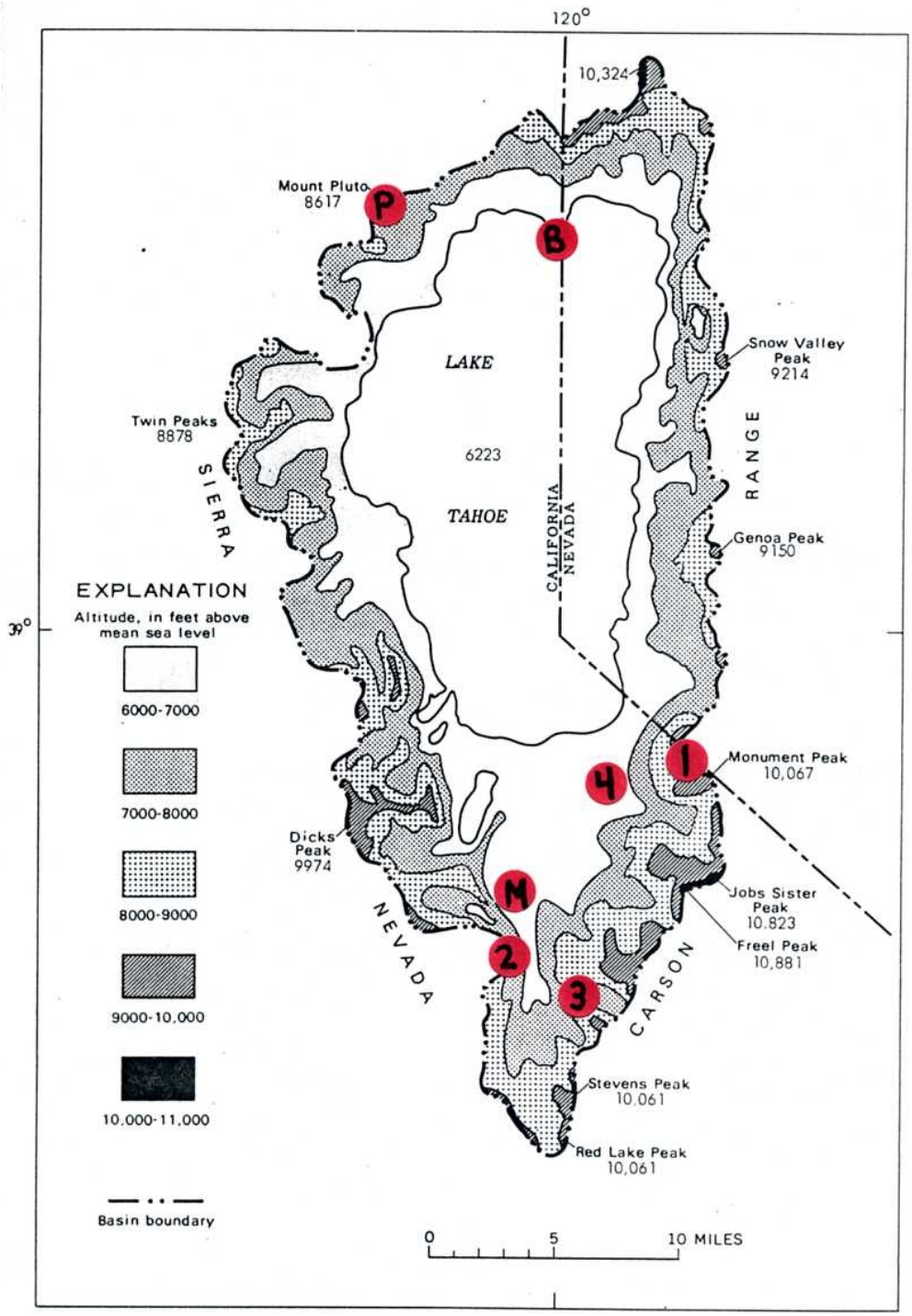

Figure 3-2. Land surface elevation ranges in Tahoe Basin. Large dots show locations of five hardrock wells that were profiled and of two thermal springs: P-Mt. Pluto well site, B-Brockway Hot Springs, M-Meyers Warm Springs. Numbered dots show locations of granitic bedrock wells profiled, in order of decreasing elevation (ft amsl): 1-Heavenly Gondola (9170), 2-Echo Pass (7385), 3-Big Meadows (7300), 4-Ralph (6360). Map modified from USGS (Crippen and Pavelka, 1970).

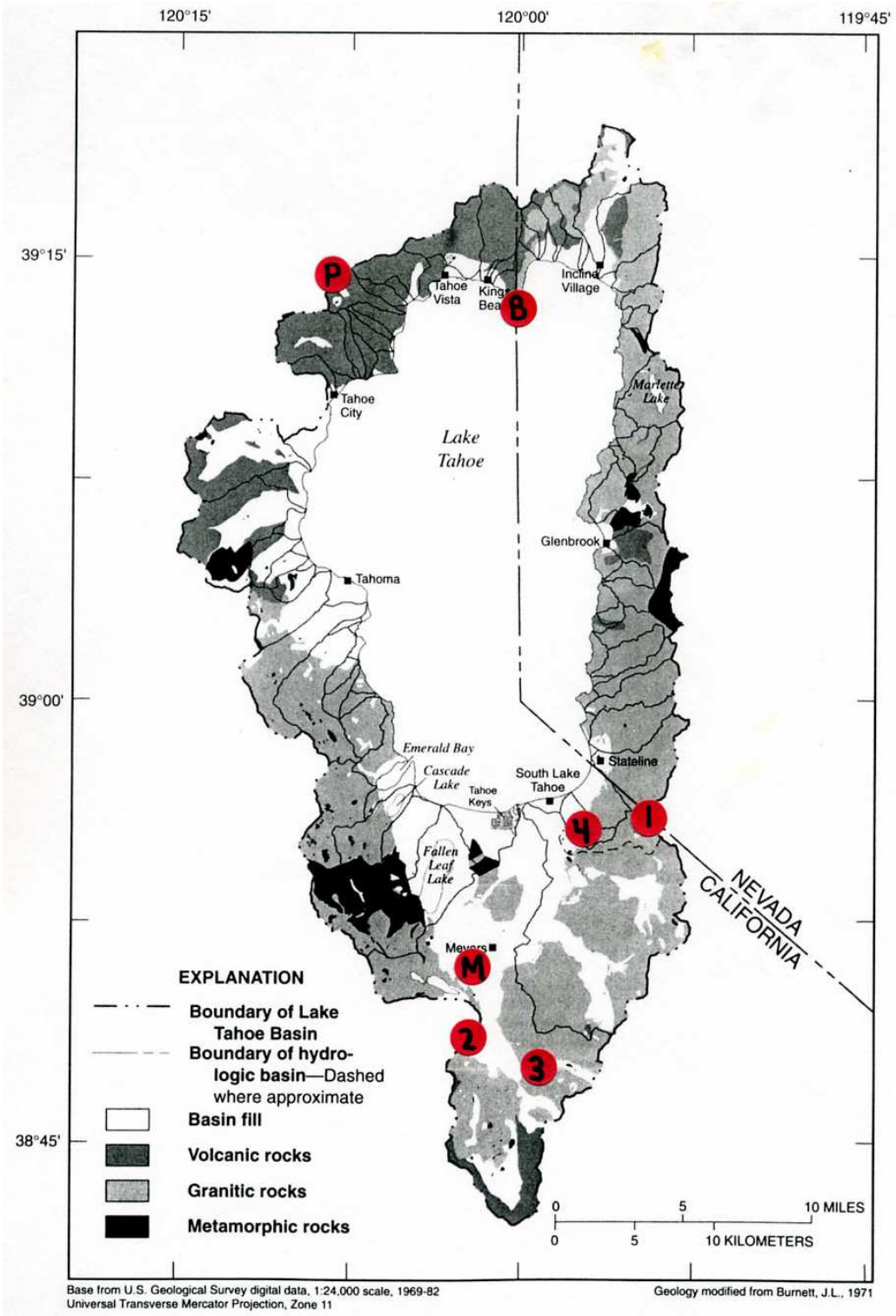

Figure 3-3. Generalized Geology of Tahoe Basin. Large dots show locations of five hardrock wells that were profiled and of two thermal springs: P-Mt. Pluto well site, B-Brockway Hot Springs, M-Meyers Warm Springs. Numbered dots show locations of granitic bedrock wells profiled, in order of decreasing elevation (ft amsl): 1-Heavenly Gondola (9170), 2-Echo Pass (7385), 3-Big Meadows (7300), 4-Ralph (6360). Map modified from USGS (Thodal, 1997).

Appendix 1 reviews aspects of hardrock hydrogeology pertinent to Tahoe area watersheds. Shallow bedrock is generally not as permeable as the basin-fill aquifer sediments in the Tahoe area. However, due to steep hydraulic gradients typically present at bounding mountain-front areas, shallow bedrock in mountain-front areas is likely a significant source of mountain-front recharge to many valley aquifers. Deep bedrock generally is less permeable than shallow bedrock. However, there are large areas of high-elevation mountain block where some groundwater recharge to depth can occur, and often large head gradients between these high-elevation mountain block recharge areas and nearby valley discharge areas. Therefore, as reviewed in appendix 1, it is plausible that discharge up into the bottom of valley area basin-fill aquifers sourced from high elevation mountain block recharge areas could be a significant source of recharge to many valley sedimentary basin-fill aquifers in the Tahoe Basin area.

The eastern side of the Tahoe Basin has undergone relatively little glacially scouring (Burnett, 1968). Many areas of exposed bedrock are deeply weathered and decomposed to grus. Thickness of grus has been reported to reach as much as 100 ft in the eastern Tahoe Basin (Thodal, 1997). Permeability is high within such decomposed granitic bedrock (Burnett, 1968, Thodal, 1995). Weathered bedrock areas have a much higher water storage capacity than areas of unweathered bedrock, likely affecting the magnitude of stream baseflow. Gaged streamflow in the baseflow season (July-Sept./Oct.) is much larger (as a percentage of annual mean streamflow) for streams on the eastern side of the basin than for streams on the western side of the basin (Trask, 2007).

The quaternary history of the Tahoe Basin has been described by Birkeland (1963,1964) and includes episodes of volcanic activity and of glaciation. These have been associated with highstands of Lake Tahoe to hundreds of feet elevation above the current sill. Valley basin-fill consists of quaternary sediments of fluvial and lacustrine origin, with predominant glacial genesis of sediments on the western side of the basin. Much of the glacial derived sediment has been transported and reworked by fluvial processes, and much consists of non-stratified and non-sorted tills and moraines. Lacustrine deposits above the current Lake Tahoe shoreline include beach sand, silt, and clay deposits. Basin-fill deposits to over 1,000 ft thick have been found in the South Tahoe and Incline Village areas (Blum, 1979, Markiewicz et al, 1992, Bergsohn et al, 2007).

3.3 General Hydrology: Mean annual precipitation ranges from less than 1.5 ft/yr near Glenbrook on the central eastern shore of Lake Tahoe, to over 6 ft/yr at high elevations near the Sierra Nevada crest at the western basin boundary, as shown in several isohyetal maps (Crippen and Pavelka, 1970, Marjanovic, 1989, Thodal, 1997). Precipitation generally increases with increasing elevation and decreases from West to East. November-May frontal systems account for over 85% of Tahoe Basin precipitation. Most precipitation is in the form of snow, particularly in high elevation areas. Within the South Tahoe valley area at elevation <6500 ft, mean annual precipitation ranges ~2-fold from a high of nearly 4 ft/yr in the southern end of Christmas Valley to less than 2 ft/yr in the northeast near Stateline.

The large spatial variability in precipitation is amplified in streamflow, with mean annual sub-basin runoff efficiency (ratio streamflow:precip) and runoff depth (volumetric streamflow divided by contributing watershed surface area) each trending upward with increasing elevation and from east to west (Trask, 2007). For the whole Tahoe watershed, long-term annual and areal mean watershed runoff (streamflow plus groundwater outflow) has been ~55 cm/yr. Atmospheric losses have averaged ~45 cm/yr (Trask,

2007), substantially less than estimated mean Lake Tahoe evaporation (~94 cm/yr for 1968-2000).

There is large inter-annual variability in annual precipitation amounts in all areas of the Tahoe Basin. Over the period WY (water-year) 1946-2004, annual precipitation ranged from ~30% to ~200% of mean annual precipitation. Inter-annual variability in annual precipitation (as a percentage of mean annual precipitation) has been substantially larger in low elevation valley areas than in high elevation mountain areas (Trask, 2007). The large inter-annual variability in the amount of annual precipitation is reflected in watershed runoff in Tahoe Basin streams. The Upper Truckee River and Trout Ck drain most of the runoff from the South Lake Tahoe area into Lake Tahoe. Between 1958-2004, annual (water-year) volumetric runoff for Trout Ck. and the Upper Truckee R. has ranged from ~20% to over 200% of mean annual runoff for WY 1958-2004.

3.4 Stream baseflow and Groundwater storage: It has been estimated that about half of Tahoe Basin annual volumetric streamflow can be classified as stormflow and half as baseflow (Thodal, 1997 and Trask, 2007). Annual (water-year) volumetric streamflow is highly correlated not only with precipitation from the same water-year, but with precipitation from prior water-years (Trask, 2007). In the western side of the Tahoe Basin, streamflow is significantly correlated to precipitation for the current and one prior water-year only. However, in the eastern side and southern portion of the Tahoe Basin, streamflow is significantly correlated with precipitation over the past two or more water-years. The 'memory' of streamflow for precipitation from prior water-years is attributable to changes at the annual and longer time scales in subsurface storage of water. During years of high precipitation, excess water is stored in the vadose zone and as groundwater, which is subsequently released from storage during years of less precipitation.

The shorter 'memory' of the watershed for precipitation, moving from east to west within the Tahoe Basin is likely due largely to lower groundwater storage capacity in western watersheds, which have been glacially scoured, as compared to eastern watersheds, which had little previous glaciation and have extensive areas of decomposed granitic rock. This geographic pattern is also observed in stream baseflow, which is much higher for each of months July thru October (as a percentage of annual volumetric streamflow) for eastern streams than for western streams.

3.5 Evidence for deep groundwater flow: Direct evidence for groundwater flow to great depth in Tahoe area bedrock is the presence of thermal springs (Fig 3-1) in the Tahoe Basin (Brockway Hot Springs, Meyers Warm Springs) and at the eastern toe of the Carson Range. These thermal springs are all associated with fault zones.

Faults potentially can be transmissive zones for groundwater flow to depth, providing a flow path from high elevation mountain block recharge areas deep down into the bedrock, with discharge up into adjacent valleys. It is plausible that much of deep (>500 ft bgs) bedrock groundwater flow discharges upward in valley areas into overlying basin-fill aquifers. Hydraulic, thermal, and isotopic data we obtained for the South Tahoe Basin (sections 8,9.4), as well as the presence of Meyers Warm Springs and Brockway Hot Springs, indicates that deep mountain block flow likely contributes significantly to recharge of some areas of basin-fill aquifers in the Tahoe Basin.

3.6 Water supply: The quality and quantity of Tahoe Basin waters has received much attention since the 1860s, for supply both inside and outside the Tahoe Basin. About 60,000 year-round residents live in the Tahoe Basin. Additionally, nearly half of the housing units in the Tahoe Basin are classified as vacation homes, and there are numerous motels, hotels, resorts, parks, and recreational facilities. Most of this development is located in valley areas and near Lake Tahoe. It has been estimated that consumptive use (including sewage export) in the Tahoe Basin was about 12,400 acre-ft/yr by 1977 (Lind and Goodrich, 1978) and has likely grown by about 7% per decade since then, based on estimates for sewage export (Thodal, 1997).

There are limited surface water rights in the Tahoe Basin, and most water is supplied by groundwater wells. Numerous wells supply individual residences, neighborhoods, communities, and recreational facilities. Most towns in the basin have a municipal water supply, generally with large municipal wells providing most of the water. Most wells are located in valley basin-fill aquifers, however some are located in hardrock areas, particularly at high elevation. Recent groundwater quality issues in the basin have included MTBE contamination and arsenic levels.

A large system of contiguous basin-fill aquifers is located in the South Tahoe area, at valley elevations <6500 ft amsl (Figs 3-2,3 and 5-6). Nearly 7,000 acre-ft/yr is pumped from this system of aquifers by the South Tahoe PUD (Bergsohn et al, 2007) for water supply to the South Tahoe valley area, corresponding to an areal mean pumpage of about 0.25 ft/yr of water over the surface area of the valley basin-fill.

The sole natural surface water outlet from the Tahoe Basin is the Lower Truckee River (Fig 3-1), which supplies most of the water for the Reno-Sparks area. During many years (notably circa 1930 and 1990) Tahoe Basin water yield (Lower Truckee R. outflow plus Lake Tahoe storage change) has been <0; i.e. atmospheric losses from Lake Tahoe and the watershed have exceeded precipitation. The water supply to the Reno-Sparks area is highly sensitive to drought in the Tahoe Basin, and to any long-term changes in Tahoe precipitation. Over WY (water-years) 1958-2004, there was no statistically discernable overall trend or shift in response of annual volumetric streamflow of major Tahoe Basin streams to volumetric precipitation (Trask, 2007), despite increase in mean annual air temperature, decreasing percentage of annual precipitation as snow, increased groundwater pumping and wastewater export, and land cover changes. However, there has been a marked trend of increasing inter-annual variability in the amount of annual Tahoe Basin precipitation over the period 1915-2004 (Trask, 2007), which is reflected in independent records of Tahoe Basin water yield.

4: Investigative Approach

We have proposed that measurement of temperature (T) profiles in existing wells and boreholes, which is simple and inexpensive to perform, can be used to address and substantially help to resolve groundwater recharge sources, flow depth, and flow patterns in foothill and montane regions.

The use of subsurface T measurements to estimate groundwater recharge and discharge rates began in the 1960's (Bredehoeft and Papadopulos, 1965). Recent reviews by leading groundwater scientists have concluded that there is under-used potential for thermal studies to help better define groundwater flow fields (Anderson, 2005). Subsurface heat and groundwater flow are innately coupled (reviewed appendix 1). Subsurface movement of heat is analogous to that of solute. Heat is conducted down a T gradient, similar to solute diffusion down a concentration gradient. Like nonreactive solute mass, heat energy is conserved, and is advected with moving groundwater. Groundwater advection of heat energy in the subsurface is a major determinant of 3D subsurface T fields, which can be easily probed in the shallow soil and to depth in accessible wells or boreholes.

The approach is particularly suited to montane and other high-relief areas, since subsurface T is particularly sensitive to the magnitude and pattern of groundwater flow in these areas. The substantial topographic relief in montane regions enhances groundwater recharge to depth from high elevation areas. Subsurface vertical T gradients are highly sensitive to recharge rates to depth and discharge rates from depth. In the Tahoe Basin region, the USGS investigated stream recharge of an aquifer near Carson City, by means of thermocouples deployed within and below a stream, to log the arrival of thermal pulses advected with recharging streamwater (Ronan et al, 1998). These initial investigations were expanded in stream surface and subsurface T monitoring studies within the South Tahoe Basin by the USGS.

5: Field Methods

The thermal approach to areal groundwater flow tracing is based on accurate determination of mean annual subsurface soil temperature (Ts) and precision measurement of T-profiles in existing wells and boreholes. Ts for a given location or over an area can be estimated using available GIS coverages for several land surface attributes (see appendix 4), with improved confidence thru calibration using Ts monitoring data for the area of interest. Recent improvements in sensor and probe technology have enabled easily performed soil T monitoring and T-profile measurements. These measurements are made at a small fraction of the cost of standard hydraulic methods of well/aquifer yield testing, and with much less associated expense than standard geophysical methods (e.g. ground-penetrating radar, seismic) often used to characterize sedimentary aquifers. Field measurements of subsurface T had been performed prior to this investigation, including (i) monitoring of shallow Ts at over 90 sites for periods of 1-3 years in the South Tahoe Basin. (ii) measurements of T-profiles in several dozen wells and boreholes in the Tahoe Basin region. Sensors and probes were calibrated before and after use, using a well-mixed temperature bath with an NIST-referenced temperature probe, to check stability of calibration. Appendix 2 describes details of probes and measurement techniques.

Figure 5-1. Photo of inexpensive thermister devices used to monitor and log temperature for periods of up to a year or more in many South Tahoe area shallow soil sites and a few Tahoe area wells: Onset 'temperature Tidbit' (center) and Onset 'Hobo' temperature logger (upper right). Note quarter in center (to left of tidbit) for scale.

5.1 Field monitoring survey of soil T: The purpose of the soil T investigation was to determine Ts (mean annual soil T) over the range of different elevation, radiation, and plant cover environments in the South Tahoe area. Seasonal surface T oscillations propagate by conduction into the subsurface with exponentially decreasing amplitude with depth, and are damped out to <0.2C amplitude at ~40 ft bgs in sediments. At depths of ~40 ft bgs in sediments, subsurface T is usually determined primarily by Ts of the overlying ground surface. Areas of very rapid shallow lateral groundwater flow, or areas of vertical recharge rate >5-10 ft/yr can significantly perturb T at 40 ft depth, depending on T of this recharge water. For most lateral flow rates, and for vertical recharge rates <~3 ft/yr, conduction of heat to/from the ground surface dominates lateral or vertical advection of heat above ~40 ft bgs. Thus Ts is usually the main determinant on the T of shallow groundwater. Knowledge of Ts enables determination of a specified-T boundary condition at the surface or shallow subsurface, in analytic and numerical models of combined heat and groundwater flow.

Robust and inexpensive self-logging T sensors with very small drift specification were purchased ('Hobos', Onset Corp.), shown in Fig 5-1 above.

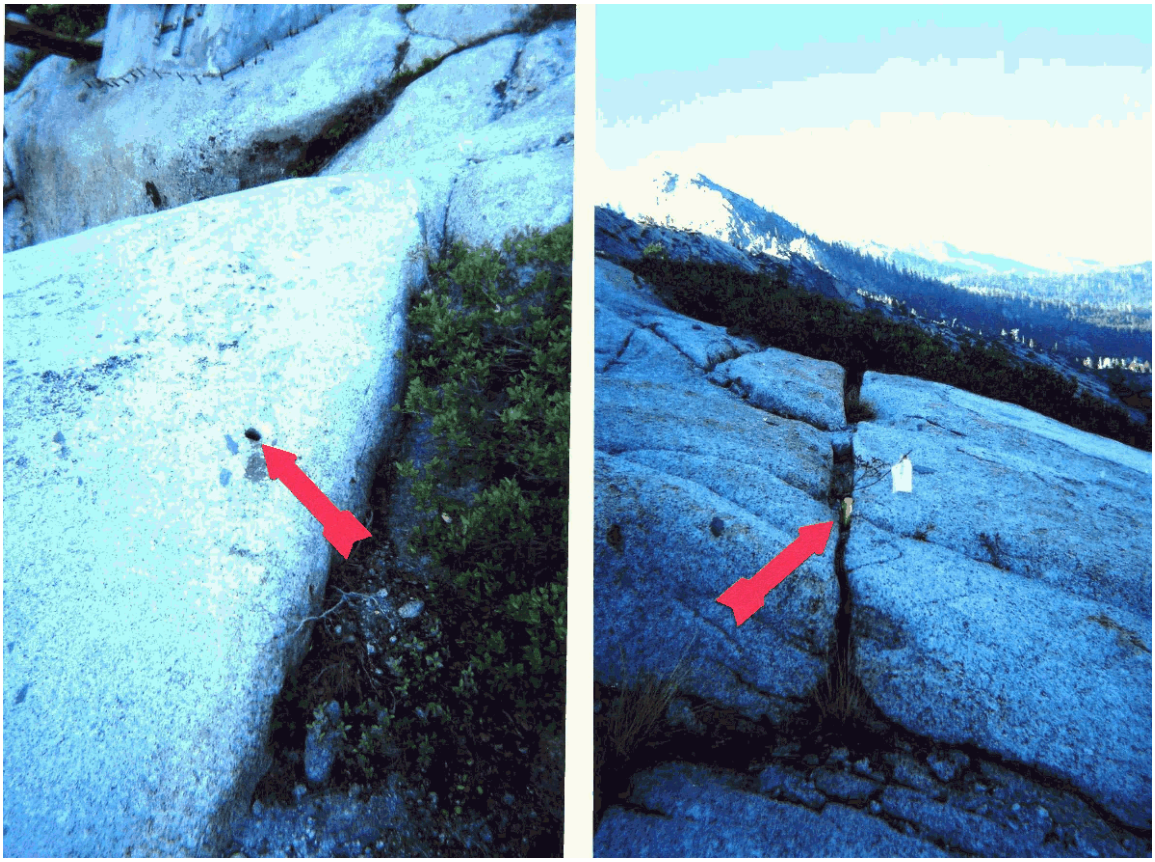

Figure 5-2. Photos of soil T monitoring sites in exposed, glacially scoured granitic bedrock near Echo Lake (~7400 ft elevation). Left: Arrow tip indicates blasting hole drilled in bedrock, which had a diameter just large enough to fit the Hobo temperature probe (Echo Lake site #2). After probe placement, the hole was filled with granitic sand to restrict air circulation. Right: Arrow tip points to plastic stake and flag marking position of spot within narrow soil-filled crevice (just wide enough to fit probe) where Hobo temperature probe was buried (Echo Lake site #6).

Probe calibration was carefully checked over the range 0C to 30C in a temperature bath with an NIST-referenced standard probe. All probes were accurate to within +/- 0.15C over this T range. Many probes were checked for calibration drift after >1 yr of field deployment; drift was consistently within +/- 0.15 C.

Deployment of each sensor consisted of activation to log T at 30 minute intervals (to capture diurnal soil T variations) and burial of sensor (with minimal soil disturbance) so that the thermister element was located ~6" deep. Exposed granitic bedrock T was monitored in a few locations by placing probes within narrow sediment-filled fractures, or in abandoned holes that had been drilled for construction, as shown in figure 5-2.

A total of 97 soil T sensors were emplaced in a number of clusters distributed widely within the South Tahoe basin area (Fig 5-4) between spring and fall, 2004. A chief objective of the soil T monitoring program was to determine Ts over a wide range of different surface environments. As documented in a large literature for many regions, Ts can vary laterally by as much as ~4 C over small distances (see appendix 4, section 7), depending mainly on radiation exposure, surface albedo, soil moisture, and plant cover environments. A soil probe cluster typically consisted of several soil probe sites located within a few hundred feet of each other, but with each site having a different surface environment. The following land surface effects on soil T were sampled:

- Slope of land surface (flat to maximum slope sampled ~35^0)
- Aspect of land surface (dominant N,S,E,W all sampled)
- Elevation of land surface (range 6240 to 7605 ft amsl)
- Vegetative cover (dense forest, sparse forest, thick brush, grasses, sun-exposed bare soil or bedrock)
- Surface color (light or dark; for areas of sun-exposed bare soil or bedrock)
- Soil moisture (several probes sited in perennial wet meadows)

Sensors were downloaded *in situ* via infra-red interface on one to several occasions during deployment periods of ~1 to ~3 years.

Figure 5-3. Photo of soil T monitoring site, shaded under manzanita at ~7300 ft elevation (Angora Ridge site #2). Height of brush is ~1.5-3 ft; typical for many areas of the Tahoe Basin. Probe burial spot indicated by arrow tip (marker flag & stake faintly visible).

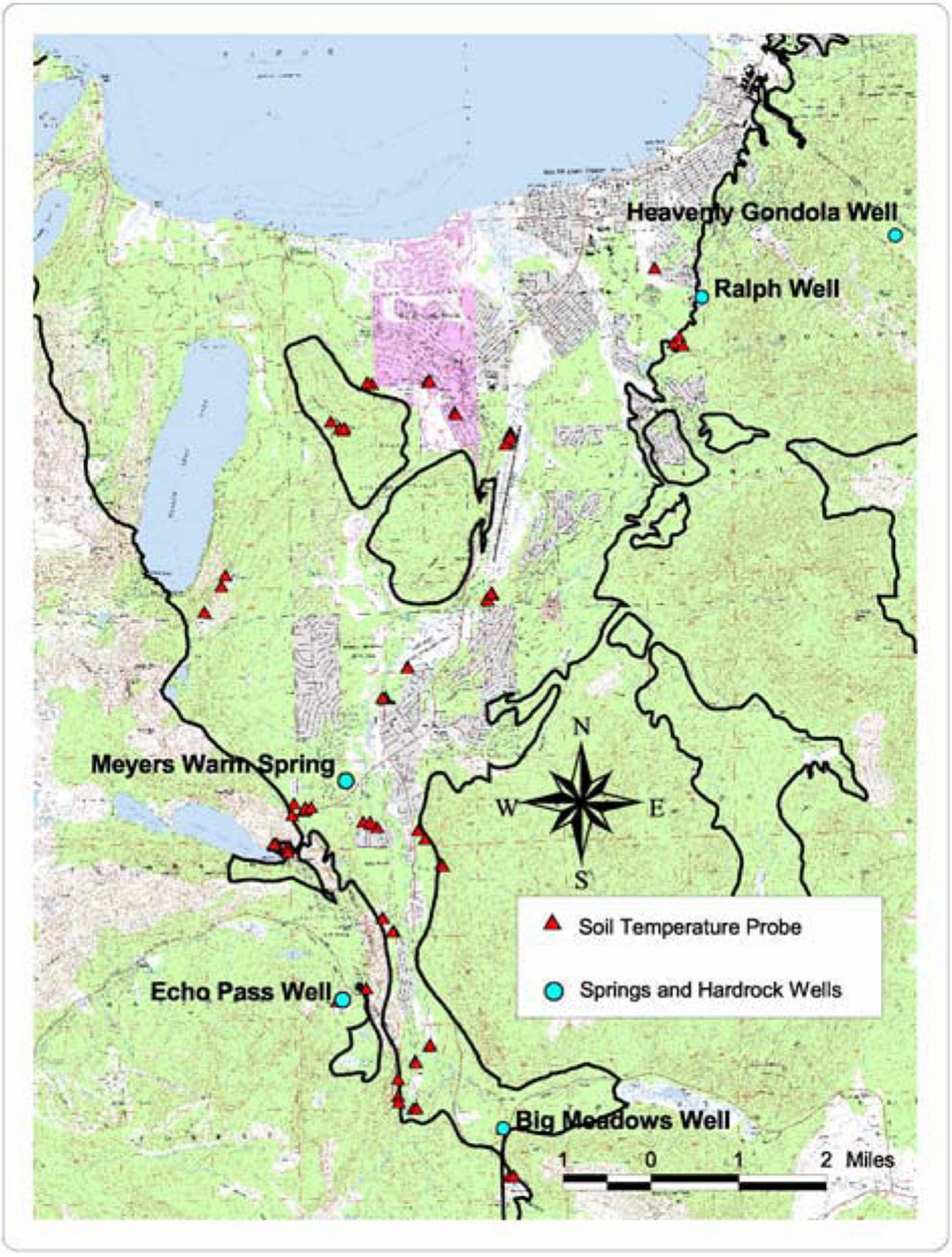

Figure 5-4. South Tahoe area, showing locations of soil T probe clusters, granitic hardrock wells that were T-profiled in the South Tahoe area, and Meyers Warm Spring. Heavy black lines demarcate edges of bedrock contact. The southern tip of Lake Tahoe is located along the top portion of the map (Map courtesy Dr. Eric Labolle).

5.2 Field measurements of well and borehole T-profiles: Accurate heat flow estimates and analyses depend on accurate and precise T-profile measurements, to resolve subsurface T gradients and changes of T gradients with depth. Recent improvements in probe technology have enabled quick, easy, inexpensive measurement of T-profiles at high resolution. T-profiles in wells and boreholes were measured using several different probes, as described in appendix 2. All probes used had calibration checks in a well-mixed insulated temperature bath with an NIST-referenced standard probe. Calibration offset and drift were small to very small for all probes used.

An exceptional quality custom T probe (Chandra and Associates) with millidegree resolution and stability was used for most T-profiles.

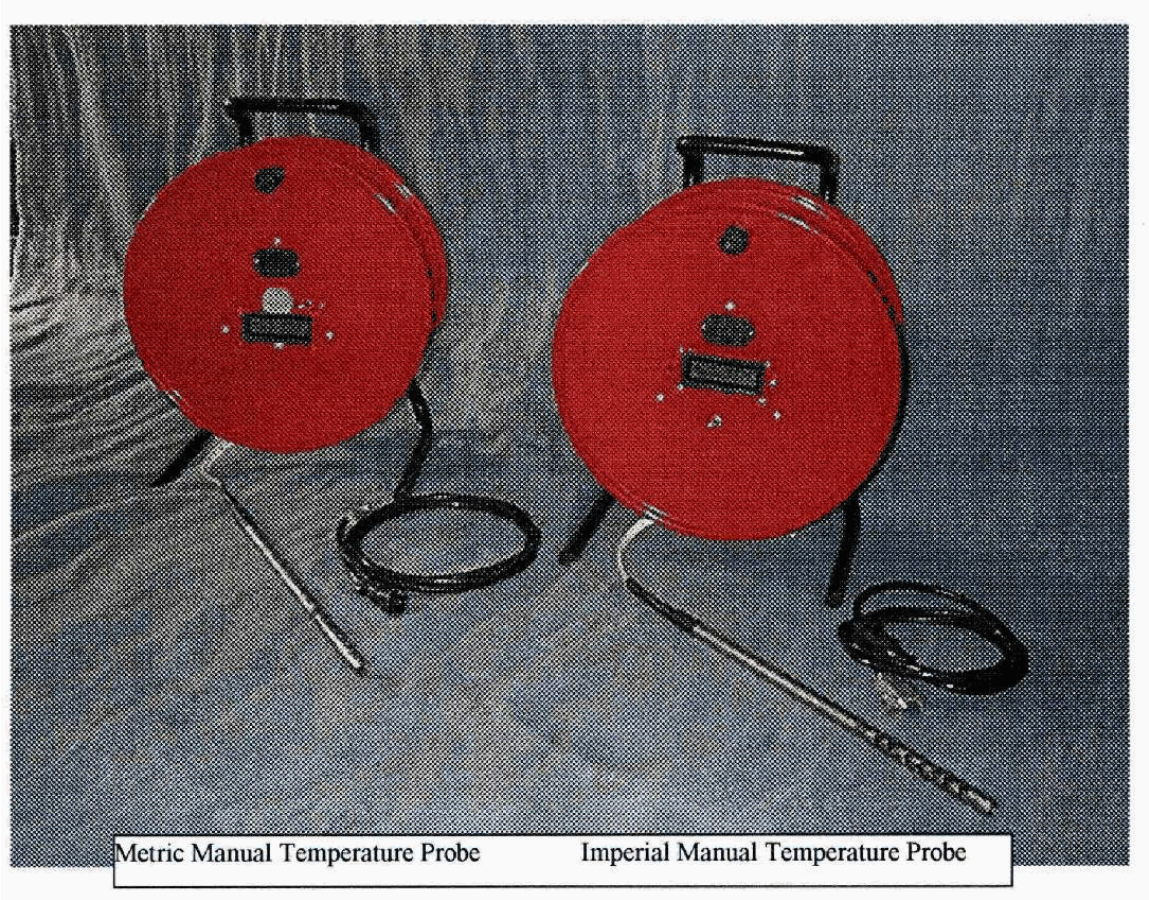

Figure 5-5. Photo of commercial well T-profiling devices (Chandra and Associates). Two of these portable, hand-reeled devices were used for most (but not all) of the well T-profiles we measured in the Tahoe Basin. The probe OD is 1 cm; and the platinum thermister element (located near probe tip) is mechanically protected by a perforated stainless steel shield. Probe temperature is displayed on the reel, and the device can be connected to a laptop for user-directed automated logging of temperature data.

The probe is small diameter (quick response time and low thermal mass), and has a pre-aged platinum thermistor to minimize drift. The analog sensor signal is digitized within the sensor housing, eliminating cable distortion of analogue signals, and enabling real-time communication with the probe logger during profiling. Other probes (appendix 2)

were used for some wells due to limited cable length for the Chandra probe, and to occurrence of technical problems with the Chandra probe starting late summer of 2005.

Many wells profiled were in active service for water supply, so profiling times were scheduled near the end of shut-off periods for that well. A minimum of several days of no pumpage (or longer for large-radius wells) and negligible intra-borehole flow is required for intra-borehole T to equilibrate with T in the formation in the immediate vicinity of the well. Equilibration of the formation T in the immediate vicinity of the well with the formation T in the area may require much more time, depending mainly on rates of vertical groundwater flow in the formation that may have been induced by prior pumping, and also by the prior pumpage rate and the ambient lateral groundwater flow rate (after pump off) in the area near the well. For wells that were in active service for water supply, T-profiles were measured after as long a time interval as possible of no pumping (> 1-2 weeks).

The procedure for T-profile measurement consisted of manually lowering the probe into a well or borehole using a length-calibrated cable reel. When the shallowest depth desired for first reading was reached (usually the well water level) the probe was locked into stationary position. The stationary position was maintained for several minutes (or more, depending on response time of the probe used), in order for the probe sensor to equilibrate with the borehole T at that depth. When the sensor reading stabilized, the depth and T reading was recorded. The process was repeated at depth intervals ranging from 2 to 20 ft (usually 5 to 10 ft) down the borehole until an obstruction was reached (e.g. pump, borehole bottom), and then the probe was reeled up. The recordings of depths and T measurements constitute the T-profile data for that well.

5.3 Selection of wells for T-profile measurements: We measured well T-profiles in several areas of the Tahoe basin region (Fig 3-1), including several dozen wells in the South Tahoe area (Figs 5-4, 5-6). Depths profiled ranged from ~50 ft to ~1,000 ft bgs. Most of the wells profiled were used for local, community or municipal water supply, and some were test or monitoring wells. Most of the wells available for T-profile measurement were located in basin-fill sediment areas, although many of these wells terminated in or near the underlying bedrock. One of the basin-fill well sites (Clear Ck.) is located at the eastern base of the Carson Range (Fig 3-1). Many other basin-fill wells are located in the South Tahoe area (Fig 5-6), as listed in appendix 6. Five wells and boreholes were located in hardrock areas, with very shallow sedimentary cover and varying thickness of weathered bedrock (Figs 3-1, 5-4).

We gained the active support of the South Tahoe PUD in measurement of district well T-profiles, in a cooperative investigation described in Bergsohn et al (2007). We sought to measure T-profiles in as many South Tahoe PUD district wells as possible, given well accessibility and pumping schedules. Also within the South Tahoe valley, we were given permission by the USGS to measure T-profiles in a USGS nested piezometer site, and by the US Forest Service for a monitoring well in the Meyers landfill. A total of several dozen wells completed in South Tahoe basin-fill sediments were T-profiled during 2004 and 2005. Additional T-profiles had been measured during 2001, and are included in the results presented. Some wells were T-profiled more than once, to check for seasonal and inter-annual temporal stability in T-profiles.

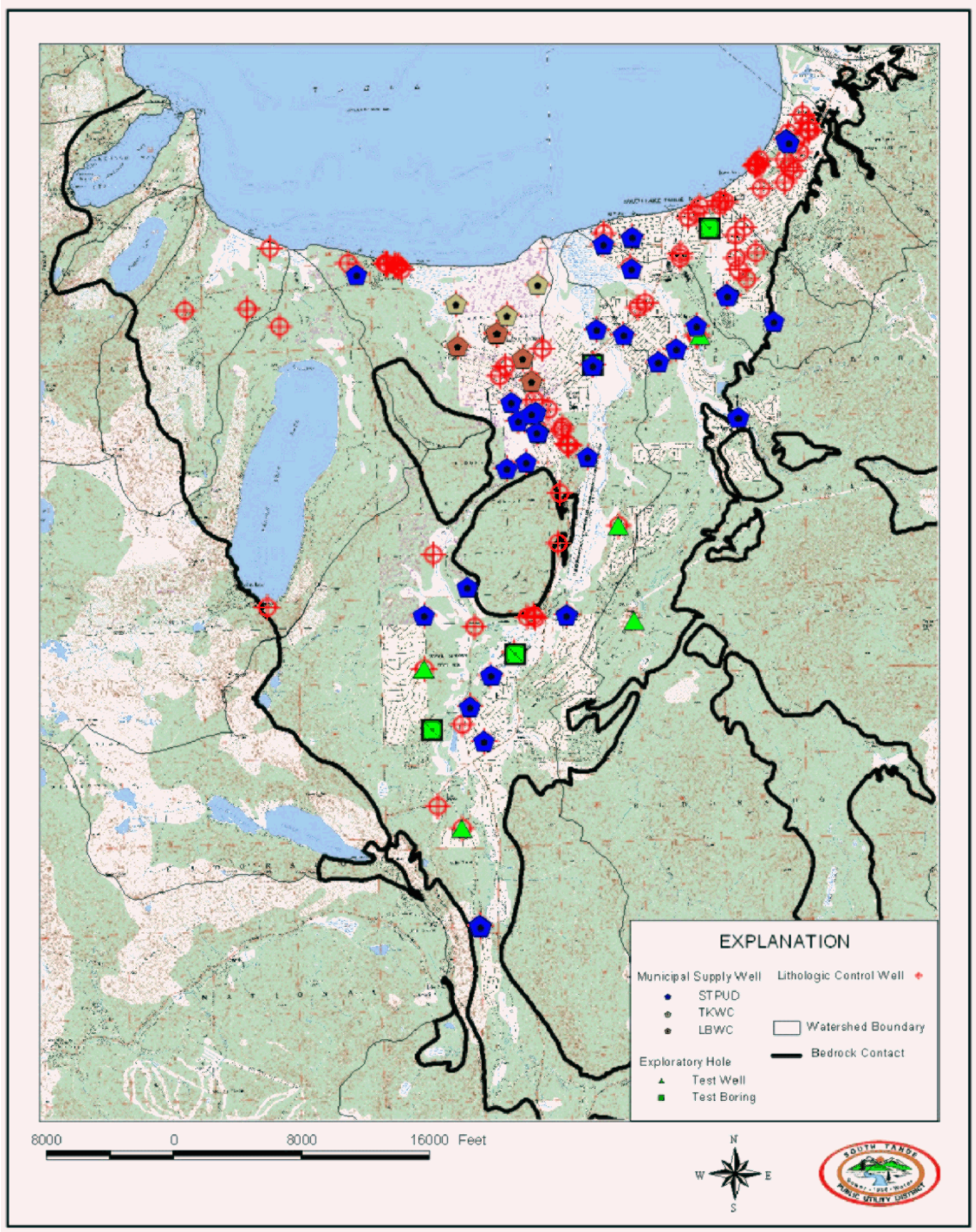

Figure 5-6. Distribution of basin-fill wells in the South Tahoe area. Black lines demarcate edges of bedrock contact. The southern tip of Lake Tahoe is located along the top of the map. All municipal supply wells and exploratory holes are located in valley lowlands between Lake Tahoe elevation (~6225 ft amsl) and 6500 ft amsl; many (but not all) of these wells were T-profiled. Some privately owned non-municipal wells are also shown (denoted 'Lithologic Control Wells'; not T-profiled). (Map courtesy Dr. Eric Labolle)

There are a number of hardrock boreholes in the Tahoe Basin area that were drilled for single household water supply, for snowmaking and lodge facilities (e.g. Heavenly Valley Resort, Northstar Resort), recreational facilities (U.S. Forest Service) and for use by government agencies (Caltrans, Civilian Conservation Corp). Most hardrock wells are located at high elevation, where suitable basin-fill aquifers are not available for water supply. Wells completed in hardrock are not currently major sources of water supply for Tahoe municipalities, and are not anticipated to be a major source of municipal water supply in the foreseeable future. However, discharge from bedrock likely contributes significantly to recharge of Tahoe Basin valley basin-fill aquifers.

Four South Tahoe area wells (Ralph, Heavenly Gondola, Big Meadows, and Echo Pass) completed in granitic bedrock were found available for hydraulic and thermal analyses (Fig 5-4). Additionally, a test well drilled deep into volcanic rock at the peak of Mount Pluto, located in the northern boundary of the Tahoe Basin (Fig 3-1), was available for T measurements. All but the Ralph well are located at elevation >7200 ft amsl. The Echo Pass and Heavenly Gondola wells were drilled ~1000 ft deep into granitic bedrock, and the Mount Pluto peak well is 800 ft deep in volcanic bedrock. The Ralph well was formerly operated by the South Tahoe PUD, and had been inactive for many years prior to T-profile measurement. The other three wells are non-district wells that had been drilled for private (Heavenly Gondola, Mount Pluto), public (Big Meadows), and government agency (Echo Pass) water supply.

Well construction and lithology information were available for each hardrock well except for the Mount Pluto well. The location and elevation of each well were determined by GPS. With the exception of the Mount Pluto test well (dry hole), each hardrock well had been pump tested shortly after installation, and also at later times for the Ralph and Heavenly Gondola wells. Water level measurements were available from during and/or shortly after drilling for each well. We performed one or more manual static water level measurements on each well. Additionally, an automated levelogger probe was suspended in the Big Meadows well from summer 2004 thru fall 2005, recording hourly water level data. A T-profile was measured in each well on one or more occasions, using one or more high precision temperature probes, as described above and in appendix 2.

5.4 Additional field data: Air T and precipitation data were obtained from ncdc archives for the South Tahoe Airport, located in the South Tahoe Basin at elevation ~6300 ft amsl, for comparison with our soil T measurements. Air pressure was monitored semi-continuously in the Mt. Pluto well using a Solinst Barologger, for comparison with borehole T monitoring results at Mt Pluto.

Well construction and lithology logs were obtained for most wells that were T-profiled, and well test records were obtained for some wells. These records were used to help in interpretation of observed T-profiles, as detailed in results for each well.

6: Analytic Methods

Heat flow can be used to trace groundwater flow, due to the intrinsic physical coupling of heat and groundwater flow. Subsurface temperature gradients imply groundwater density gradients, which can drive groundwater flow. Heat flows upward from depth toward ground surface in all areas of the earth's crust. At areas of the subsurface where there is significant groundwater flow, a substantial fraction of this heat energy is commonly diverted laterally or vertically by the groundwater flow. In this way, groundwater flow influences subsurface temperature fields. Small groundwater flow rates are indicated by conductive subsurface heat flow patterns, and departure from purely conductive heat flow indicates advection of heat with moving groundwater.

Analytic or semi-analytic solutions exist for a few simple patterns of heat and groundwater flow. Numerical methods are needed for irregular boundary conditions and more complex flow patterns.

6.1 Determination of conductive T gradients*:* For purely conductive geothermal heat flow upward from depth (negligible groundwater advection of heat), the subsurface vertical T gradient dT/dz is described by Fourier's Law:

$dT/dz = Q/\lambda$

Q = areal geothermal heat flux (heat energy/area/time)

λ = bulk thermal conductivity of subsurface rock or sediment body

The value of Q for the Tahoe Basin has been determined (see results). For hardrock, λ can be approximated by tabulated handbook values for that rock type. Alternatively, for rock or sediment standard relations can be used to approximate bulk λ using estimated mineral, rock, water, and air fractions & handbook values of λ for these constituents. For most rock and sediment types, λ varies over only a small range, such that handbook based estimates of λ are typically accurate to well within a factor of two.

For granitic rocks, quartz has a several-fold higher λ than the feldspars, thus a higher quartz:feldspar ratio, which can occur thru natural chemical weathering of granitic-derived sediments, will increase λ and thus decrease dT/dz (if feldspar-derived clay fraction washed out). Clay minerals and feldspars have comparable low λ values, thus partial diagenetic alteration of granitic sediments *in situ*, without appreciable washout of the clay fraction, might not alter λ of the sediment significantly. Clay-dominated layers found in Tahoe basin-fill, attributable to paleo-lacustrine depositional environments, may have somewhat smaller λ and thus larger conductive geothermal dT/dz than silt or sand dominated layers. At depth in sediments, compaction might reduce porosity by several percent, resulting in reduction of T gradient of several percent (slight concave-down curvature of T-profile). However diagenetic changes in mineral composition might eclipse the effects of compaction on λ at depth.

Departures of observed T-profiles from purely conductive T gradient are indicative of various patterns of groundwater flow.

6.2 Subsurface propagation of surface T warming: Substantial warming of ~1-2C has been documented for mean winter and annual air T in the Sierra Nevada over the last several decades (Dettinger et al, 1995, 2002, Anderson, 2006, and Barnett et al, 2008). This air warming is expected to have increased mean annual soil T (Ts) in the Tahoe Basin, and to propagate warmer T beneath the soil profile by conduction. Since there have been several decades of substantial surface warming, T-profiles are expected to be substantially altered in the shallow subsurface (<100 ft depth), and perturbed by a decreasing amount with increasing depth.

Abrupt and/or gradual increases in surface T propagate by heat conduction into the subsurface. Under conditions of negligible groundwater advection of heat, the depth of propagation of influence of a step change in surface T is approximated by:

$d = 2*[\alpha*t]^{0.5}$ = depth to which ambient temperature is changed by > 16% of the step change in surface temperature

α = thermal diffusivity

t = time since initiation of surface temperature warming at t=0

For a gradual increase in T over t, perturbation of subsurface T does not penetrate as deeply as for a step change.

Analytic expressions for transient conductive heat flow within a semi-inifinite slab undergoing either a step-change in surface temperature or a steadily increasing surface T are (Carslaw and Jaeger, 1959, p. 63):

$T(z,t) = To + a*z + \Delta T*[erfc(\eta)]$

(step-change ΔT in surface temperature)

$T(z,t) = To + a*z + b*t*[(1+2\eta^2)*erfc(\eta) - (2/\pi^{1/2})*\eta*exp(-\eta^2)]$

(linear ramp increase in surface temperature at constant rate b (C/yr))

t = time since initiation of surface temperature change at t=0

z = depth below ground surface z = 0 (positive in downward direction)

To = initial (t<0) ground surface temperature Ts

ΔT = magnitude of step-change in temperature (C) at time t = 0

a = ambient conductive geothermal gradient = dT/dz = constant (for t<0)

b = rate of change of surface temperature (initiating at t=0)

$\eta = z/[2*(\alpha*t)^{1/2}]$ (dimensionless) where α = thermal diffusivity

erfc = complementary error function

In these expressions, the first two terms (To+a*z) represent the steady-state geothermal T gradient at t<0, and the remaining terms account for the transient increase in surface T. The value of 'b' closely approximates the rate of increase in mean annual air T (Ta) in the Sierra Nevada over the last 30-40 years. Ts does not necessarily change at the same rate as Ta, since there are many factors in the surface energy balance that influence Ts. Notably, the annual average duration of snow cover likely has changed together with warming air T, which could have a large impact on Ts. However, compilations of worldwide data indicate that changes in surface T closely follow changes in air T in most areas (e.g. Huang, 2000). A warming rate of ~0.04 C/yr for Ts in the Sierra Nevada over the last 30-40 years is estimated; similar to the estimated rate of increase of Ta.

Examples of these relations are graphed in figure 6-1 below for granitic bedrock and granitic-derived sediment.

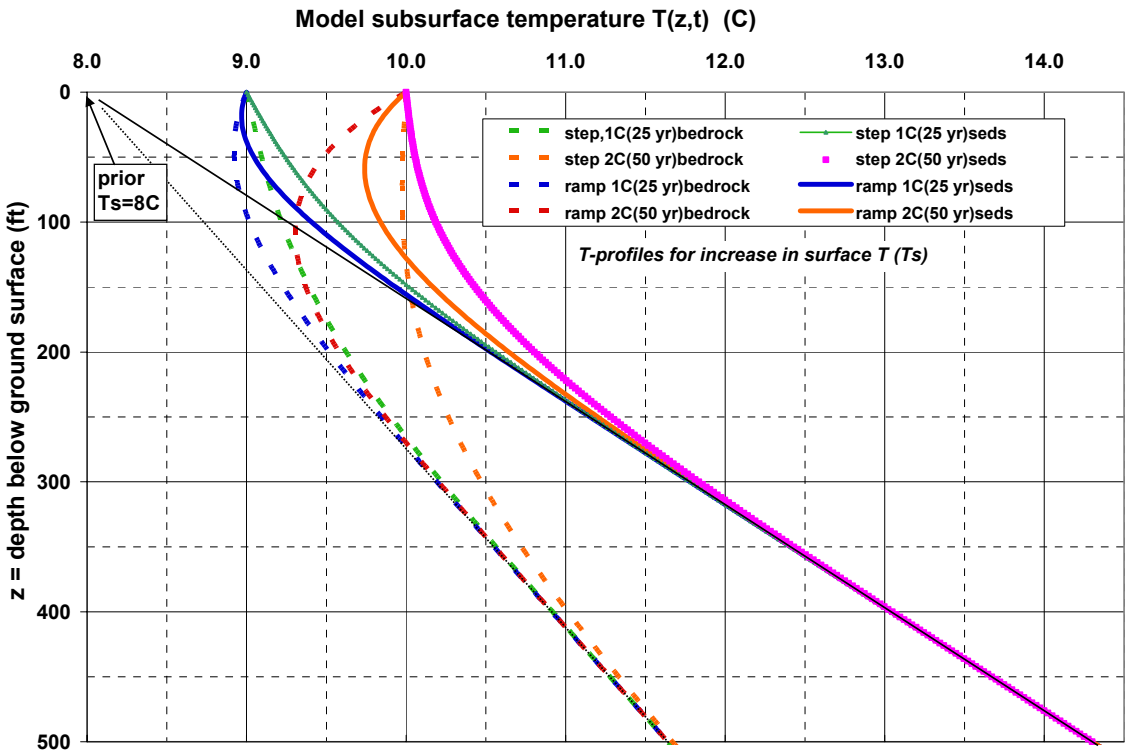

Figure 6-1. Model transient T-profiles in subsurface for surface T (Ts) warming initiating 25 or 50 years prior, for granitic bedrock (λ =2.76 W/m/^{o}C, α = 420 ft^2/yr) and sediments (λ = 1.60 W/m/^{o}C, α = 186 ft^2/yr) in the Tahoe area (Q = 66 mW/m^2). Initial Ts is 8C, then Ts warming of 1-2C to 9-10C takes place either suddenly (step-change 25-50 years prior) or gradually (ramp over 25-50 years). Model assumes conductive heat flow only (i.e. negligible groundwater advection of heat). Analytic model described in section 6.2.

As figure 6-1 shows, the effect of Ts warming penetrates more deeply into bedrock than into sediments, due to the higher α of bedrock. Figure 6-1 shows that shallow T inversions could result from gradual warming of Ts due to the recent trend of warming air T in the Sierra Nevada. Shallow T inversions can also result from a recent large step change in Ts (more recent and/or larger than shown in figure 6-1), due to recent clearing of forest or other dense vegetative cover.

The effect of surface warming on T-profiles is especially important in interpretation of observed concave-up T-profiles and T inversions (see results section 8).

6.3 Intra-borehole water flow: Intra-borehole water flow can substantially alter the borehole T-profile from that of the formation in the area. Intra-borehole flow is generally possible in uncased wells, which are typical in hardrock areas. Intraborehole flow can also occur if there are gaps between the casing and formation, or between two or more screened intervals in the same well, or within one long screened interval. Downward intra-borehole flow in the presence of steady upward geothermal heat flow in the surrounding formation results in cooling of the borehole T-profile and nearby formation T, relative to the formation at $r >> r_w$ at the same depth, as per Ramey (1962):

$$T(z,Vb,t) = To + a*[z+A*(\exp(-z/A)-1)]$$

where $A = [r_w^2*\rho_w*Vb*C_w/(2*\lambda)]*f(t)$

To = T(0,Vz,t) (assumed constant)

z = vertical position in borehole (z=0 at entrance to flow)

Vb = rate of intra-borehole flow (units L/T)

a = vertical T gradient in formation (and in borehole at t=0)

r_w = well or borehole radius

λ = thermal conductivity of formation

ρ_w,C_w = density, heat capacity of water

($C_w*\rho_w = 4.196X10^6$ (mks units) at 10C)

This solution is for a condition of constant intraborehole flow from z=0 to $z=z_e$ at rate Vb initiating at time t=0. Ramey presents f(t) for a constant heat flux cylindrical source:

$$f(t) = -0.29 - \ln[r_w/(2*(\alpha*t)^{1/2})] \qquad \text{for } t>>r_w^2/(4\alpha)$$

α = thermal diffusivity of formation

This solution has been found to be accurate at long times (Ramey, 1962), although the rate of heat exchange between the borehole and formation decreases with time, starting near the entrance of the intra-borehole flow. However, the assumption of constant heat flux leads to a derivation that is valid for a cylinder of effective length proportional to $[T(z_e,Vb,t)-To]$. As the effective cylinder length decreases with time as $[T(z_e,Vb,t)-To]$ decreases, the proportion of the cylinder exchanging heat at a constant rate does not change substantially until most of the cylinder has cooled to To.

The relations above show that wellbore cooling is a complex function of both the duration and rate of intraborehole flow. For spontaneous intraborehole flow induced by borehole short-circuiting of vertical head gradients in the formation, the flow rate would typically gradually slow down after flow initiation (e.g. post-drilling). However the relations above are a good approximation for quasi-steady Vb.

Figure 6-2 below shows the relation above for T(z,Vb,t) at several conditions of Vb and t, illustrating the influence of downward intra-borehole flow on the borehole T-profile in a formation with steady upward conductive heat flow. Note the T-profiles are characteristically flattened near the entrance to intraborehole flow, and that the undisturbed formation T gradient is often recovered upstream of the exit of intraborehole flow (for sufficiently small t, Vb). Figure 6-2 shows that the intra-borehole flow rate is much more important than the flow duration (years) in altering the well T-profile. Note the computed T-profiles are based on a model that does not account for lateral groundwater flow which may be present in the formation surrounding the portion of the borehole in which the intraborehole flow is occurring. Rapid lateral groundwater flow in the formation would advect heat to the borehole, resulting in less cooling (warmer T-profiles) than those shown in figure 6-2. Just below the exit to intra-borehole flow, the borehole T can increase very sharply with depth (not shown), given adequate lateral groundwater flow rate in the formation to laterally transport and disperse the cooler water transported down the borehole.

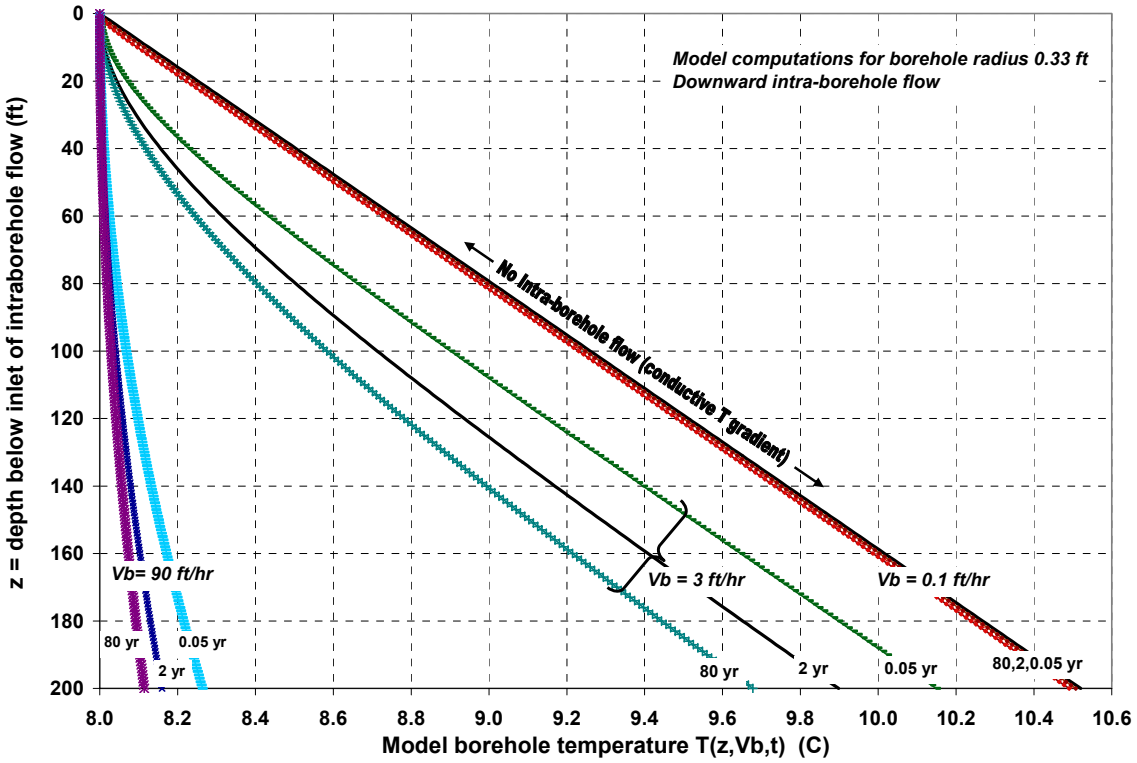

Figure 6-2. Model transient T-profiles in well with downward intraborehole flow starting at a single depth (inlet depth defines vertical coordinate z=0). Results shown for flow initiating 0.05, 2, and 80 years prior, at rates 0.1, 3, and 90 ft/hr. Model uses Q= 66 mW/m^2 for Tahoe area, and α = 186 ft^2/yr, λ = 1.60 W/m/^{o}C for granitic sediments. Model assumes negligible vertical or lateral advection of heat by groundwater in the formation surrounding the borehole. Analytic model described in section 6.3.

6.4 1D combined heat and groundwater flow: Bredehoeft and Papadopulos (1965) presented the analytical solution for 1D steady coupled groundwater and heat flow:

$$T(z) = T(0) + [T(L) - T(0)]*[\exp(\beta*z/L) - 1]/ [\exp(\beta) - 1]$$

where z = depth below $z = 0$

$\beta = C_w*\rho_w*V_z*L/\lambda$

V_z = vertical Darcy velocity of groundwater in formation

This relation is typically used as a curve fit to T-profile data to obtain a numerical estimate of the curve-fit parameter β. This enables estimation of V_z using the T-profile and an estimate of λ, independent from any hydraulic data. Downward groundwater flow results in a concave-up T-profile shape; and upward groundwater flow results in a concave-down T-profile shape.

Heat and groundwater flow is often predominantly 1D across aquitard layers. This 1D solution is also accurate in steady 2D flow, such as may be present within an aquifer, under the following condition (Lu and Ge, 1996):

$$V_x*(dT/dx) << V_z*(dT/dz) \text{ where } x = \text{lateral dimension}$$

Analytic solutions to 1D groundwater and heat flow in the presence of transient surface T warming have been presented by Taniguchi (1999a,b). These solutions are extremely cumbersome and complex and therefore are not reproduced here.

6.5 2D modeling of thermal energy balance near mountain-front: A novel energy balance on cool mountain front recharge into an adjoining valley basin-fill aquifer is developed under steady-state conditions in a rectangular cross-section extending away from the mountain-front (Fig 6-3). The model is 'black-box': processes within the domain are not modeled, only heat and groundwater flow across the domain boundaries.

Net advective heat flow across any enclosed domain boundary d_b in 3D can be expressed in general form as:

$$E_{ad}\{d_b\} = C_{v,w} * \oint_s [V_{\perp}(s) * \Delta T(s)] ds = \text{advective heat flow across boundary } d_b$$

(units energy/time)

$C_{v,w} \equiv$ volumetric heat capacity of water $\equiv \rho_w * C_w$

$s \equiv$ spatial location on boundary d_b (any coordinate system)

$ds \equiv$ differential boundary area at location s (units L^2)

$V_{\perp}(s) \equiv$ darcy velocity component perpendicular to d_b at location s

$\Delta T(s) \equiv$ T at location s (on d_b) minus T_{ref}

where $T_{ref} \equiv$ reference T (fixed value)

Net conductive heat flow across any enclosed domain boundary d_b in 3D can be expressed in general form as:

$$E_c\{d_b\} = \oint_s [Q_{\perp}(s)] ds = \text{conductive heat flow across boundary } d_b$$

$Q_{\perp}(s) \equiv$ conductive heat flux component perpendicular to d_b at location s

(units energy/time/area)

The condition of conservation of thermal energy is applied in a domain with no internal heat sources or sinks at steady-state: net conductive heat flow across the domain boundaries must balance net advective heat flow across these boundaries:

$$E_{ad}\{d_b\} = E_c\{d_b\}$$

$$C_{v,w} * \oint_s [V_{\perp}(s) * \Delta T(s)] ds = \oint_s [Q_{\perp}(s)] ds$$

This general steady-state condition of thermal energy conservation in 3D is applied to the 2D model domain shown in figure 6-3 below.

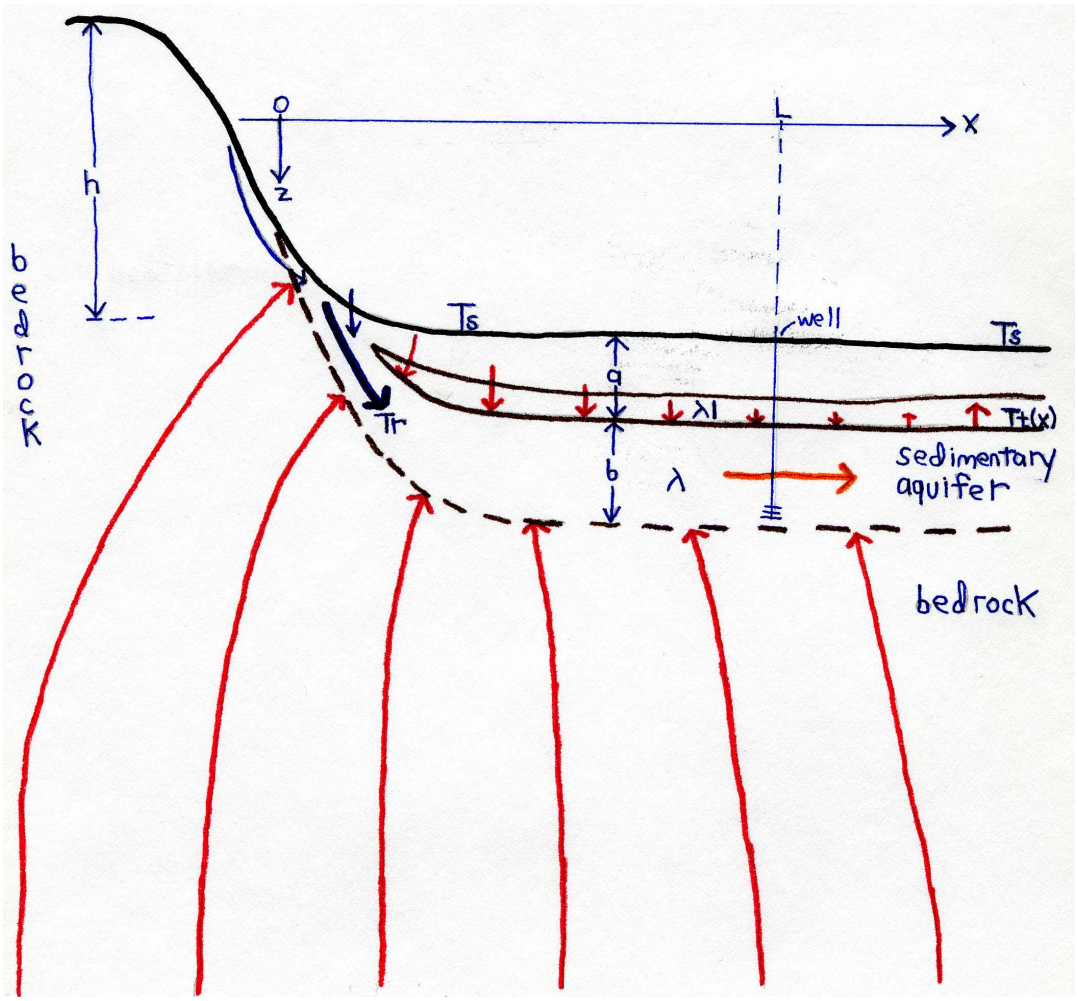

Figure 6-3. Schematic cross-section of mountain-front groundwater recharge, for use in thermal model of mountain-front recharge of sedimentary aquifer spanned by depth interval 'b'. Red arrows indicate conductive heat flux into this lower aquifer. Groundwater recharge at the mountain-front cools the subsurface; thus ambient conductive geothermal heat flow from depth is diverted toward the mountain-front area, increasing conductive heat flux near the mountain-front. Conductive heat also flows into the aquifer from the top (since Tr<Ts) near the mountain-front and for some distance into the valley. As the aquifer becomes warmer with increasing distance from the mountain-front, the direction of heat flow across the top surface of the aquifer reverses direction. The blue arrows at the left edge of the aquifer denote cool groundwater recharge into the mountain-front lateral side of the aquifer. The orange arrow in the aquifer near the right side denotes warming of groundwater in the aquifer with distance away from the mountain-front due to conductive heat flow into the aquifer. The model is also applicable for a single aquifer on top of bedrock, with the depth interval 'a' consisting of an unsaturated zone.

The model assumes steady downflow of cool recharge water at temperature T_r into the edge of the aquifer at the mountain front, and 1D steady lateral groundwater flow within the aquifer, directed away from the mountain front. Heat flows by advection with groundwater out of the domain across only the valley-side lateral boundary of the domain at x=L. For steady lateral flow of groundwater in the aquifer, setting $T_{ref} = T_r$;

$$E_{ad}\{x=L\} = C_{v,w} * \int_{z=a+b}^{z=a} [V_x(z) * (T\{z,L\} - T_r)]dz$$

= net advective heat flow out of domain (units energy/time/width)

where $V_x(z)$ = lateral Darcy velocity of groundwater in aquifer

For this 2-D domain, the differential area *ds* is replaced by a differential length *dz* on the domain boundary; and units of E_{ad} are energy/time/width perpendicular to the plane of the domain. For uniform lateral groundwater flow; $V_x(z)$ = constant = Vx

$$E_{ad}\{x=L\} = C_{v,w} * V_x * b * \Delta T_m$$

where $\Delta T_m \equiv \int_{z=a+b}^{z=a} (T\{z,L\}/b)dz - T_r$ = mean value of ΔT at x=L

Heat energy flows into the domain by conduction across all four domain boundary sides shown in figure 6-3. Heat flux relations presented by Lachenbruch (1968,1969) account for the focusing of deep geothermal conductive heat flux toward mountain-front areas. Appendix 3 shows how heat flux relationships along each of the domain boundaries is integrated and bounded, such that net conductive heat flow $E_c\{d_b\}$ across all four sides of the domain is bracketed:

$$[0.64*(a+b)]*Q + L*[Q+Qt\{x=L\}] < E_c\{d_b\}$$
$$< (1.97*Hl)*Q + L*[Q+(Qt\{x=0\}+Qt\{x=L\})/2] \quad \{Tr<Ts\}$$

where Hl= a+b+h+h' (see appendix 3 for definition of h')

Q = areal ambient conductive heat flux from depth

$Qt\{x=0\} = \lambda 1*(Ts-Tr)$ and $Qt\{x=L\} = \lambda 1*(Ts-Tt\{x=L\})$

At steady-state, energy conservation requires $E_c\{d_b\} = E_{ad}\{x=L\}$. Combining the relations above;

$$[0.64*(a+b)]*Q + L*[Q+Qt\{x=L\}] < C_{v,w} * V_x * b * \Delta T_m$$
$$< (1.97Hl)*Q + L*[Q+(Qt\{x=0\}+Qt\{x=L\})/2] \quad \{Tr<Ts\}$$

Vx from a mountain front recharge source is bracketed by this expression, using the T-profile data from a well located at x=L to obtain ΔTm and $Qt\{x=L\}$. The range is small when the value of the term $Qt\{x=L\}$ is significantly different from the value of Q (e.g. for Tr<Ts if there is a T inversion reaching to the top of the aquifer at x=L). An example of using this model to determine a lower bound on Vx is presented in section 8.7.

A different approach to quantifying the heat flow balance in the domain shown in figure 6-3 was undertaken by Cermak (1989), who solved the differential equation of heat flow within the aquifer under the assumption that dT/dz ~ 0 within the aquifer, so that $T(x,z) = T_{aq}(x)$ within the aquifer. The solution presented by Cermak is:

$$T_{aq}(x) = T_{eq} + [Tr-T_{eq}]*\exp(-n*x)$$

where $n = -[C_{v,w}*Vx/(2*\lambda)]*[1-[1+(4*\lambda*\lambda_1)/(b*a*(C_{v,w}*Vx)^2)]^{1/2}]$

$T_{eq} = Ts + (Q/\lambda_1)*a$

Examples of the black-box and Cermak solutions are shown in appendix 3. The black-box approach has the following advantages over the Cermak (1989) approach for estimation of the rate of mountain-front groundwater recharge Vx:
(1) The Cermak method assumes dT/dz ~0 within the aquifer. Such an approximation may be acceptable for deep, thin aquifers (a>>b), but is not good for thick or shallow aquifers, particularly not for a<b. The 'blackbox' energy balance approach presented here is not dependent on any simplifying conditions on the T distribution within the aquifer.
(2) The Cermak solution does not account for focusing of deep geothermal heat flow near the recharge zone x=0, therefore the Cermak solution for change of T near the mountain front is less than the actual change in T. Thus the black-box is more realistic than Cermak for Vx at small distances from the mountain-front (a+b)<x<~5*(a+b). The black-box approach should be accurate for all distances x>(a+b) where $T(x)-Tr < T_{eq}-T(x)$; e.g. for cool recharge at distances where there is a T inversion present. Neither solution is likely to be highly accurate near the mountain front x<(a+b), since subsurface T is sensitive to realistic departures from model assumptions near the mountain.
(3) The black-box solution is analytic for Vx, whereas the Cermak relations must be solved iteratively or numerically for Vx.

For thin deep aquifers (a>>b) at large distances from the mountain front where more than half the change of aquifer T from Tr to T_{eq} has occurred, the Cermak solution may be more useful, since the energy balance bracketed range of Vx becomes wide as Tt(x) approaches T_{eq}.

Other analytic approximations to simple symmetric geometries of steady 2D groundwater and heat flow have been published (e.g. Lu and Ge, 1996, and Reiter, 2001). Numerical techniques are needed to approximate combined heat and groundwater flow under conditions of asymmetric boundary conditions and more complex flow patterns.

6.6 Finite Element Numerical Modeling: Advances in processing speed of inexpensive desktop computers and the availability of powerful data processing software have recently enabled routine analysis of coupled heat and groundwater flow; with heat flow measurements acting as a robust constraint on groundwater flow. We used the USGS finite element modeling code SUTRA (Voss, 1984) to model the nonlinear but deterministic interaction between subsurface groundwater flow and heat flow. SUTRA accounts for the T dependence of water density, which influences groundwater flow. Large 2-D and 3-D models can be run using this software on standard inexpensive desktop computers.

Boundary conditions and bulk subsurface parameters (hydraulic conductivity k and thermal conductivity, hydraulic storativity Ss, heat capacity Cp, thermal dispersivity) for groundwater and heat flow are specified as part of model input. Groundwater head and flow rate, and subsurface T and heat flow rate are output from the model and compared to field observations. Input can be adjusted iteratively so that modeled results are consistent with field observations. Typically, there is much larger uncertainty in the hydraulic than in the thermal parameters, since bulk thermal conductivity λ and Cp vary only over a small and known range for most common rock and sediment types. Thus typically only the hydraulic parameters (k and Ss) need adjustment, and in this way groundwater flow rates are better constrained.

7: Results for Soil Temperature

A detailed description of soil T monitoring results is presented in appendix 4, and summarized below. 93 of 97 soil sensors were recovered and downloaded during fall 2005. All recovered sensors had successfully logged soil T at 30 minute intervals for the entire period of deployment, which was >1 year at most sites. Four probes were not recovered; it appeared that each of these probes was removed and possibly redeployed by digging or burrowing animals. All of the dozen probes left in place for 1-2 additional years were recovered; although data from several of these probes could not be recovered.

7.1 Examples of soil T time series: Figure 7-1 below shows time series of daily mean soil T measured at each of three sites from summer 2004 to fall 2005. Two of these sites were located very close to each other on the floor of Christmas Valley (near Meyers), one in unshaded bare soil and the other in a nearby dense forest copse (Fig 7-2). The third site was in exposed bare soil ~1 mile upslope near Echo Lake, about 1,250 ft higher in elevation. Figure 7-1 illustrates the sites have similar winter soil T near 0C, but large differences in summer soil T. The ~1,250 ft elevation difference between sites did not affect soil T nearly as much as inter-site differences in vegetative cover.

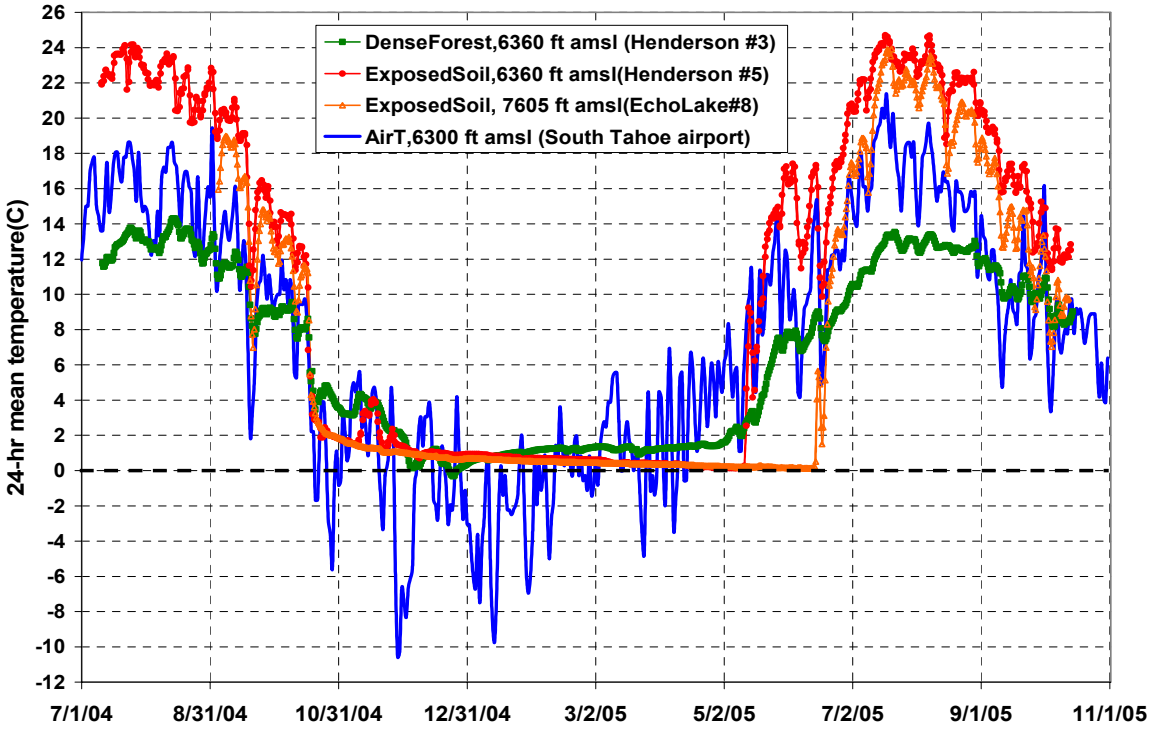

Figure 7-1. South Tahoe area soil and air T monitoring data (24-hr mean), July 2004 thru Oct. 2005. Data are shown from two sites near each other in Christmas Valley (Henderson #3,5) and one site ~1 mile westward on top of a ridge near Echo Lake (Echo Lake #8). The 'exposed soil' sites were located in bare soil with very little vegetation shading (although the Christmas Valley site has significant terrain shading), whereas the 'dense forest' site received no direct sunlight (photos figure 7-2). Air T data from the nearby South Tahoe airport is shown for comparison.

Figure 7-2. Photos of two soil T probe sites ~200 yards apart from each other on the floor of Christmas valley (~6360 ft amsl). Top: Meadow with well-exposed bare grey/brown soil (Henderson site #5). Bottom: Dense tree copse within pine forest area, with soil covered by needles and dead twigs (Henderson site #3). Each site is in a flat area (slope <2^{o}). The upper site is exposed to sun for nearly all daylight hours; in contrast the deeply shaded lower site receives no direct sunlight. T monitoring data are shown in figure 7-1.

7.2 Winter soil T: During winter, soil T dropped to near 0C at all sites, but did not freeze at any sites during winters 2004/05 and 2005/06 (winter minimum soil T>-1C), including the highest elevation sites near 7600 ft amsl (Note: the freezing point T is depressed slightly below 0C in partially saturated soils). Most sites had minimum T in the range 0.0 to +0.5C. This indicates that infiltration in valley areas and surrounding slopes was not significantly impeded by frozen topsoil during snowmelt. During January 2007 soil did freeze (T<-1C) at about half the monitored sites during periods of sub-freezing air T and no snow cover. However, this frozen condition only persisted for a few days or less, with T rising >0C after snow cover was re-established. At most sites, the date of completion of snowmelt (i.e. ground surface exposure) was indicated by a sharp rise in soil T from near 0C. Many locations showed multiple such thaw dates between March and June.

7.3 Summer soil T: In contrast with winter T, warm season T varied widely between sites. Figure 7-3 shows mean August 2005 soil T for each site vs a regression relation:

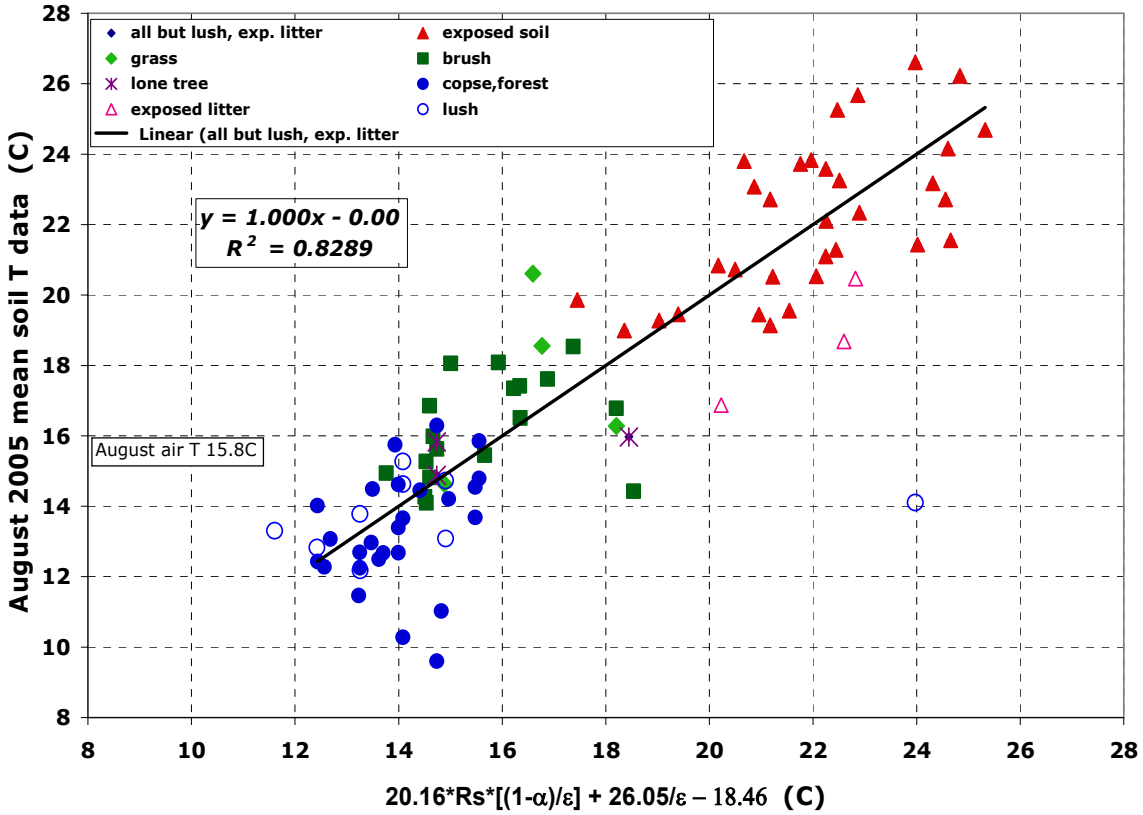

Figure 7-3. August 2005 mean measured soil T at monitoring sites vs regression against model function of surface radiation related parameters (see section 7.5). Rs (mean August incident short-wave radiation flux at surface) is normalized to 1.000 (dimensionless) for a level non-shaded surface. There was no correlation of July or August mean soil T with elevation over the range of site elevations (~6240-7600 ft amsl). Mean August soil T was as much as 11C warmer than to 6C cooler than mean August air T (South Tahoe airport, 6300 ft amsl). 'Exposed litter' sites were exposed sites of soil completely covered by pine needles, leaves, and/or bark & twigs. 'Lush' sites were sites that had very damp topsoil thruout August (water table very near ground surface).

During summer, forest soil T was substantially cooler than air T, and exposed (non-shaded) soil T was substantially warmer than air T. Summer soil T peaked between mid-July and late August at each site for each summer monitored (summer 2004 thru summer 2007 at some sites). Peak 24-hr mean summer soil T ranged from ~11C to ~31C between all sites, as compared to ~20C for peak 24-hr mean summer air T. Peak daily mean summer soil T at a given site (and peak daily mean summer air T at the South Tahoe airport) did not change by more than +/-2C between summers. Higher summer soil T is associated primarily with less vegetative cover, more radiation exposure, and darker, dryer soils. Elevation over the range monitored had little influence on summer soil T, with no statistically significant summer soil T lapse from 6230 ft to 7600 ft amsl. Similar results were found for mean July 2005 soil T (appendix 4).

7.4 Annual mean soil T: Annual mean soil T (Ts) varied substantially between sites, as shown in figure 7-4 below. Since nearly all sites had winter soil T near 0C, the rank order of sites by Ts is similar to the rank order for mean July and August T. Figure 7-4 below graphs Ts data for each site vs a regression relation (described in section 7.5):

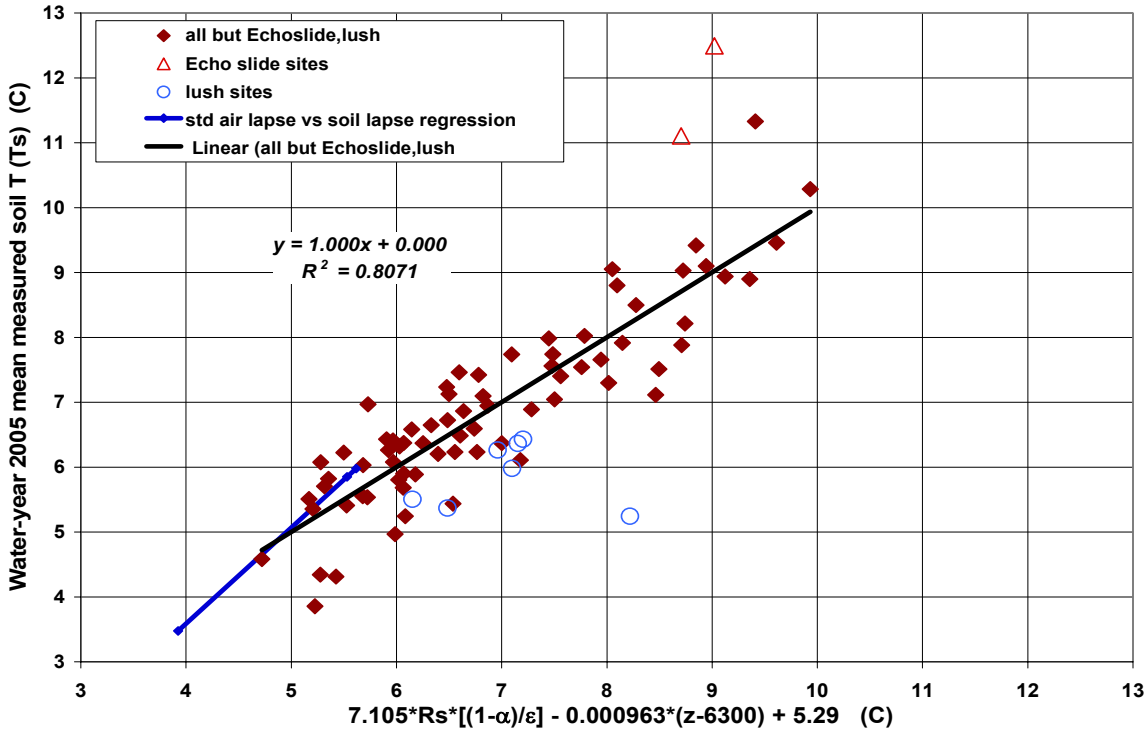

Figure 7-4. Mean annual measured soil T (Ts) for water-year 2005 at monitoring sites vs regression against model function of elevation and surface radiation related parameters (section 7.5). Mean annual air T over the range of site elevations (lapse 6C/km) also shown. Rs (mean annual short-wave radiation flux incident at surface) is normalized to a value of 1.000 (dimensionless) for a flat non-shaded surface. The range of site elevation z was ~6240-7600 ft amsl. There is no correlation of Ts with the 1/ε regression term (section 7.5) over the range of site ε. Two 'Echo slide' sites were on steep bedrock near Echo Lake where snow slid off during warm spells in winter, and thus were anomalously warm. 'Lush' sites were sites that had very damp topsoil throughout summer and early fall (water table near ground surface).

The effect of elevation (thru Ta) on Ts is removed in figure 7-5 below, which shows soil T corrected for air T lapse (~6C/km) vs the regression relation:

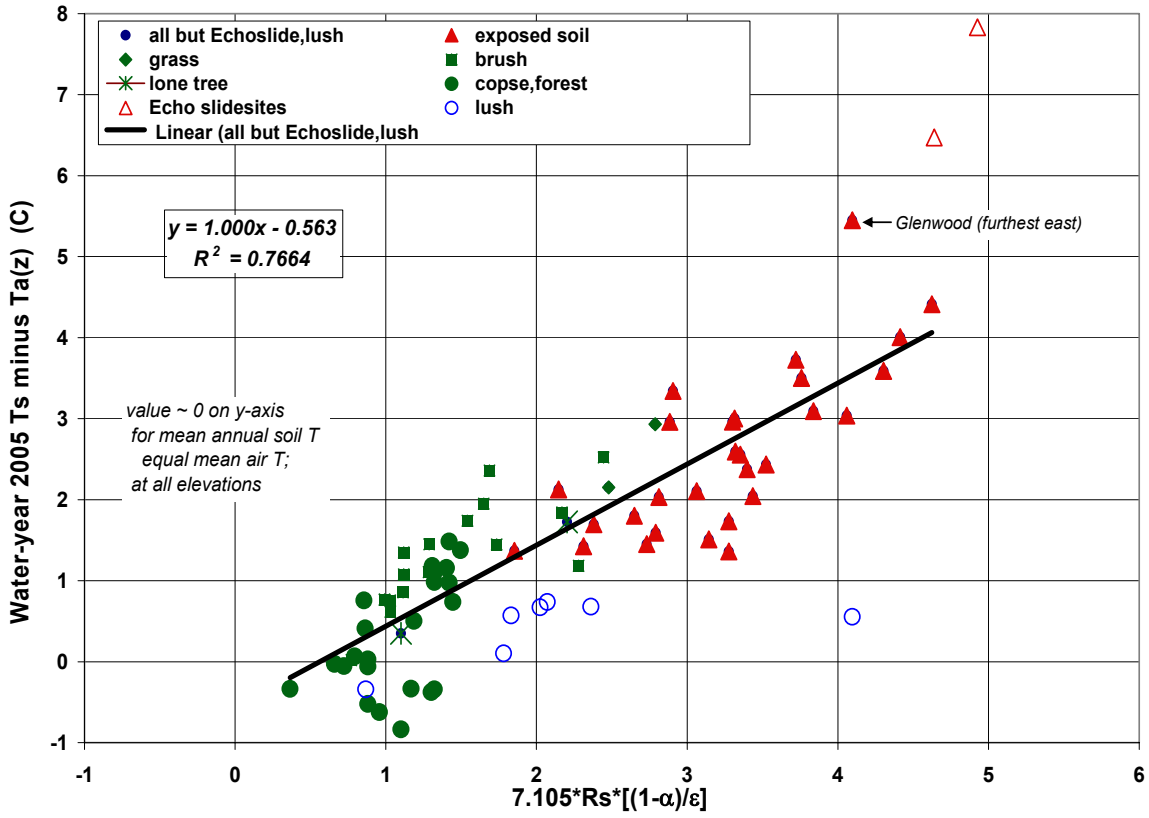

Figure 7-5. Mean annual measured soil T (Ts) for water-year 2005 at monitoring sites, corrected for mean annual air T(Ta) at site elevation, vs regression against model function of surface radiation related parameters (see section 7.5). This graph shows the value of Ts relative to Ta at that elevation, using the same data as figure 7-4 (corrected for elevation). This graph shows Ts (with exception of outliers) was as much as ~5C warmer or 1C cooler than Ta at that elevation.

Figure 7-5 shows Ts ranges from ~1C below to ~5C above annual mean air T (Ta) for that elevation. Note the y-intercept in figure 7-5 is <0, due to latent heat loss (i.e. evapotranspiration), which can cause Ts in completely shaded locations to be cooler than Ta (this effect is most pronounced in summer; see figure 7-3 and appendix 4).

7.5 Modeling of soil T: In figures 7-3, 7-4, and 7-5 above, the regressions for summer soil T and for Ts were fit to the same model form; shown below for Ts:

$$Ts = C1 + C2*z + C3*[(1-\alpha)*Rs]/\varepsilon + C4/\varepsilon \qquad R^2 = 0.808$$

where C1, C2, C3, C4 are regression coeffients
z = site elevation
α = estimated site surface albedo
Rs = est. annual mean incident short-wave radiant energy flux at surface
ε = estimated site surface long-wave radiation emissivity

For soil T during summer months (July, August), mean annual values of the parameters Rs, α, ε are replaced by monthly values for these parameters in the equation above (appendix 4). In figures 7-3,4,5 above Rs values (August or annual mean short-wave radiation flux incident at surface) are normalized to a value of 1.000 (dimensionless) for a flat non-shaded surface (for monthly or annual timescales); dimensional values of Rs in energy flux units corresponding to these normalized values are estimated in appendix 4.

Estimated values of Rs were computed based on estimates of slope, aspect, and shading by terrain and vegetative cover at each site. Most of the inter-site variations in both summer soil T and in Ts are attributable to inter-site differences in Rs. The regression result for elevation lapse of Ts (~3.2 +/- 0.8 C/km) is significantly less than that of air T (~6 C/km in Tahoe Basin). Differences in elevation affect Ts thru differences in incident short-wave and long-wave radiation and differences in the duration of winter snow cover, as well as thru lapse in Ta.

Scatter of soil T data (monthly and annual) about the least squares regression fit to the model is not attributable to errors in soil T measurement or primarily to imperfections in the model form approximation of the physical processes determining soil T (see appendix 4). Instead, the scatter is due mainly to errors in specific site estimates of the values of the regressors Rs (from uncertainty in shading estimates), α, and ε, and to non-monitored inter-site differences in soil moisture (affects latent heat loss). Several sites observed to have damp topsoil thru late summer were removed from the regression (negative outliers figs 7-3,4,5), as were two sites in steep exposed granitic bedrock, where snowpack slid off during warm spells in winter (positive outliers, fig 7-4,5). The presence of litter on top of the soil surface helps insulate the underlying soil from heating during summer (Fig 7-3), but also helps insulate the underlying soil from cooling during winter, such that sites with substantial litter cover were not outliers for Ts.

The regression equations for summer soil T and Ts are semi-empirical, with functional form based on a simplified lumped-parameter physical model of surface energy exchange processes (see appendix 4). With this model approach, soil T maps over a landscape area can be simulated using data typically available as GIS coverages (slope, aspect, elevation, leaf-area index or other measure of vegetative cover, and surface albedo and emissivity, or soil color). Additionally, data from an air T monitoring site in the general area, and an index of typical seasonal cloud cover are required. Other closely related soil T mapping methods have been reported in the literature, cited in appendix 4.

8: Results for Well Temperature Profiles

Seasonal surface T oscillations propagate by conduction into the subsurface with exponentially decreasing amplitude with depth, and are damped out to <0.2C amplitude at ~40 ft depth in South Tahoe area basin-fill sediments. The T-profile below ~40 ft depth is of most practical value in determining groundwater flow patterns since complicating transient effects of seasonal changes in surface T are damped out.

For wells installed across fairly uniform types of geologic material, a purely conductive T-profile increases linearly with increasing depth at steady-state. A purely conductive T gradient depends on the underlying geothermal heat flow upward from depth, the bulk λ value(s) of the geologic materials, and Ts in the area near the well.

More generally, T-profiles have a curved shape. Curvature of a Tahoe T-profile is typically attributable to one or more of the following: (i) spatial changes in bulk λ, due to changes in rock type or rock mineral composition with depth (ii) decadal or longer time-scale changes in Ts, which can strongly affect the shallow portion of the T-profile (iii) intraborehole water flow and (iv) groundwater flow patterns in the formation surrounding the well. The effect of these influences on well T-profiles are modeled in section 6 and are observed in many Tahoe wells described in this section.

8.1 Tahoe Basin Heat Flow: The T-profile at depth for a deep granitic bedrock well at Echo Pass, located near the southwestern corner of the Tahoe Basin (Figs 3-2,3, 5-4), provides a calibration point for regional geothermal ambient conductive heat flow from depth for the South Tahoe area. Figure 8-1 below shows the Echo Pass well T-profile:

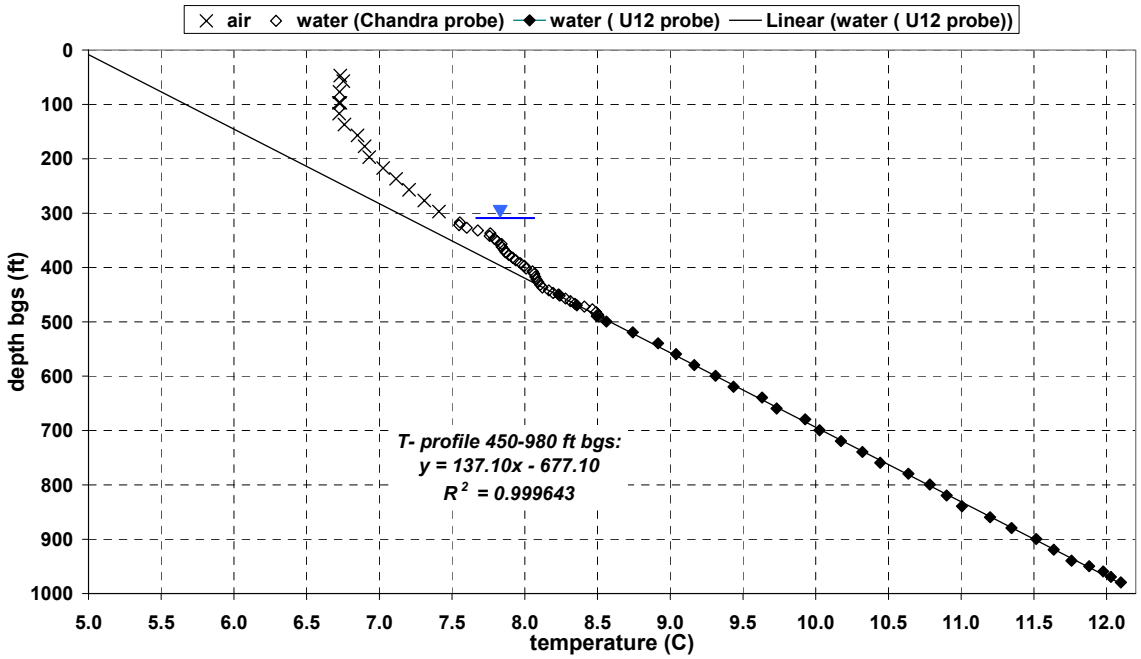

Figure 8-1. Temperature profile of well at Echo Pass, to 980 ft bgs in granitic bedrock. The static water level in this well was ~315 ft bgs during 2004/05.

The T-profile from about 450 ft depth to the deepest measured point (~1,000 ft depth) is a nearly perfect straight line ($R^2 = 0.99964$), indicating negligibly small disturbance of conductive heat flow by groundwater flow or topographic effects below ~450 ft depth:

$dT/dz = (7.28 +/- 0.03)x10^{-3}$ C/ft (+/- 1σ)

The thermal conductivity λ of the granitic rock at depth is estimated based on measured mineral compositions of samples of non-weathered rock from this Bryan Meadows granodiorite unit (Loomis, 1981) and tabulated values of mineral λ, using standard methods (appendix 5). The value of computed λ depends on the mineral proportions of each sample, with mean λ = 2.76 W/m/C (range 2.38 to 3.27 W/m/C) for Bryan meadows granodiorite. This estimate of λ is near the center of a range reported for granodiorites (Schon, 1996) and is supported by thermal diffusivity measurements in a nearby quartz diorite unit (appendix 5).

Steady conductive geothermal heat flux Q = (dT/dz) * λ:

Q = 1.58 HFU (=66.0 mW/m^2) (range 1.36 to 1.87 HFU = 56.9 to 78.2 mW/m^2)

This estimate of Tahoe Basin geothermal heat flux falls near the center of a range reported by Henyey and Lee (1976) based on measurements in Lake Tahoe bottom sediments. High confidence in the magnitude of geothermal conductive heat flow for the Tahoe region is provided by this new calibration point together with the prior measurements under Lake Tahoe. This heat flux value is intermediate to the higher flux of the neighboring basin and range, and the lower flux of the western slope of the Sierra Nevada (Henyey and Lee, 1976).

8.2 Conductive ambient geothermal temperature gradient in sediments: For saturated sediments, the steady-state conductive geothermal gradient dT/dz due to ambient flow of geothermal heat Q upward from depth, undisturbed by groundwater flow, is related to that of parent bedrock (in the same region) by:

$(dT/dz)_{seds} = (dT/dz)_{bedrock} * (\lambda_{bedrock}/\lambda_w)^{\theta}$

$\lambda_{seds} = \lambda_{bedrock} * (\lambda_w/\lambda_{bedrock})^{\theta}$

θ = total volumetric porosity of sediments

subscript 'w' denotes water

This formulation holds under conditions where the sediment mineral composition is the same as that of the parent bedrock; and thus may not be an accurate approximation for sediment layers that have been substantially chemically weathered or diagenetically altered. For Tahoe basin sediments with granodiorite mineral composition, given $(dT/dz)_{bedrock}$ from section 8.1 and $\lambda_w = 0.58$ W/m/C; substituting into the relation above;

$(dT/dz)_{granitic\ seds} =\sim 0.00728 * (4.76)^{\theta}$ (C/ft)

Thus for sediment porosities of 25%, 35%, and 45%; dT/dz ~ 0.0108 C/ft, 0.0126 C/ft, and 0.0147 C/ft, respectively for Tahoe basin granitic derived sediments (with negligibly

altered mineral proportions), substantially larger than the conductive geothermal gradient 0.0073 C/ft in granitic bedrock.

Focusing of deep geothermal heat flow toward valley areas is neglected in these analyses. Such focusing is reduced by the presence of thick insulating layers of sediments in many Tahoe valley areas. However, enhanced geothermal conductive heat flow is likely significant near valley margins where sediments are thin, and in deep narrow valleys such as Christmas Valley in the South Tahoe area.

8.3: Borehole at Mt. Pluto summit: nonsteady temperature to 800 ft depth

Figure 8-2. View from near peak of Mt. Pluto (el. 8617 ft amsl) facing E-SE, showing Lake Tahoe and the Carson Range in background. The summit is a broad, fairly flat area of about 100 yards diameter. The land surface gradually falls downward on all sides of the summit area, with slopes>10% on all sides within ~100 yards from the summit area.

Peak well description: An 800 ft deep dry well is located at the summit of Mt. Pluto (elevation 8617 ft amsl), on the northern boundary of the Tahoe Basin watershed (Fig 3-2). A day lodge has been operated at the summit of Mt. Pluto, which is also the terminus for several ski chairlifts operated by Northstar-at-Tahoe Resort. This well was originally drilled in the mid 1980s as a test well for water supply to the summit day lodge and for snowmaking (Jim Lochridge, Mountain Operations Manager, personal communication). Because the well was dry, it was not developed for water supply. The peak well is near

the base of the upper terminus of the Comstock chairlift. PVC casing (~6" OD) is present at the top of the borehole; within which a narrower (~4"OD) pvc casing initiates at depth ~12 ft bgs. The downward extent of casing is not known; drilling or construction logs for this well have not been found. Permission to access this well for T and air pressure measurements was given by Northstar-at-Tahoe. Measurements initiated July 2002 and continued thru fall 2003.

Geology of Mt. Pluto area: The northwest portion of the Tahoe Basin where Mt. Pluto is located (Fig 3-1) has a predominantly volcanic geology (Fig 3-3). The area has not been volcanically active during the Holocene. However, several volcanic flows in the area have been dated to the late Tertiary period and early Pleistocene epoch (Burnett, 1971). Two 7.5 minute Quads that include the Mt. Pluto area have recently been mapped in detail (Wise and Sylvester, 2004a,b). Most of the rock in the area near the peak of Mt. Pluto is part of the Late Miocene Martis Peak Formation, consisting of basaltic andesite to andesitic lava flows and pyroclastic deposits.

Water table: This well was nearly dry during 2002/03, with only ~1-2 ft of water at the bottom, near 800 ft depth (elevation ~7815 ft). This bottom water may be locally perched or trapped, rather than part of the areal water table. An irrigation supply well located about 0.6 mile downslope to the N-NE (near the bottom terminus of the Rendezvous chairlift) at ~7700 ft elevation had a measured depth to water of about 100 ft, or about 7600 ft elevation. Thus the water table under the peak of Mt. Pluto is likely at >7600 ft elevation; or less than 1,000 ft depth. A reasonable estimate of water table depth under the peak is about 900 ft bgs, or ~7700 ft amsl. However, drilling of the peak well may have short-circuited groundwater flow to depth; therefore the ambient water table at the peak (prior to drilling) may have even been above 800 ft depth.

Mean hydraulic head gradient for groundwater below the peak of Mt. Pluto to the shoreline of Lake Tahoe to the SE (distance ~3 miles , elevation ~6225 ft amsl) is ~ 9.2%. Mean hydraulic head gradient below the peak of Mt. Pluto to the Martis Valley to the north (distance ~4 miles, elevation ~ 5900 ft amsl) is ~ 8.4%. Mean hydraulic head gradient below the peak to the Truckee River valley to the west (distance ~3.5 miles, elevation ~6000 ft amsl) is ~ 9.2%.

T-profile: T profile measurements were performed on a number of dates using several different probes (appendix 2). The large number of measurement dates was required due to slow equilibration time for probe T readings in air (dry hole), equipment problems, and depth limitations of some probe reels. Also, initial measurements indicated that T readings at depths >100 ft bgs were not stable between measurement dates. Additional T-profile measurements were performed to confirm whether or not this apparent instability was real or due to errors in probe calibration or other equipment problems.

Figure 8-3 is a composite T-profile for this well, including data from measurements performed on several dates and using several T probes from July 2002 thru June 2003. A large and deep T inversion is present; T decreases by ~2C from near ground surface to ~300 ft depth. The magnitude of the T inversion is compatible with Ts warming. Ts warming has occurred due to removal of dense forest in the area around the well during construction of the ski runs and peak facilities, and also due to the trend of rise in Sierra Nevada air T over the past few decades or more (see section 6.2 and appendix 5 for effects of Ts warming on T-profiles). The T-profile indicates a large and relatively abrupt change in T gradient near 300 ft depth. Such an abrupt change in T gradient at depth is not consistent with Ts warming alone, and suggests intraborehole airflow may affect the T-profile gradient near 300 ft bgs. During winter, snow covers the

well top (~1 ft above ground surface) thus restricting airflow into the well during winter but not during summer, which may contribute to the deep T inversion in this well. From ~300 ft depth to the well bottom, subsurface T increases, with mean gradient ~0.0021 C/ft, which is very close to the Tahoe Basin ambient air lapse of ~0.0018 C/ft.

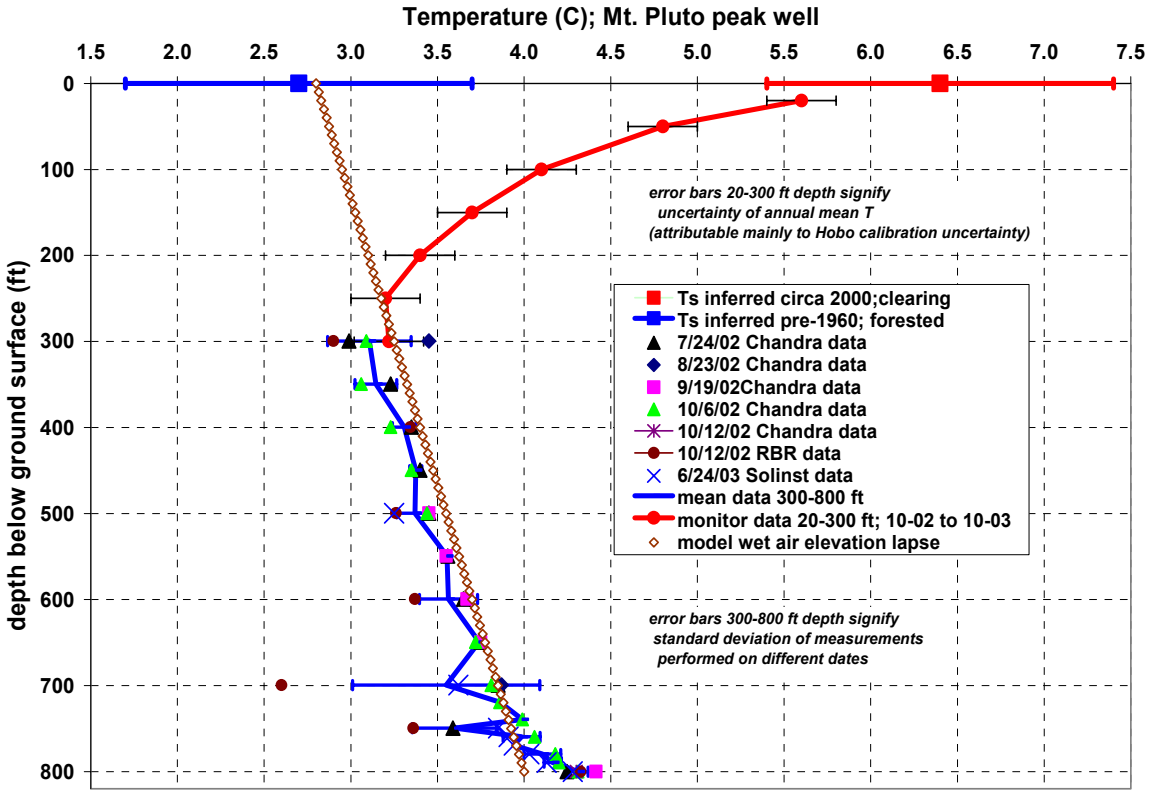

Figure 8-3. Mt. Pluto peak well T measurements, summer 2002 to fall 2003. Mean annual surface T (Ts) inferred based on elevation, observed site surface characteristics and results from our soil T investigation (section 7). Well T was monitored semi-continuously between Oct 2002 and Oct 2003 at many depths between 20 and 300 ft (see figure 8-4); the mean T at each depth is shown. T between 300 and 800 ft depth was measured on multiple dates to check for the presence of apparent temporal changes in T at depth, using several different probe types. Uncertainty in each plotted data point is ~+/- 0.1C (not shown), due mainly to slow equilibration of probes in air. Thus at many depths below 300 ft, apparent differences in T readings of >~0.2C on different dates reliably reflect actual temporal changes in T (see also figure 8-4). The well was a dry well (air in borehole) to ~798.5 ft depth (only bottom readings at ~800 ft are water-submerged).

Figure 8-3 also shows that at most depths, T was apparently not stable between measurement dates. Most of the probes used had calibration confirmed to within +/- 0.02 C accuracy for the T range in this well. Temporal changes in measured T at a given depth were often much larger than this uncertainty in calibration accuracy. Thus the actual well T-profile, from the top to the bottom of the well, was not stable over time, but instead changed between measurement dates.

Long-term T monitoring: To confirm and characterize temporal changes in the T-profile, T was monitored semi-continuously for ~1 year at many depths between ground surface and 300 ft bgs. A Solinst Barologger was used to monitor air pressure and T 20 ft down the well. There was a hole in the well cap, ensuring that the pressure in the top of the well was the same as ambient atmospheric air pressure at the peak during summer months; however during winter snowpack covering the well top (well top was less than 1 ft above ground surface) may often have isolated the well air pressure from rapid response to atmospheric pressure changes. Additional probes used for T monitoring at several depths between ground surface and 300 ft depth included Onset Hobo Water Temp Pros and Onset Temperature Tidbits (see section 5.1). These probes were attached at different places on a length-calibrated line 300 ft long, activated to log T at intervals of 20-30 minutes, and suspended down the well from Oct. 2002 to August 2003. The depth limit of 300 ft was chosen due to practical difficulties in setting up and operating a line of probes longer than 300 ft. Results of this monitoring are shown in figures 8-4 and 8-5 below.

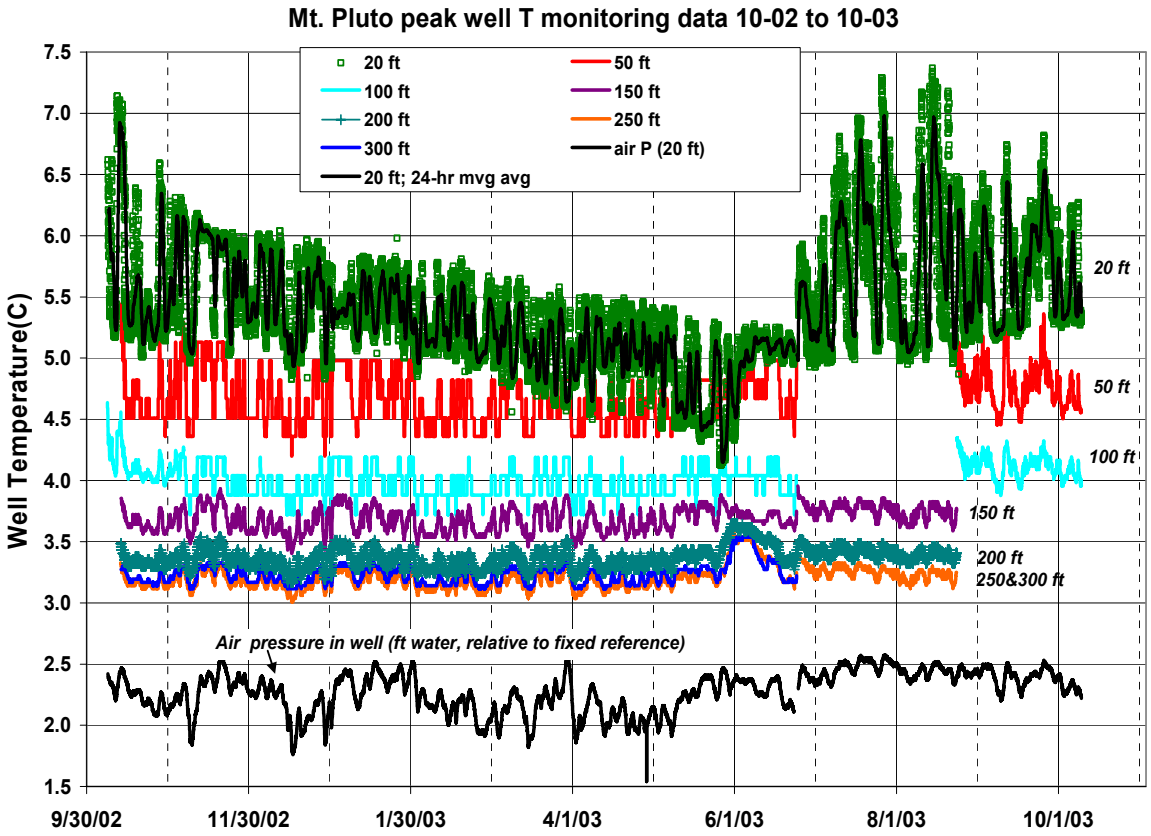

Figure 8-4. Mt. Pluto peak well (dry well) T monitoring data from Oct. 2002 to Oct. 2003. T monitoring data was obtained using either Onset 'Hobos' (fine T resolution) or 'temperature tidbits' (coarse T resolution) suspended at 50 ft depth intervals between 50 to 300 ft depth. Additionally, a Solinst 'barologger' was suspended at 20 ft depth to log air pressure and T. Logging intervals ranged from 15 to 30 minutes.

The monitoring data displays many episodes of synchronous changes in well T with time, logged by autonomous probes at widely different depths from near ground surface to as deep as 300 ft. Many of these changes in T initiated during a change in air pressure.

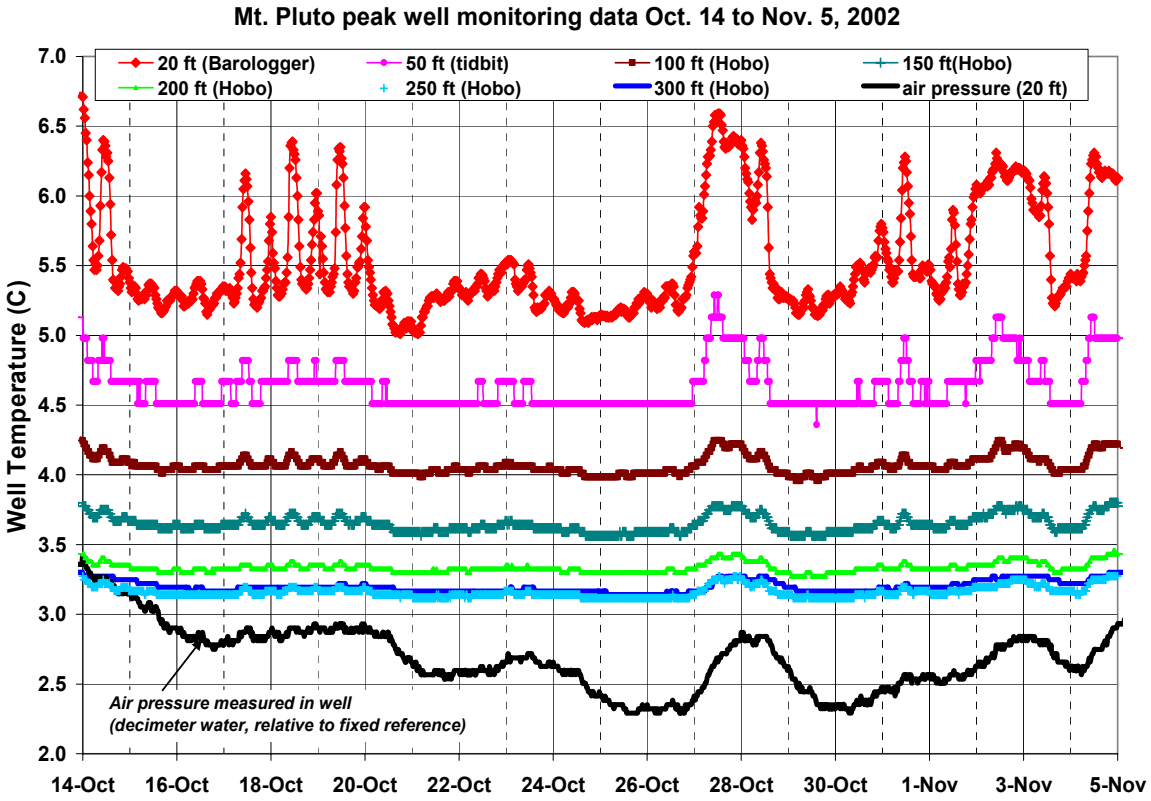

Figure 8-5. Mt. Pluto peak well (dry well) T monitoring data; blow-up of time scale in figure 8-4 from Oct. 14 2002 to Nov. 5 2002. This shorter time scale clearly illustrates that temporal changes in borehole T to 300 ft depth are synchronous with temporal changes in air pressure. Logging intervals ranged from 15-30 minutes. This figure illustrates that borehole T decreases with increasing depth, and that the amplitude of temporal peaks in T decrease with increasing depth. These observations indicate that the direction of airflow is downward during initiation of a temporal peak in T. The T peak occurring about Oct 28 has an amplitude at 250 & 300 ft depths that is much larger than the mean difference in T between 250 and 300 ft depths; indicating that air in the borehole has moved downward by > 50 ft near 300 ft depth during this airflow event.

The only plausible mechanism for the synchronous changes in well T at widely separated depths is intraborehole airflow between the surface and depths of 300 ft or more.

The amplitude of these T oscillations is larger than could be produced by barometric expansion and contraction (causing vertical movement of air) of the column of air within the borehole radius alone, which can move the air only small distances (for 2% change in air pressure, air column near well top would move 0.02*800 ft = 16 ft). An air column movement of >50 ft is required to account for the amplitude of some of the abrupt and synchronous changes in well T. If the well borehole below 300 ft depth is connected to fractures of total volume > several-fold that of the borehole volume; then it

is possible that the column of air in the borehole above 300 ft depth could move more than several-fold further (i.e. >50 ft) in response to atmospheric pressure changes transmitted from the top of the well. Thus it is plausible that the top of the well is the only route for exchange of air between deep sections of the borehole and the atmosphere.

It is also plausible that air travels between the borehole and ground surface thru a fracture network in the volcanic rock that connects deeper sections of the borehole with ground surface below the peak of Mt. Pluto. The amplitude of the T oscillations decreases with depth, indicating that the direction of such airflow is downward from the well top to depths of 300 ft or more.

It should be noted that borehole air movement results not only in advection of heat, but also of moisture: condensation and evaporation of water to/from the probe & borehole surfaces may also contribute to the registered T changes. The occurrence or potential magnitude on registered T of condensation and evaporation (due to borehole air column movements) have not been investigated.

Intra-borehole airflow: In summary, several types of observations together demonstrate significant intraborehole airflow between the top of the well to >750 ft depth:
(i) synchronous changes in well T from near ground surface to 300 ft depth; the deepest depth that was semi-continuously monitored. These changes often coincide with changes in air pressure, and have too large of a T amplitude to be produced by barometric expansion and contraction of the column of air contained within the borehole radius.
(ii) temporal instability (monthly timescale) of entire T-profile to depth >750 ft bgs.
(iii) mean T gradient ~0.0021 C/ft from ~300 ft depth to the bottom of the well (800 ft bgs), which is only slightly more than the Tahoe Basin ambient air lapse ~0.0018C/ft. Such a T gradient in a dry hole is consistent with airflow as the main control on the borehole T gradient.

We have not determined whether the airflow routing is:
(a)Thru-flow of air between the top and deeper sections of the well, and thru fractures that are connected to the surface of the mountain slope and the borehole at depth.
(b) Dead-end barometric pumping of air between the top of the well and into large volume fracture openings located below 300 ft depth in the well. These fracture openings might not be connected to the atmosphere other than thru the borehole up to the well top.

If there is thru-flow routing of air, then the borehole airflow rate must be slow, since even during periods of warm summer weather the borehole remains cool (Figure 8-4). A detailed analysis of the existing well T monitoring data might help in better evaluating the likelihood of each of these two hypotheses for airflow routing.

The hydraulic significance of these findings is summarized as follows: the very deep water table below the peak of Mt. Pluto suggests good groundwater drainage, and thus significant permeability of the volcanic bedrock to depth >800 ft bgs. The small T gradient from ~300-800 ft bgs is attributable in part to borehole airflow; but is also likely attributable in part to downward groundwater percolation (above water table) in the formation to depth below the bottom of the borehole, resulting in downward advection of some of the upward ambient conductive geothermal heat flow. Observations of well T show that airflow is often present in the borehole, and implicates a fracture or fracture network at depth that is connected to the borehole. It is not clear whether the airflow route is thru-flow or dead-end barometric pumping. In either case, significant fracturing of bedrock at depth is implicated, suggesting significant hydraulic permeability of the volcanic bedrock to depth at the borehole scale.

8.4: Clear Creek fan: groundwater discharge from deep bedrock: A piezometer nest emplaced by USGS researchers is located near the apex of the Clear Ck alluvial fan at the eastern base of the Carson Range, near the southeast border of the Eagle Valley and of Carson City, NV (Fig 3-1). A local site map and cross-section is shown below:

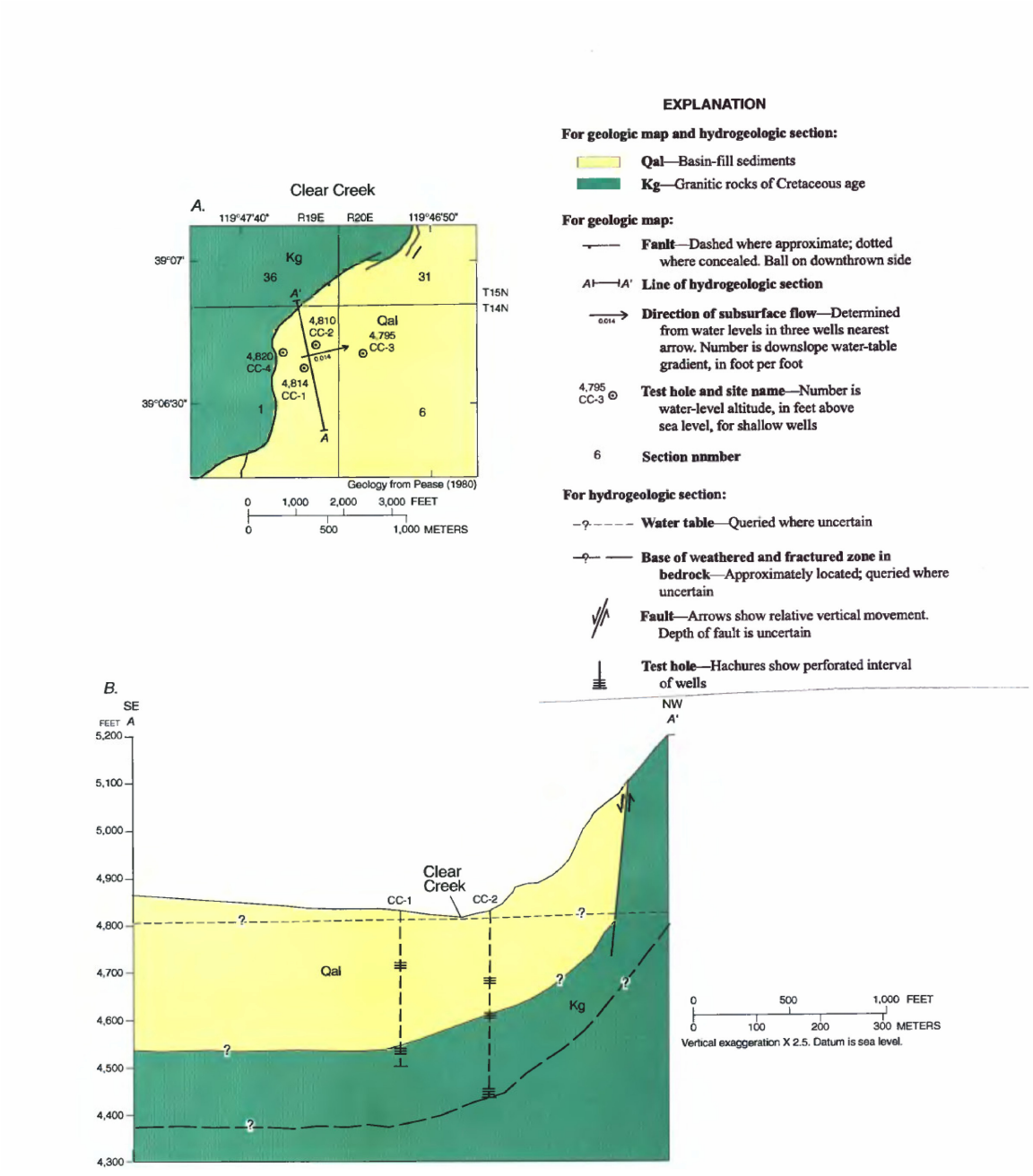

Figure 8-6. A) Plan view of upper portion of Clear Ck alluvial fan, located at base of Carson Range near Carson City and Highway 50 (Fig. 3-1). Shows location of wells, direction of groundwater flow, and surficial geology. B) Cross-section thru transect A-A' from upper diagram, showing locations of Clear Ck, piezometer nests, screening depths, and depth to granitic bedrock. Map copied from Maurer and Berger (1997).

This area of Clear Ck is located about 5 miles east of the eastern boundary of the Tahoe Basin, and is lower in elevation (4800 ft amsl) and dryer (mean precipitation ~14 inch/yr) than the Tahoe Basin proper, but shares the bedrock geology of the Carson Range with the eastern side of the Tahoe Basin. The piezometer nest is located about 700-1000 ft off the base of steep mountain-front slopes to the west and northwest (Fig 8-6), and about 150 ft from the Clear Ck channel. Clear Ck flows perennially most years, with mean annual flow ~4,000 acre-ft/yr, and wide seasonal and inter-annual variation in flow rate. The water table has been shallow in this area of the Clear Ck alluvial fan (<20 ft bgs).

The piezometer nest is designated 'CC-2 test hole' and described in detail by Maurer and Berger (1997). The deepest piezometer tube is 400 ft deep, thru about 230 ft of alluvial sediments ranging from clayey sand to sand and gravel, and about 170 ft of fractured granitic bedrock, most of which is weathered (decomposed) and friable. This deep tube is gravel-packed from 375–400 ft bgs, and screened from 389-399 ft bgs.

The USGS has thoroughly characterized the groundwater hydrology in this area using standard hydraulic, hydrologic, and geophysical methods (Maurer and Berger, 1997 and Maurer and Thodal, 2000). The water table has been shallow near the well, ranging from about 11 to 13 ft depth bgs during 1996 (Maurer and Berger, 1997) and also in 2001 and 2002, according to several sounder measurements we performed. An exception was a water table of 7 ft bgs during late May 2001, a warm day in the snowmelt season. The lateral hydraulic gradient was determined by the USGS as ~1.5% downward to the East in this area of the Clear Ck alluvial fan, at all depths from the water table to 400 ft bgs.

Hydraulic estimate of Vz: The vertical hydraulic gradient from ~230 to 400 ft depth was measured using water levels in the bottom two piezometers (one screened at bedrock top near 230 ft depth) in the CC-2 test hole by the USGS during 1996, and by us using several sounder measurements from 2000 thru 2002. The vertical hydraulic head gradient in the fractured granitic bedrock ranged from 0.25% to 0.60% (upward) between measurement dates, with mean ~0.40% upward.

The USGS performed resistivity vs. depth measurements in the CC-2 and other test holes in the area, and calibrated the results to slug test results from numerous area piezometers, yielding continuous estimates of Kx with depth (Maurer and Berger, 1997). Using these results for the 170 ft of fractured granitic rock spanned by the CC-2 test hole, arithmetic mean Kx ~2.8 ft/day and harmonic mean Kz ~ 1.7 +/-0.7 ft/day.

Thus the hydraulic estimate of lateral Darcy velocity Vx in the granitic bedrock is computed as (2.8 ft/day)*(0.015) = 15 ft/yr = Vx. The vertical Darcy velocity Vz in the granitic bedrock is computed as (1.7 ft/day)*(0.0040) = 2.5 ft/yr (upward) = Vz. Given the uncertainty in the estimates of the vertical hydraulic gradient and of Kz, the hydraulic estimate of Vz ranges from 0.9 ft/yr to 5.2 ft/yr upward.

Thermal estimate of Vz: An independent estimate of Vz in the fractured granitic bedrock is performed here using thermal data alone, as described in section 6.4. All or parts of the T-profile in the CC-2 test hole were measured several times during 2000, 2001, and 2002. Figure 8-7 below shows the deep half of the T-profile measured in this well; within the granitic bedrock logged from 230 to 400 ft depth bgs. Figure 8-7 also shows several Bredehoeft curve model T-profiles (see section 6.4) resulting from selection of several different values of Vz in the granitic bedrock at 230-400 ft bgs. There is no independent data for the bulk thermal conductivity λ of the fractured granitic rock. Because the granitic bedrock is described by Maurer and Berger (1997) as extensively fractured and weathered (decomposed), and friable in many depth intervals, it is assumed that λ is

intermediate to that typical of unweathered crystalline granitic rock (λ ~ 3.0 W/m/C from Schon, 1996) and granitic sediment of porosity 25% (λ ~ 2.0 W/m/C). Thus it is estimated that for the weathered granitic sediments from 230-400 ft bgs, λ = 2.5 +/- 0.5 W/m/C. Thus from methods, for a vertical length L = 170 ft, Vz = (1.19 +/- 0.24 ft/yr)*β, where β is the curve-fit parameter. From figure 8-7 it is evident that a good match to the T data occurs for β ~0.84, yielding Vz = 1.0 +/- 0.2 ft/yr.

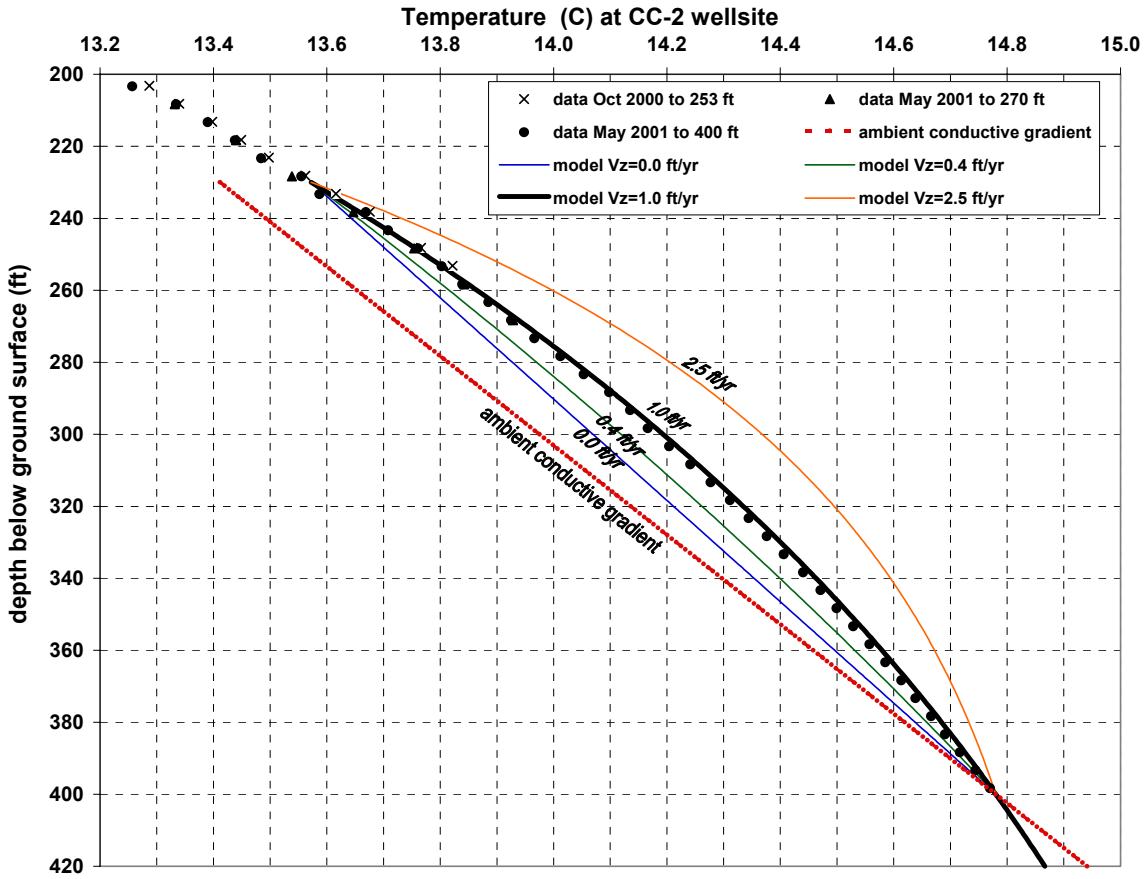

Figure 8-7. T-profile data in deep half of CC-2 well, and model T-profiles. Model T-profile depth spans from the granitic bedrock contact (~230 ft depth) to bottom of well (~400 ft depth). Model T-profiles computed as described in section 6.4 using thermal parameter values from section 8.4, shown for Darcy flow rates of 0.0 (conductive heat flow), 0.4, 1.0, and 2.5 ft/yr of groundwater flow upward in the depth interval 400 to 230 ft bgs. This graph shows good fit of T-profile data to model with 1.0 ft/yr of upward groundwater flow. The graph also shows that near 400 ft depth the observed T gradient is substantially smaller than the purely conductive T gradient; indicating that upward groundwater flow originates below 400 ft depth.

This thermal estimate for Vz of 1.0 +/- 0.2 ft/yr is near the low end of the range of the independently determined hydraulic estimate of 0.9 to 5.2 ft/yr for Vz. The discrepancy in Vz estimates could be due to anisotropy in permeability (Kz<Kx) in either the weathered or unaltered intervals of granitic bedrock, resulting in overestimation of the hydraulic result for Vz. Additionally or alternatively, the discrepancy could result from

possible significant lateral T gradients associated with the lateral component of groundwater flow in bedrock (see section 6.4), which could result in underestimation of the thermal result for Vz. The best estimate is judged to be Vz~1.5 ft/yr upward, close to the thermal result for Vz, since lateral T gradients are likely to be small at depth, and Kz<Kx is not unusual (for Vz~1.5 ft/yr upward, Kz~0.6*Kx).

T gradient at 400 ft depth: Figure 8-7 above also shows the slope of the conductive T profile in the bedrock for ambient geothermal heat flow upward from depth; from $dT/dz = Q/\lambda$; where ambient heat flow Q ~ 66 mW/m2 (see section 8.1; note this value of Q does not account for topographic focusing of ambient geothermal heat flow toward the edge of valley areas that normally occurs, which results in enhanced heat flow) and λ = 2.5 W/m-^{o}C; resulting in dT/dz = 0.00805 C/ft. If upward groundwater flow originates at or above 400 ft depth; this large T gradient would be present near 400 ft depth. However, the measured T gradient near 400 ft depth is substantially smaller, indicating that upward groundwater flow originates at depth below 400 ft; and not at or above 400 ft depth.

Upper half of T-profile: Figure 8-9 (section 8.5) shows that the shape of the T-profile above the weathered bedrock, within the granitic sediments from ~50 to 230 ft depth, is also concave down; even though the hydraulic gradient direction in the sediments is downward (Maurer and Berger, 1997) rather than upward. For 1-D heat and groundwater flow, downward groundwater flow is associated with a concave-up T-profile (Bredehoeft and Papadopolus, 1965). The observed concave down profile above 230 ft depth is likely attributable in part to the gradual transition from sediments to fractured rock with depth described by Maurer and Berger (1997), which would cause a gradual decrease in λ and thus a gradual increase in dT/dz with decreasing depth in the sediments above 230 ft depth. Also, a 1-D approximation of heat flow may not be accurate in the sedimentary layers, because: (i) the sedimentary layers are shallower and more exposed to areal heterogeneity in Ts. (ii) the T-profile in the sedimentary layers is likely more affected by lateral groundwater flow, since the ratio Vx/Vz in many of these sedimentary layers is larger than in the bedrock layers. Cool streamflow infiltration nearby (downward and lateral components) complicates interpretation of the shape of the upper half of the T-profile (see section 8.5).

In summary, the observed deep half of the T-profile in granitic bedrock at the CC-2 site is used in an established 1D model of heat flow; yielding a vertical advective heat flow rate with associated Vz upward in the granitic bedrock that is within the lower end of the range of an independently determined standard hydraulic estimate of Vz. The small discrepancy between the two estimates is likely due to anisotropy in permeability (Kz<Kx), and possibly also to a significant lateral T gradient at depth. The small vertical T gradient near 400 ft depth shows that the upward groundwater flow does not initiate at or above 400 ft depth; but significantly below 400 ft depth. These observations indicate significant amounts of groundwater flow in the granitic bedrock below 400 ft depth in this area of the Clear Ck alluvial fan. It is plausible that such deep bedrock flow originates from deep recharge into the nearby high elevation mountain-block areas.

8.5: Clear Creek fan: groundwater recharge and thermal energy balances: The dominant sources of groundwater recharge in the area of the Clear Ck alluvial fan upgradient from the CC-2 well site to the mountain-front are determined using thermal and hydraulic data and the groundwater mass balance. The T-profile is used to check the consistency of the groundwater mass balance with the thermal energy balance. The 3D subsurface domain for both the groundwater mass balance and subsurface thermal energy balance underlies the ~60 acre land surface area between section A-A' (Fig 8-8) and the mountain-front, with depth extending from the water table (~12 ft bgs) to the bottom of the CC-2 well (400 ft depth bgs).

Groundwater recharge sources are classified as follows:
(1) precipitation recharge: distributed over alluvial fan (into top of aquifer).
(2) infiltration of Clear Ck: along axis of fan (down into top side of aquifer; then lateral).
(3) mountain-slope recharge: groundwater flow initiating in the mountain slope and flowing thru fractured bedrock (laterally into upgradient side of alluvial fan aquifer).
(4) mountain-block recharge: up from granitic bedrock at depth (into bottom of aquifer).

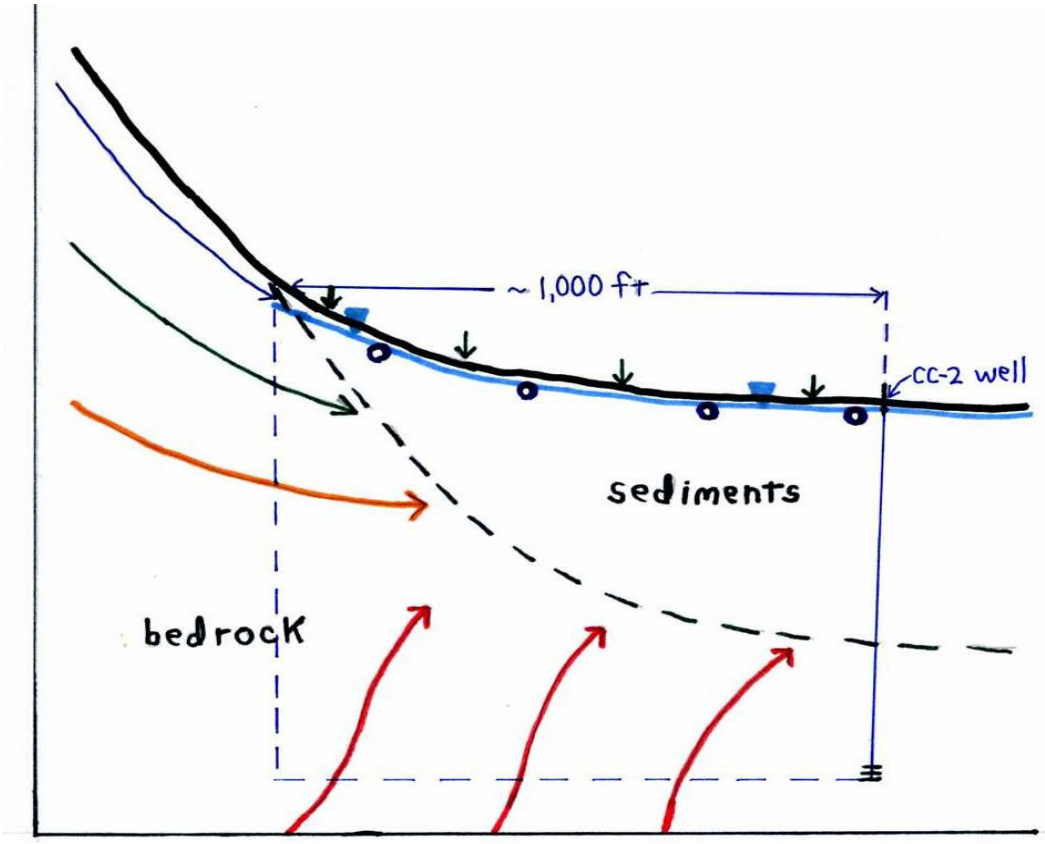

Figure 8-8. Schematic cross-section of model domain for thermal energy and groundwater mass balances at Clear Ck. Vertical scale exaggerated. Domain is bounded by water table on top, well on right (valley) side, and dashed lines at bottom (400 ft depth) and left (mountain-front) sides. Arrows denote groundwater recharge sources for the domain. Groundwater enters the domain from the top (percolation of cool precipitation and snowmelt), left side (cool to warm mountain-slope recharge), and bottom (warm mountain-block recharge). Also cool recharge from Clear Ck. occurs (denoted as blue circles under water table); initiating as vertical infiltration in the streambed and spreading laterally in the shallow subsurface. Heat energy flows across domain boundaries by advection with moving groundwater, and also by conduction down T gradients.

Groundwater Balance: The estimated subsurface outflow is ~1,000 acre-ft/yr from the upper part of the Clear Ck alluvial fan (Maurer and Berger, 1997). Maurer and Thodal (2000) conclude this flow is fairly steady, varying by ~20% between dry and wet years.

Distributed recharge of precipitation in this area has been estimated as <0.1 ft/yr (Maurer and Thodal, 2000). Thus annual precipitation over the 60 acre top surface of the domain supplies <6 acre-ft yr to recharge of the water table, accounting for at most only ~0.6% of the total estimated subsurface flow.

Previous investigations indicate there is about 500 acre-ft/yr of Clear Ck stream infiltration within ~0.5 mile upgradient from the CC-2 site (Maurer and Thodal, 2000), sufficient to supply ~50% of total estimated subsurface flow.

The presence of mountain-block discharge upward into the aquifer is shown by the observed hydraulic gradient upward from depth; with Vz estimated using either hydraulic or independent thermal data as described in section 8.4. The estimated Vz is ~1.5 ft/yr from depth near CC-2. There is likely several-fold higher upward discharge rate Vz at the break in slope at the toe of mountain-front 1,000 ft upslope (see section 9.2). A mean Vz of 3.0 ft/yr upward from deep bedrock into sediments between transect A-A' (figure 8-6, runs near the CC-2 site) and the upgradient mountain-front yields ~180 acre-ft/yr of recharge. Thus flow from mountain block deep bedrock is estimated to supply ~18% of the total estimated subsurface flow.

Summing these amounts, about 686 acre-ft/yr, or ~69% of the total estimated subsurface flow is accounted for by recharge into the top and bottom sides of the Clear Ck. alluvial fan. The remaining 314 acre-ft/yr (~31%) must recharge into the sides of the domain at the upgradient edges of the alluvial fan, from subsurface flow in the neighboring mountain slopes to the west and northwest.

Thermal energy balance: A thermal energy balance on groundwater flow is performed in the remainder of this section, using the above estimates of groundwater recharge. The measured T-profile is used together with estimated temperatures and quantities of each recharge source, and estimates of conductive heat flow into the aquifer to define a 'black-box' macroscopic steady-state thermal energy balance on advective and conductive heat flow crossing the boundaries of the domain (see section 6.5):

$$\int_{Aad,out} [Q_{ad,out}]dA = \int_{Aad,in} [Q_{ad,in}]dA + \int_{Ac} [Q_c]dA$$

In the equation above, the Q symbols denote thermal energy flux (energy/time/area) and the A symbols denote boundary surface areas of the domain (units L^2). Subscripts: 'ad' = advection, 'c' = conduction, 'in' = into domain, 'out' = out of domain.

Surface and shallow subsurface T: Mean annual air T (Ta) at Carson City was 10.2C from 1948-2006 (WRCC, Station 261485). For scrub and chaparral vegetation, which has covered most of the alluvial fan area, our Tahoe surface T investigation (see section 7.4) indicates that Ts (mean annual surface T) is likely ~1.5 to 3C warmer than Ta. Other wells we investigated near Carson City with similar areal vegetation have T-profiles (not shown) that indicate Ts is in the range ~11.5C to 13.5C. It is estimated that in the area near the CC-2 site, Ts = 12.5 +/- 0.7C, which is 2.3 +/- 0.7C higher than Ta.

This estimate for Ts is consistent with shallow subsurface T monitoring data at the CC-2 site. Several small, robust temperature sensors with automated datalogging ('temperature tidbits', Onset Corp, see section 5.1, appendix 2) were suspended in the CC-2 well at depths between 6 ft and 18 ft bgs from July 2001 thru October 2002. These

sensors successfully logged T semi-continuously over the period of deployment. Figure 8-9 shows mean annual T data from these sensors at 6,10,12,14,16, and 18 ft depth bgs. Mean annual T at each depth is defined as the average of peak summer T (mean of peak T for summers 2001 and 2002) and the low T for winter 2001/02. Figure 8-9 shows mean annual T decreases monotonically from 6 to 18 ft depth from ~12.7C to ~11.0C; presumably due to the cooling effect of lateral dispersion of Clear Ck streamflow infiltration in the shallow subsurface. Tidbit monitoring data for mean T at 18 ft depth matches closely with mean T from two T-profile measurements at 18 ft depth performed ~5 months apart (Fig 8-9).

T-profiles: Figure 8-9 below shows the complete T-profiles of the CC-1 and CC-2 wells, using depth vs. T measurements performed during fall and spring seasons, and the tidbit monitoring data at shallow depths in CC-2 described above.

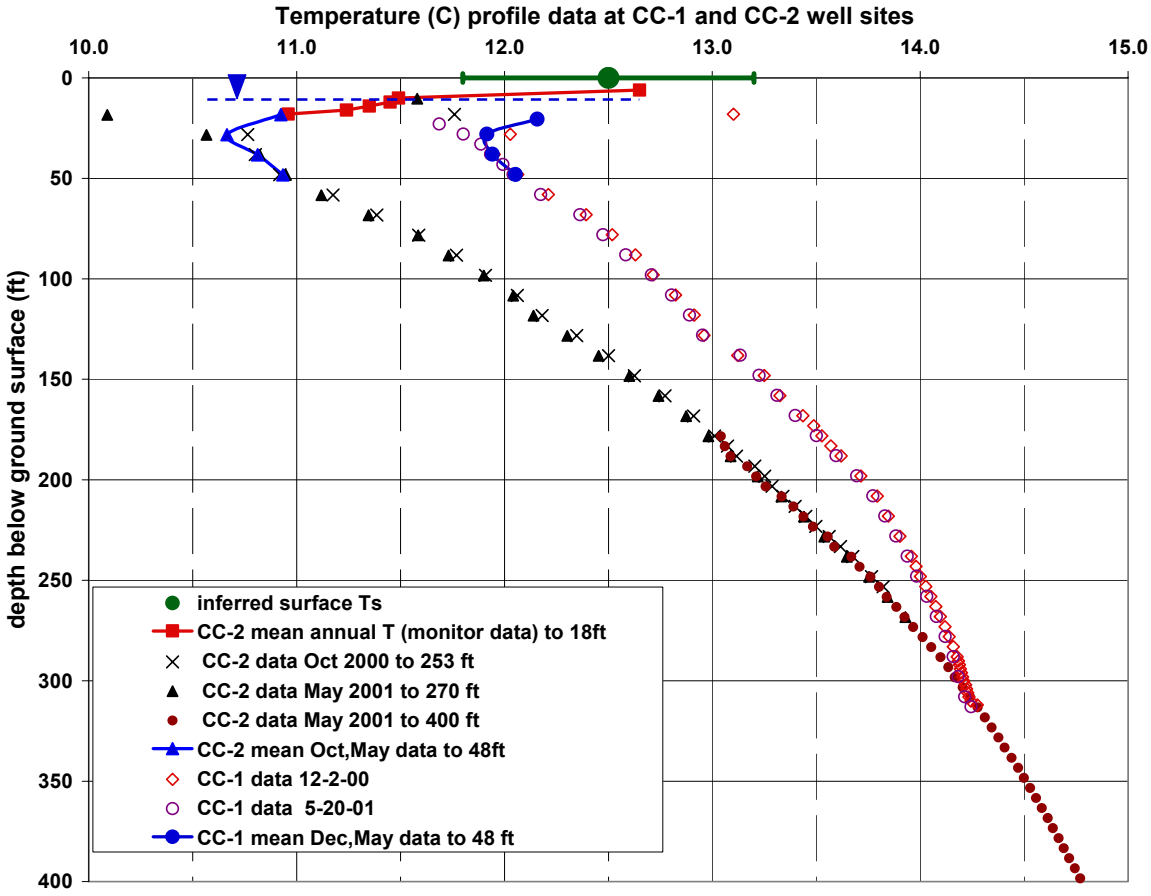

Figure 8-9. Complete T-profile data for CC-1 and CC-2 wells (locations shown figure 8-6). Mean annual surface T (Ts) inferred based on site elevation and surface radiation exchange parameters, using results from section 7. This inferred Ts is seen to be consistent with results of shallow T measurements/monitoring. Two T-profiles at each well were measured about ½ year apart, thus the mean of the T data at shallow depths is likely very close to the mean annual T at these depths (confirmed in CC-2 well by semi-continuous data logging for ~1 year). A shallow, sharp T inversion is present at both well sites, attributed to infiltration of Clear Ck streamwater (see text). Granitic bedrock at the CC-1 site is located at ~295 ft depth, whereas bedrock is substantially shallower (~230 ft bgs) at the CC-2 site. The T gradient near the bottom of each well is small, indicating substantial groundwater flow in the bedrock below the bottom of each of these wells.

Below about 40 ft depth, there was no change (<0.1C) in the T-profiles between seasonal measurement dates. Thus the depth of seasonal surface T damping is ~40 ft bgs in this area. Note that shallow (~25 ft bgs), sharp T inversion at these wellsites, which can be accounted for only by shallow cool groundwater flowing laterally to the area near these wells. The CC-1 T-profile was about 1C warmer than in CC-2 from 20 ft to 50 ft depth, consistent with CC-1 being located further from Clear Ck (~300 ft) than CC-2 (~150 ft), and thus less influenced by cool infiltration of Clear Ck.

Another USGS test and monitoring well (Kings 1) in the mountain-front area near Carson City has a T-profile indicating a very shallow T inversion, consistent with shallow recharge of nearby cool streamflow. Other wells in Kings, Ash, and Vicee Canyons have T-profiles (not shown here) displaying deeper T inversions, attributable to deeper recharge of more distant stream infiltration, or another source of cool recharge originating near the mountain-front or mountain slopes.

CC-1 is the same temperature as CC-2 at 320 ft depth. Note the very small T gradient near the bottom of CC-1, which terminates within the top of the granitic bedrock, indicating substantial groundwater flow upward from the underlying bedrock.

Outgoing Advection of Heat: In order to compute the thermal energy balance on groundwater in the domain, the rate of heat energy exiting the domain by advection with groundwater needs to be estimated. This requires that the groundwater flow rate averaged T (Tg) of the subsurface be estimated where the groundwater exits the domain:

$$Tg = \int_{12\,ft}^{400\,ft} [T(z) \bullet Vx(z)]dz \,/ \int_{12\,ft}^{400\,ft} Vx(z)dz$$

Groundwater exits the domain laterally across transect A-A' (Fig 8-6), near the CC-1 and CC-2 test well sites. The lateral groundwater velocity profile with depth Vx(z) was roughly estimated using Vx estimates from Maurer and Berger (1997) for transect A-A'. On average, Vx is larger in the sediments than in the granitic bedrock; thus shallower portions of the T-profiles influence Tg more than deeper portions of the T-profiles. The resulting estimate is Tg ~ 13.0 +/- 0.4C from the water table (~12 ft bgs) to 400 ft depth.

Incoming Advection of Heat: The T of distributed precipitation recharge to the water table is close to the mean annual T at the top of the water table, which is ~11C at the CC-2 site (fig) and ~12C at the CC-1 site (not shown). There is likely substantial areal heterogeneity in water table T over the 60 acre domain, and thus uncertainty in any estimate of the areal annual mean water table T. However mean areal annual water table T likely falls in the range ~9.5C (mean stream infiltration T) to ~12.5C (Ts).

For the perennial lush vegetation and shading near Clear Ck (willows line the channel), results for our Tahoe surface T investigation (see section on results for surface T) indicate that Ts in and near the stream channel falls between Ta to Ta-1C. Since Clear Ck emerges from a narrow canyon at a steep slope, it is estimated that mean annual stream recharge T ~9.5C, lower than Ta by ~0.7C.

The CC-2 well T gradient shows that T of mountain-block recharge upward at 400 ft depth is 14.75 C near the CC-2 well site. However, numerical modeling indicates that it is likely that T at depth is significantly warmer closer to the break of slope at the mountain-front (associated with higher discharge rate near the mountain front; see results for numerical modeling). The difference between shallow subsurface T and T at 400 ft depth may be on average as much as 2-fold higher (average between CC-2 site and the

mountain-front); thus mean T at 400 ft depth between CC-2 and the mountain-front is likely between ~15C and ~19C.

Using the volumetric water recharge rates and associated recharge temperatures above, simple mixing of these recharge waters yields Tmix = 10.8C to 11.8C; which is cooler than estimated Tg = 12.6 to 13.4 C.

Conduction of Heat: In addition to advection of heat with recharge water, heat energy flows into the domain by conduction across the domain boundary surfaces. The heat energy flux Qc conducted into the domain across any boundary is determined using Fourier's Law of heat conduction $Qc = \lambda*(dT/dz)$. The amount of warming ΔT of 686 acre-ft/yr of water (estimated amount of recharge into top and bottom surfaces of domain, from above) resulting from a heat flux Qc is $\Delta T = Qc*Ac/(\rho_w*C_w*686 \text{ acre-ft/yr}) = 8.918x10^{-6} (^oC/W)*Qc*Ac$ where Ac is the area over which Qc flows into the domain.

At 400 ft depth in the granitic bedrock at the wellsite, λ ~2.5 W/m/^{o}C and dT/dz ~ 0.0049C/ft, thus Qc ~ 0.0402 W/m^2. As noted earlier, it is likely that heat flow is enhanced several-fold as the mountain front is approached from the CC-2 well site. Thus between the well site and the mountain-front, the mean dT/dz could be as much as ~2x that at the CC-2 site; thus mean Qc is likely in the range 0.0040 to 0.0080 W/m2. For the 60 acre area of the bottom of the domain, this corresponds to a total areal thermal power inflow of 9,760 to 19,520 W; or ΔT = 0.09C to 0.17C.

The observed T gradient near the water table (~12 ft depth bgs) is much larger than at 400 ft depth; due to the presence of the sharp and shallow T inversion the amount of thermal conductive energy input from the ground surface is unusually large. In the shallow sediments near and below the water table, it is estimated that the porosity is ~35%, thus λ ~ 1.7 W/m/^{o}C. At the CC-2 well site near 12 ft depth bgs the T gradient (see fig) is ~0.10 C/ft, thus Qc ~ 0.558 W/m^2. However, the CC-2 well site is only ~150 ft from the Clear Ck streambed; whereas the mean distance to the streambed is ~600 ft over the domain. Since Clear Ck infiltration is the likely source of the T inversion, it is likely that this inversion is weaker at further lateral distances from the streambed. It is estimated that over the area of the domain, the mean T gradient near the water table is about 1/2 to 3/4 that observed at the CC-2 site; thus over the top of the domain, mean Qc ~ 0.28 to 0.42 W/m2. For the 60 acre area of the bottom of the domain, this corresponds to a total areal thermal power inflow of 67,800 to 101,600 W; or ΔT = 0.60C to 0.91C.

Heat conduction across the lateral edges of domain is likely negligible, due to predominant vertical orientation of T gradients near the edges of the domain, and the small surface area of the cross-sectional area of the domain relative to plan view.

Summing the quantities of conductive heat flow in from the top (~12 ft bgs) and bottom (400 ft bgs) of the domain, this heat energy warms 686 acre-ft/yr of water by 0.69C to 1.08C. Adding this to Tmix yields a mean subsurface T of 11.5 to 12.9C. The upper end of this range overlaps the range of Tg = 12.6 to 13.4C.

Mountain-slope advection: The only remaining component in the thermal energy balance is heat advection from the upgradient lateral edge of aquifer (mountain-slope recharge). The water balance indicates mountain-slope inflow accounts for ~32% of water inflow to the domain. This lateral water inflow will also contribute thermal energy to the domain if it enters the domain at moderate depth. From above, the amount of cooling or heating needed in the domain ranges from -0.3C cooling to +1.9C warming. This cooling or heating is provided by mountain-slope recharge. The T of this recharge is somewhere in the range 12C<Ts<13.4C + (1,000/320)*1.9C, or <13.4C+5.9C = 19.3C. Recharge water

with T ~12C can be provided by shallow mountain-slope flow (mean depth <50 ft bgs), whereas recharge water with mean T ~19 C requires deep mountain-slope flow (mean flow depth ~500 ft bgs). Thus mean depth of mountain-slope flow is somewhere between ~50-500 ft bgs in order to close the estimated thermal energy balance in the domain.

In summary, hydraulic and thermal data show mountain-block recharge upward accounts for ~18% of groundwater flow in the upper portion of the Clear Ck alluvial fan, and streamwater infiltration ~50%. The remaining ~32% of groundwater recharge is attributed to lateral inflow from the neighboring mountain slopes. These estimates of groundwater recharge are consistent with the thermal energy balance and the measured T-profiles at the CC-1 and CC-2 well sites. If the ratio of streamwater infiltration to mountain slope plus deep bedrock groundwater discharge upward into the aquifer was substantially higher than 1:1, the mean T of the T-profiles would be cooler than observed (insufficient heat energy). If this ratio was substantially smaller than 1:1, the mean T of the T-profiles would be warmer than observed (excess heat energy). Previous USGS estimates of volumetric quantities of Clear Ck streamflow infiltration (Maurer and Thodal, 2000) are additionally supported by the thermal data and analyses presented here.

A substantial amount of warm groundwater recharge from depth is needed to account for the observed heat energy in the T-profiles. There is not nearly enough ambient conductive geothermal heat flow upward from depth to warm the cool, proximal stream recharge to the temperatures observed in the T-profiles. However, advective heat flow upward from the underlying granitic bedrock provides about half or more of the needed heat. A significant amount of heat is conducted downward from ground surface, opposite to the typical upward direction of conductive heat flow due to shallow cooling resulting from nearby Clear Ck streamwater infiltration. A small cooling to moderate amount of warming may be advected in with shallow to deep (~50-500 ft mean depth bgs) groundwater flowing sublaterally down neighboring mountain slopes and recharging the alluvial fan laterally at the mountain-fronts. A significant amount of mountain-slope recharge (~1/3 of total groundwater recharge) is consistent with both the water balance and energy balance in this area of the Clear Ck alluvial fan. More field investigation would be required to determine the temperature and depth of this mountain-slope recharge.

8.6 Results for Granitic Bedrock Well Investigations: Overall, the field measurements of T-profiles were successful. Accurate, precise, high-quality T-profiles were obtained for each of the 4 granitic bedrock wells profiled. T-profiles for each of these wells are presented graphically in appendix 5, together with detailed analyses and interpretation. Some hydraulic parameters are presented in table 8-1 below.

Available water level data indicates that seasonal variation in static water levels in these hardrock wells has been less than 10 feet. Water elevations measured in the deep high elevation hardrock wells (Echo Pass and Heavenly Gondola) are likely lower than areal water tables. Vertical hydraulic gradients are large in these high elevation areas, and the well installation has short-circuited the formation to depth in the vicinity of these wells. During drilling it was noted that the water level in the Heavenly Gondola well dropped substantially as drilling progressed to depth. The water level also dropped substantially post-drilling in the low-permeability Echo Pass Well. Well pump test data were used to compute specific capacity, and to estimate lateral hydraulic conductivity (K_h). As detailed in appendix 5, several methods of analysis were applied to pump test

data for each of the deep bedrock wells (Echo Pass and Heavenly Gondola); these methods all yielded comparable estimates of K_h. The table above shows that specific capacity and K_h values for bedrock well sites are small, below the range of values for well sites in valley-fill sediments in the South Tahoe area (Bergsohn et al, 2007), with the exception of the Heavenly Gondola well. Specific capacities of all the bedrock wells fall within a range typical for granitic bedrock in the Sierra Nevada (Davis and Turk, 1964), with the exception of the remarkably high specific capacity measured for the Heavenly Gondola well. The Heavenly Gondola well has exceptionally high specific capacity and K_h for a deep bedrock well. As detailed in appendix 5, this is attributable to intersection of the borehole with a fault zone at depth, as inferred from the drilling log and indicated by the presence of a fault mapped striking within several hundred yards from the well site and dipping toward the well.

Table 8-1: Hydraulic Parameters for Wells Completed in Granitic Bedrock in South Tahoe area

Parameter	Ralph	Big Meadows	Echo Pass	Heavenly Gondola
Ground surface elevation (ft amsl)	6360	7300	7385	9170
Well depth (ft bgs)	230	110	1040	995
Mean static water level (ft bgs)	~10	~12	~315	~835
specific capacity (gpm/ft drawdown)	0.47	0.061	0.0071	2.0
K_h (ft/day)	~0.080	~0.013	~0.005	~3
Recharge rate to depth (ft/yr)*	-	-	<0.03	<1.5
K_z (ft/yr)	-	-	<0.3**	NB

* Recharge estimates based on analyses of temperature data
** For depths below 450 ft bgs; upper bound from vertical flow (recharge) rate bound
NB: not well-bounded between ground surface and deep fault zone

The groundwater recharge rate to depth and vertical hydraulic conductivity K_z can often be estimated using T-profile data: the T-profiles in the deep Echo and Heavenly wells are each related to the vertical groundwater recharge rate v_z to depth >500 ft in granitic bedrock. From the estimated upper limit of v_z and estimate of vertical hydraulic head gradient, K_z is bounded for the Echo pass well. T-profiles in the Big Meadows and Ralph wells indicate the presence of substantial advection of heat by sub-lateral (downward) groundwater flow near or below the bottoms of these wells; however recharge rates to depth cannot be estimated with confidence. A brief summary of main findings for each of these hardrock wells is presented below (see appendix 5 for details):

Big Meadows well: The observed deep T inversion is attributable in part to gradual surface T warming over the last several decades. However, the inversion is also caused in part by diversion of conductive geothermal heat flow from the well area, due to sub-lateral flow in the lower portion of the borehole sourced from higher elevation recharge, or sub-lateral to vertical groundwater flow below the bottom of the well.
Ralph well: The small and staggered T gradient in this well indicates sections of intraborehole flow in this well; and also indicates diversion of conductive geothermal heat flow by either appreciable bedrock recharge in the vicinity of this well site, or by downward groundwater flow to depths far beneath the bottom of this well.

Echo Pass well: The deep half of the T-profile for the Echo Pass well provides a calibration point for regional geothermal conductive heat flow from depth for the South Tahoe Basin region, as described in section 8.1. Below 450 ft depth, the slight concave up curvature of the T-profile can be fit by Taylor expansion of the Bredehoeft relationship; yielding stringent limits on recharge rate to depth below ~450 ft depth, including groundwater flow deep beneath the bottom of the well. Above ~450 ft depth, the curved shape of the T-profile is attributable to Ts changes and to vertical or significant lateral groundwater flow in the shallower bedrock above 450 ft depth.
Heavenly Gondola well: Hydraulic tests together with drillers log descriptions and the presence of a nearby fault together demonstrate very high permeability at over 800 ft depth within granitic bedrock, attributed to a permeable fault zone intersected by the borehole at depth. An upper limit on vertical recharge in granitic bedrock between ground surface and the deep fault zone is estimated based on well T data and inferred surface T. Additional borehole T data at depth, used in numerical modeling of heat and groundwater flow that accounts for fault geometry, could enable more accurate estimates of the rate of groundwater recharge to depth near this well, for bulk bedrock and for the fault zone.

In summary, T-profile shapes for the Heavenly Gondola, Big Meadows, and Ralph wells each indicate the presence of substantial groundwater flow rate in granitic bedrock to depths near or significantly below the bottom of the well in the area of the well. In contrast, the Echo Pass well T-profile indicates very little groundwater flow in granitic bedrock below ~450 ft depth, including deep below the bottom of the well. T-profiles indicate that mean areal vertical recharge rate (Darcy velocity) to depth >800 ft bgs in high elevation granitic bedrock is <0.03 ft/yr in the contributing area of the Echo Pass well, but possibly as much as ~1.5 ft/yr in the contributing area of the Heavenly Gondola well. Estimated bedrock permeabilities among the four well sites span most of the range reported worldwide at the borehole scale for crystalline rock (Clauser, 1992).

8.7 T-profiles in South Tahoe valley basin-fill wells: Overall, the field measurements of T-profiles were successful. Accurate, precise, high-quality T-profiles were obtained at each of 25 sites, some of which include several wells. T-profiles for each of these wells are presented graphically in appendix 6, together with detailed analyses and interpretation. Several 'signature' T-profile shapes observed in many of the South Tahoe basin-fill wells are described below:

(1) Isothermal (or near isothermal) T-profile: Very little or no change in T with depth within some depth interval of significant length (>~10 ft). This pattern is indicative of rapid intra-borehole flow (see section 6.3 and Ramey, 1962, Drury et al, 1984, and Woodbury et al, 1991). Intraborehole flow can potentially occur within any screened or sand/gravel packed interval, and between any two such intervals.
(2) Concave-upward T-profile: Observed T-profile is curved in a concave-upward shape. In the absence of lateral heat advection, this shape can result from Ts warming (see section 6.2) and/or downward recharge of groundwater in the formation, within the same depth interval as that in which the concave-upward shape is observed (Bredehoeft and Papadopulos, 1965). The contribution of Ts warming to this curve shape can be distinguished from the contribution of groundwater recharge on the basis of knowledge of site land cover history and plausible change in Ts given the land cover history. Analytical approximations, applicable to many field conditions, have been published that enable

separation of these effects, and determination of groundwater leakage rates across aquitards (Taniguchi et al, 1999a,b).

Generally, for sediments in the Tahoe Basin area, concave-upward curvature in the shallow subsurface (above ~150 ft bgs) may be attributable mainly to Ts warming (see section 6.2). Pronounced and/or deep concave-upward T-profiles within aquitards are usually attributable to aquitard leakage. Concave-up T-profile shape are also found within aquifer layers. However within aquifers, the T-profile is in general influenced by lateral as well as vertical groundwater flow, due to potential lateral advection of heat by lateral groundwater movement. Within aquifer layers, estimates of vertical groundwater flow rate using 1-D temperature data are often subject to significant uncertainty due to potential effects of lateral groundwater flow on heat transport (Reiter, 2001).

(3) Temperature Inversions: Observed T decreases with increasing depth over some depth interval.

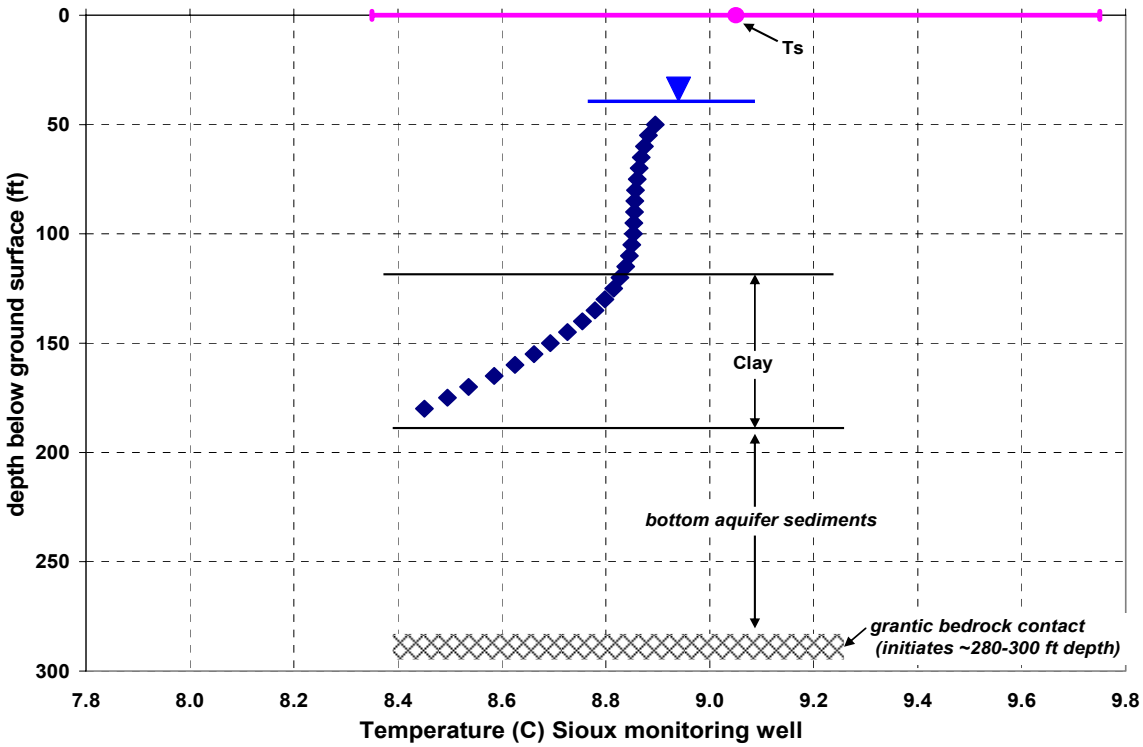

Figure 8-10. T-profile of Sioux monitoring well, sited in basin-fill sediments in central Meyers, CA (within South Lake Tahoe area). Ts near this well was not measured, but is inferred based on surface cover attributes in the area near the well and results from section 7. The shallow portion of the T-profile is consistent with this inferred Ts value. A large, deep T inversion is present in the subsurface near this well. The shape, depth, and magnitude of this T inversion indicate that it is not attributable primarily to Ts warming, but instead is caused by cool lateral groundwater flow beneath the thick clay layer. Depth to granitic bedrock is assumed to be comparable to that for the nearby Arrowhead well.

T inversions initiating near ground surface can result from recent significant increases in Ts (see figure 6-1, Taniguchi et al, 1999a,b), or from rapid cool lateral flow in the depth range of the observed inversion (see section 6.5, Cermak, 1989). These effects can be

distinguished with some knowledge of the history of land cover changes near the site that may have increased Ts significantly. Appendix 3 shows some conditions under which lateral flow from cool recharge areas can produce subsurface T inversions. Such conditions are likely present in some areas of Tahoe basin-fill aquifers.

T inversions initiating substantially below ground surface (i.e. >~50 ft bgs,) are not attributable to Ts warming effects, and are attributable solely to rapid cool lateral groundwater flow, consistent with mountain-front recharge. Figure 8-10 above is an example of a large deep T inversion at the Sioux test well location in Meyers that extends from near ground surface to >180 ft depth. Note the strength of this inversion increases with increasing depth; which is not consistent with Ts warming but is consistent with cool lateral flow at >180 ft depth in the area of this well.

A thermal energy balance is performed, as described in section 6.5, for a cross-sectional domain including the deep aquifer between the nearest mountain-front to the Sioux well (un-named peak neighboring central Meyers to the S-SE, with Tahoe Paradise Golf Course at base) and the Sioux well. The deep aquifer (cobbly sand) is located immediately beneath the bottom of the clay layer at 190 ft depth, and extends down to granitic bedrock. Depth to the top of the underlying granitic bedrock is not known precisely at the Sioux site, but is assumed to be comparable to that at the nearby Arrowhead well site, or approximately 290 ft depth. Although the T-profile within this deep aquifer was not measured, the shape of the T-profile above the aquifer (figure 8-10) indicates that the mean aquifer T is in the range 8.2 +/- 0.3C (assuming that the T inversion does not extend down into bedrock). The putative mountain-front recharge area is a N-NW facing slope, forested at higher elevations and with an irrigated golf course at lower elevation. Based on such surface attributes and results of section 7, it is estimated that Ts = 7.2 +/- 0.7C; and that the T of mountain-front recharge is about the same as Ts. Thus ΔT_m = 1.0 +/- 1.0C = amount of warming of groundwater between the mountain-front recharge source and the Sioux well site. The lower bound of ΔT_m is 0C, and does not yield a bound on Vx (see section 6.5). However, using the upper bound on ΔT_m of 2C, a lower bound on Vx (mountain-front recharge rate) can be obtained. The lower limit on the energy balance presented in section 6.5 is reproduced below:

$$[0.64*(a+b)]*Q + L*[Q+Qt\{x=L\}] < C_{v,w} * V_x * b * \Delta T_m$$

Terms in this equation are defined in section 6.5; numerical estimates of these terms are:

L = 3000 ft a = 190 ft b = 100 ft
Q = 66 mW/m^2 (section 8.1) $C_{v,w}$ = 4.196x10^6 J/m^3/C (handbook value)
$Qt\{x=L\} = \lambda_c * (dT/dz)_{190\ ft}$ = +48 mW/m^2
where λ_c denotes λ for clay (estimated from handbook ~1.5W/m/C)
$(dT/dz)_{190\ ft}$=0.0105 C/ft (from figure 8-10; slope near bottom of T-profile)

Placing these values into the equation above with ΔT_m<2.0C yields Vx > 45 ft/yr. This lower bound on mountain-front recharge holds even if there is significant leakage of groundwater thru the overlying aquitard into the lower aquifer, and/or discharge from underlying bedrock into the aquifer, since T of each of these recharge sources is >Tr for mountain-front recharge. Lateral permeability of the coarser-grain South Tahoe valley floor aquifers is > ~50ft/day (Bergsohn et al, 2007) thus a mean lateral hydraulic head

gradient < 0.24% can transport such recharge. Since the deep aquifer is ~100 ft thick, the recharge volume is equivalent to >~ 4,500 ft^3/yr of recharge from each 1 ft of length along the strike of the mountain-front. This is a large amount of recharge: if the amount of precipitation on the mountain-slope that infiltrates the subsurface (and is not evapotranspired) is ~1.5 ft/yr in the mountain-slope; all of the groundwater on the mountain-slope for a lateral distance of > 3,000 ft (about 2/3 of the distance from base to peak) would be required to recharge the deep aquifer at the mountain-front (neglecting convergence or divergence of flow parallel to the strike of the mountain-front).

14 of the 25 sites profiled in South Tahoe valley basin-fill sediments exhibited temperature inversions (appendix 6). For most of these wells, the observed T inversions are too large and deep to be attributable to increases in Ts, and are attributable to rapid cool lateral groundwater flow. Such flow is consistent with mountain-front recharge.

(4) Straight T-profile: Observed T-profile is a straight line (i.e. uniform T gradient with depth, but not near isothermal). This profile can result under conditions of very little or no vertical groundwater flow in the depth interval observed, if the lateral groundwater flow rate is very small. A straight T-profile can also occur in the presence of a substantial lateral rate of groundwater flow, if the upgradient distance of lateral flow is sufficiently long in relation to the flow rate (see section 6.5 and Cermak, 1989). The straight T-profile is not consistent with appreciable vertical groundwater flow within the formation over the depth interval in which it is observed.

(5) Large temperature gradient near bottom of well: Observed T gradient near the bottom is substantially larger than that which could result from purely conductive geothermal flow upward from depth (ambient heat flow).

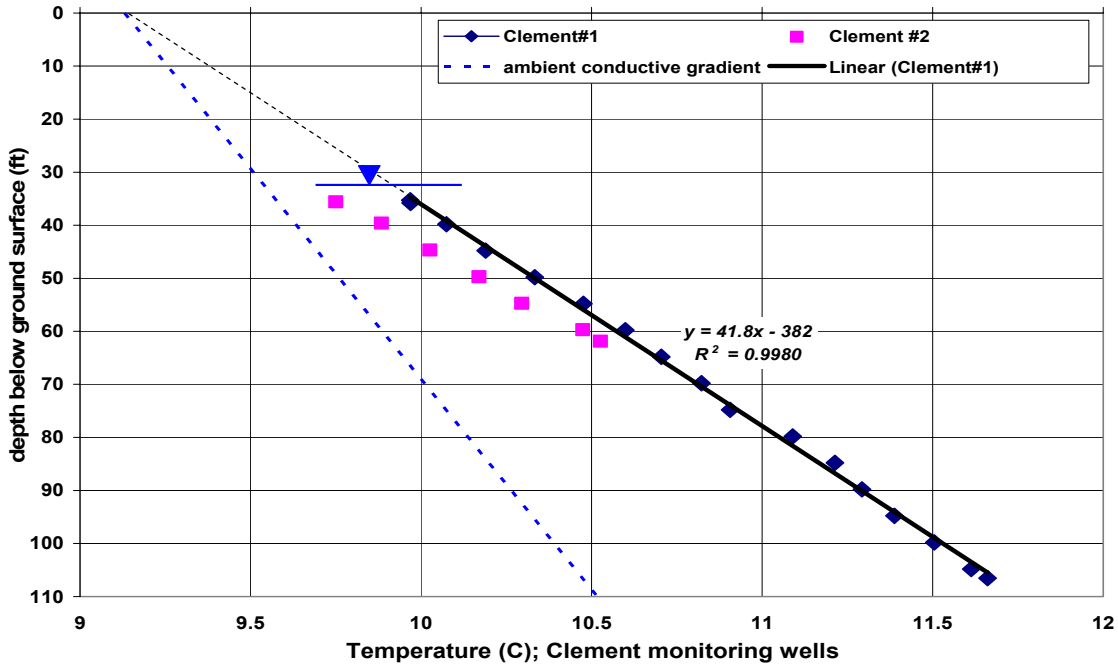

Figure 8-11. T-profile of Clement monitoring wells, located ~30 ft apart from each other in basin-fill sediments in the city of South Lake Tahoe ('South Y' area). The straight T-profile indicates very little vertical groundwater flow between the water table and 108 ft depth. A conductive T-profile for ambient geothermal heat flow (Q = 66 mW/m^2) is shown for comparison (diagram does not account for lower thermal conductivity in unsaturated sediments above water table).

In the absence of rapid intra-borehole flow downward in the interval above the large T gradient; the large T gradient indicates an advective source of heat flow upward from below the bottom of the well. This type of T-profile is observed in the ESB-2 test well in Meyers (Fig 8-12 below), the lower half of the DW-1 test well in Meyers (Fig 8-12; also type (2) T-profile in upper half), the Clement monitoring wells in South Lake Tahoe (Fig 8-11 above), and the Valhalla production well near Lake Tahoe (Fig 8-12; which is also an example of a type (4) T-profile). Figure 8-11 above shows the T-profiles for the Clement monitoring wells, together with the ambient conductive geothermal T gradient.

Note that the T gradient measured in the monitoring wells in figure 8-11 above is nearly twice that of the ambient conductive geothermal T gradient, indicating an advective source of heat flow upward to below the bottom of the area of these wells. This additional heat could be delivered either by rapid lateral groundwater flow sourced from a warmer area to below the bottom of the area of these wells, or by slow, deep upward flow of groundwater (and delivery of heat) up to some depth below the bottom of the area of the wells; i.e. a mountain-block recharge source. The Clement wells are located near Tahoe Mountain; a potential source of groundwater recharge to depth in bedrock.

All of the characteristic 'signature' patterns (1) thru (5) described above were observed among the basin-fill wells profiled. An example of each is illustrated below:

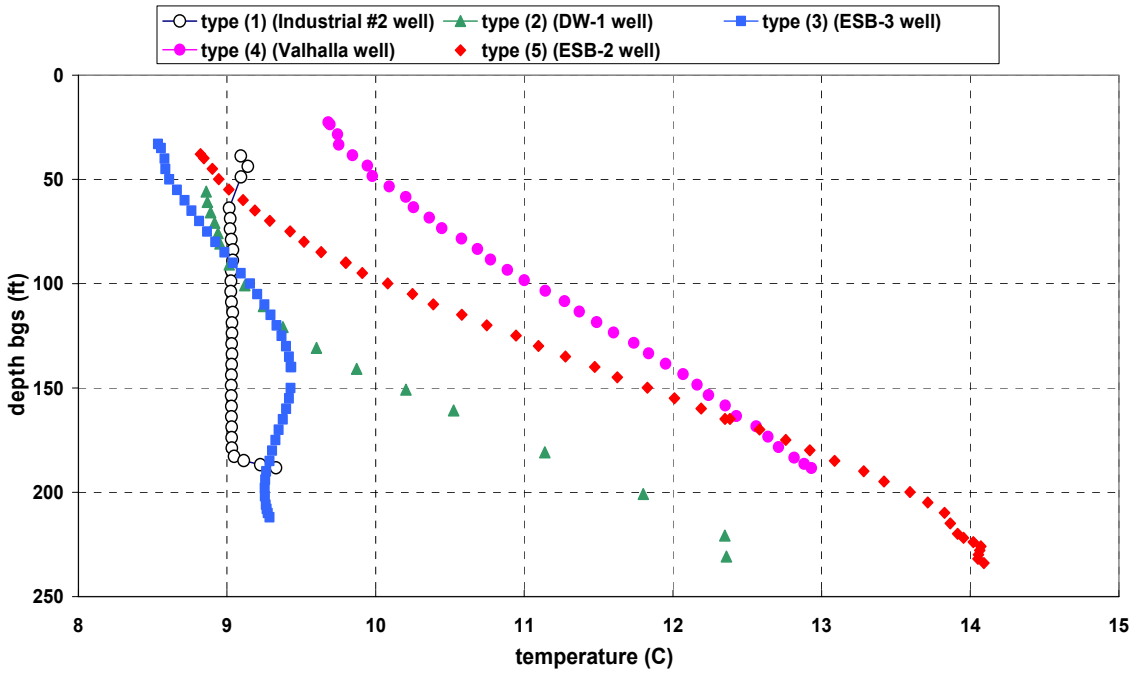

Figure 8-12. Examples of South Tahoe district well T-profiles. An example of each type of characteristic temperature profile (1) thru (5) is shown.

Results and detailed analyses for each well profiled are presented in appendix 6.

9: Additional Tahoe Field Investigations

Additional investigations of South Tahoe area groundwater flow patterns were performed as described in Bergsohn et al (2007), and include hydraulic investigations, stable isotope investigations, and characterization of Meyers Warm Springs. The isotope and Meyers Warm Springs investigations were performed by the authors of this report, and are included here in appendices 7 and 8, in order to aid in dissemination of results.

Briefly, Meyers Warm Springs demonstrates the presence of deep thermal groundwater flow and discharge up to near the edge of a basin-fill aquifer system in the South Tahoe valley. Brockway Hot Springs, located on the north shore of Lake Tahoe, have previously been investigated by us and others (see Trask and Fogg, 2000). It is plausible that there may be other locations of discharge of thermal groundwater in the Tahoe Basin, which disperse undetected beneath valley basin-fill areas.

The stable isotope results include a highly statistically significant trend of lighter isotope levels in more deeply screened wells in the South Tahoe valley basin-fill aquifer system. This trend indicates high elevation recharge sources for deep basin-fill groundwater, consistent with a significant mountain-front and/or mountain-block recharge contribution to South Tahoe valley aquifers.

10: Numerical modeling results

Conceptual numerical finite element models were used to simulate and explore groundwater and heat flow patterns in 2D cross-sections of montane topography, using the USGS SUTRA finite element modeling software (see section 6.6).

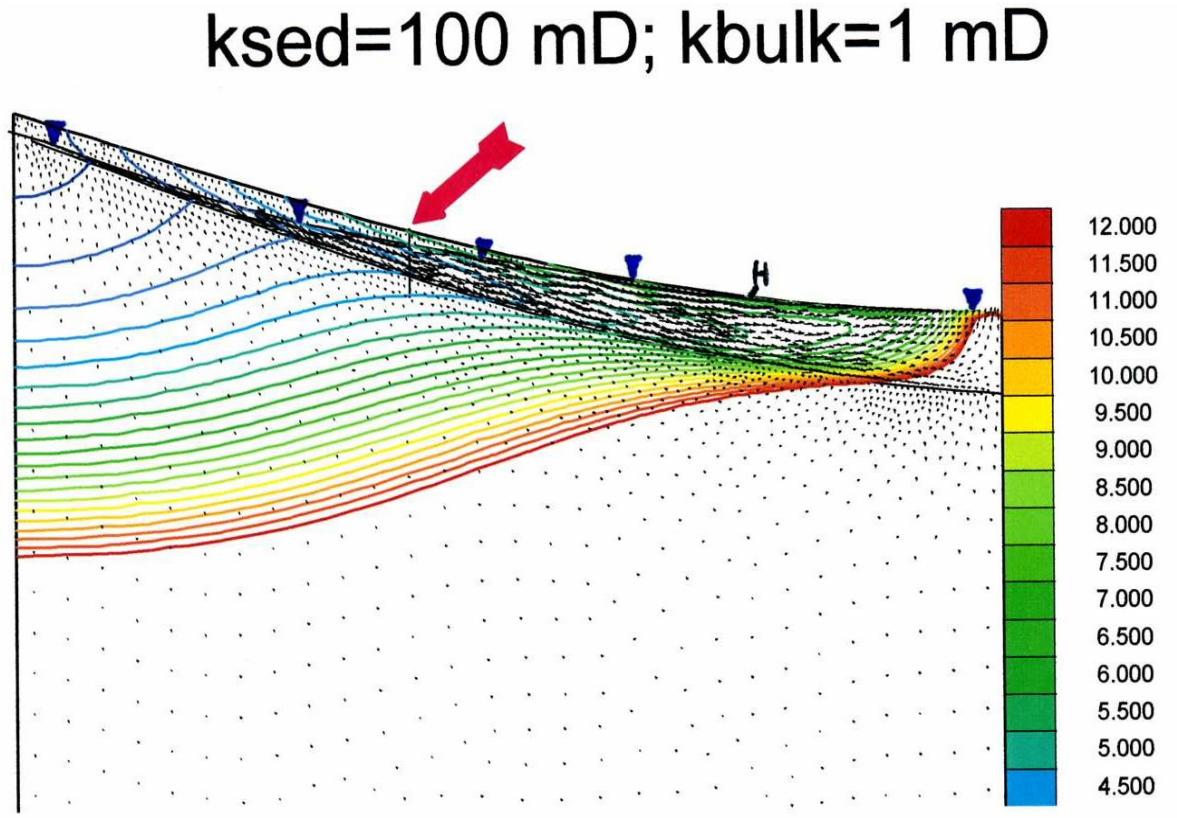

Figure 10-1a. Finite element numerical model of steady-state combined heat and groundwater flow in 2D cross-section of a generic mountain-slope. Domain is 5 km depth (upper 3.5 km shown) x 5 km length, with 1 km elevation drop from peak to valley. Slope is 17.4^{o} near peak, gradually decreasing to flat in valley. Sediment depth is 100 m at peak; gradually increasing to 400 m in valley. Sediment permeability (Ks) is set to 100 mD (millidarcy). Below the sediment layer, bedrock permeability (Kb) is set to 1 mD to ~2 km depth, then decreases semi-exponentially with depth to a value of ~0.01 mD at the bottom of the domain. Thermal parameters (λ, Cp) are set close to values for granitic sediments and bedrock as presented in sections 8.1,8.2. The lower boundary (not shown) is no-flow for groundwater, and steady Q = 66 mW/m^2 (Tahoe Basin heat flux). Side boundaries are no-flow for heat and groundwater. The top boundary is set at Ts=2C at peak, increasing at rate 6C/km of decreasing elevation to Ts=8C in valley. Steady groundwater recharge is input to top surface at 30 cm/yr from the peak down to the elevation where model output determines water table is at ground surface. Below this elevation, the upper boundary is constant head set to surface elevation. Model output shows recharge rate gradually decreases with elevation to hinge point 'H' below which upper surface discharges groundwater (valley area). Model output isotherms shown at 0.5C increments; arrows show direction and relative magnitude (arrow length) of computed groundwater flow. Large arrow at surface shows location of simulated monitoring well for figure 10-1b.

10.1 2D cross-section for areal mountain-slope flow: Simulations of both shallow mountain-slope and deep mountain-block heat and groundwater flow were run under conditions where higher permeability sediments (and/or weathered bedrock) overlay lower permeability bedrock, and Ts at higher elevations is cooler than Ts at lower elevations. Simulations were performed for moderate to steep slopes (~10-30^{o}) and a Ts elevation lapse of 6C/km, matching the Tahoe Basin atmospheric T lapse. One such simulation is shown in figure 10-1a above. The model output shows that most groundwater flow occurs in the sediments layer, due to its much higher permeability relative to the underlying bedrock. The very small T gradient near the peak is diagnostic of groundwater recharge (~5 cm/yr) to depth in bedrock, and the very large T gradient in the valley is diagnostic of groundwater discharge from depth.

Figure 10-1b below shows simulated T profiles for the domain shown in figure 10-1a, for several combinations of sediment and bedrock permeability.

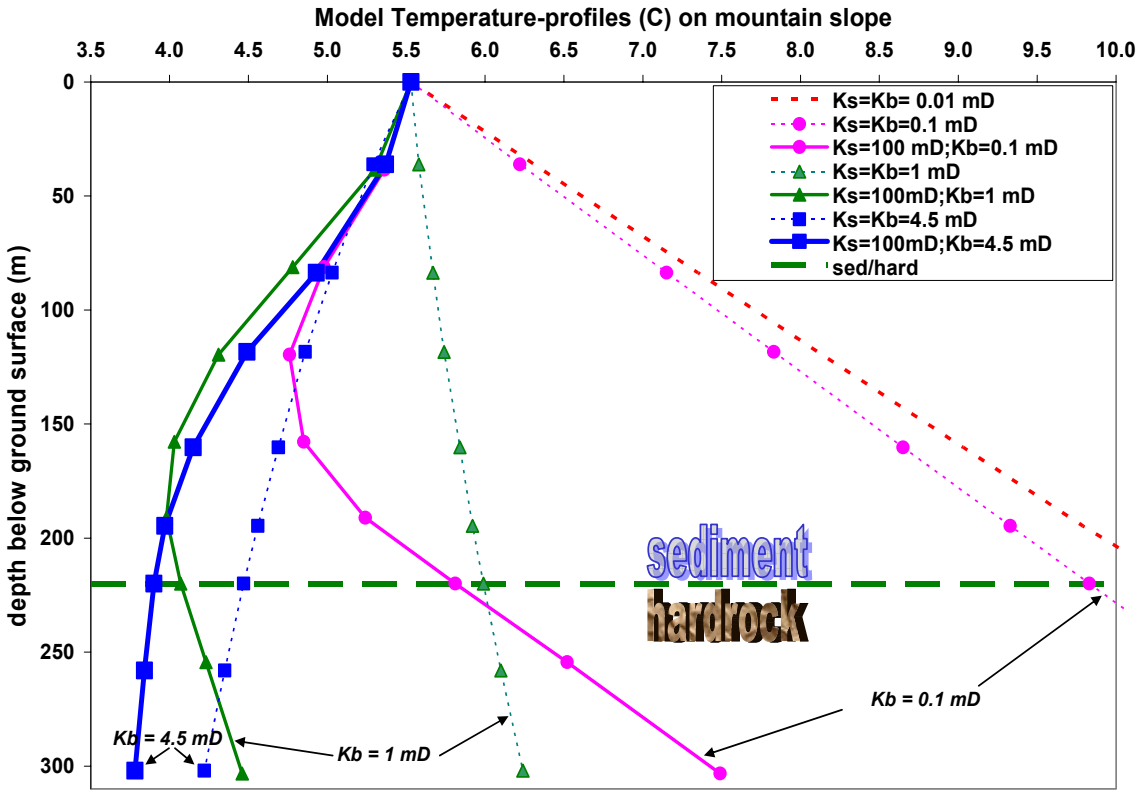

Figure 10-1b. Model output T-profiles at mid-slope location shown in figure 10-1a, for various combinations of shallow (sediment or weathered bedrock) and deep (non-weathered bulk bedrock) permeabilities. T-profiles shown in solid lines each for sediment permeability Ks=100 mD; dashed line T-profiles for Ks set equal to lower values for bedrock permeability Kb. Note T inversions result for high sediment or high bedrock permeability, and the depth of the T inversion increases with increase in bedrock permeability. Also note that the slope of each T-profile near and beneath the sediment/bedrock interface is dependent mainly on the bedrock permeability, and is not sensitive to variations in the sediment permeability.

Significant results from this and related simulations of mountain-slope flow include:
(a) Near the mountain peak, the T-profile shape is not affected by large groundwater flow rates in the sediment layers, but instead is sensitive to the rate of bedrock recharge to depth within the mountain-block, including deep recharge rates as slow as ~1-2 cm/yr.
(b) At any location on the mountain slope, high lateral groundwater flow rates in the sediment layers do not significantly affect the T-profile slope near the bottom of the sediments, or the T-profile shape below the sediment layers. Instead, near and below the bottom of the sediments, the T-profile shape is governed mainly by the magnitude of deep bedrock groundwater flow.
(c) Subsurface T inversions are produced within the mountain slope sediments, caused by cooler groundwater recharge from higher elevations flowing rapidly in the sediment layers. If the underlying bedrock is sufficiently permeable, these T inversions can extend down within the bedrock. Results of these numerical simulations for subsurface T inversions in mountain-slope sediments are similar to results for T inversions in valley sediments resulting from cool mountain-front recharge (sections 6.5, 8.7).

10.2 2D cross-section for regional mountain-block flow: Compilations of worldwide data for crystalline rock at depth show that at large length scales (>~0.5 mile), estimated permeabilities all fall within a narrow range of ~0.1 to 50 mDarcy (Clauser, 1992), corresponding to hydraulic conductivity of ~0.00026 to 0.13 ft/day (T <20C), within the range for fine to medium silt. Numerical modeling indicates that this permeability range can support high elevation deep bedrock recharge of ~0.01 ft/yr to ~5 ft/yr for typical Tahoe Basin topography. Below about 100-200 ft depth, there is often little or no decrease in permeability of crystalline rock with increasing depth (Singhai and Gupta, 1999), to depths of >2 miles (Brace 1980, 1984).

We performed numerical simulations of regional deep bedrock heat and groundwater flow in montane topography under conditions of uniform permeability at the areal scale to a depth of ~1mile, below which model permeability was gradually decreased with increasing depth. One of these simulations is shown in figure 10-2a. Similar to figure 10-1a, figure 10-2a shows a pattern of depressed isotherms at high elevation areas that are diagnostic of groundwater recharge (~5 cm/yr) to depth in bedrock, and compressed isotherms near Lake Tahoe and the eastern (Carson) valley areas, diagnostic of groundwater discharge from depth.

Figure 10-2b shows simulated T profiles for the domain shown in figure 10-2a, for several combinations of sediment and bedrock permeability:

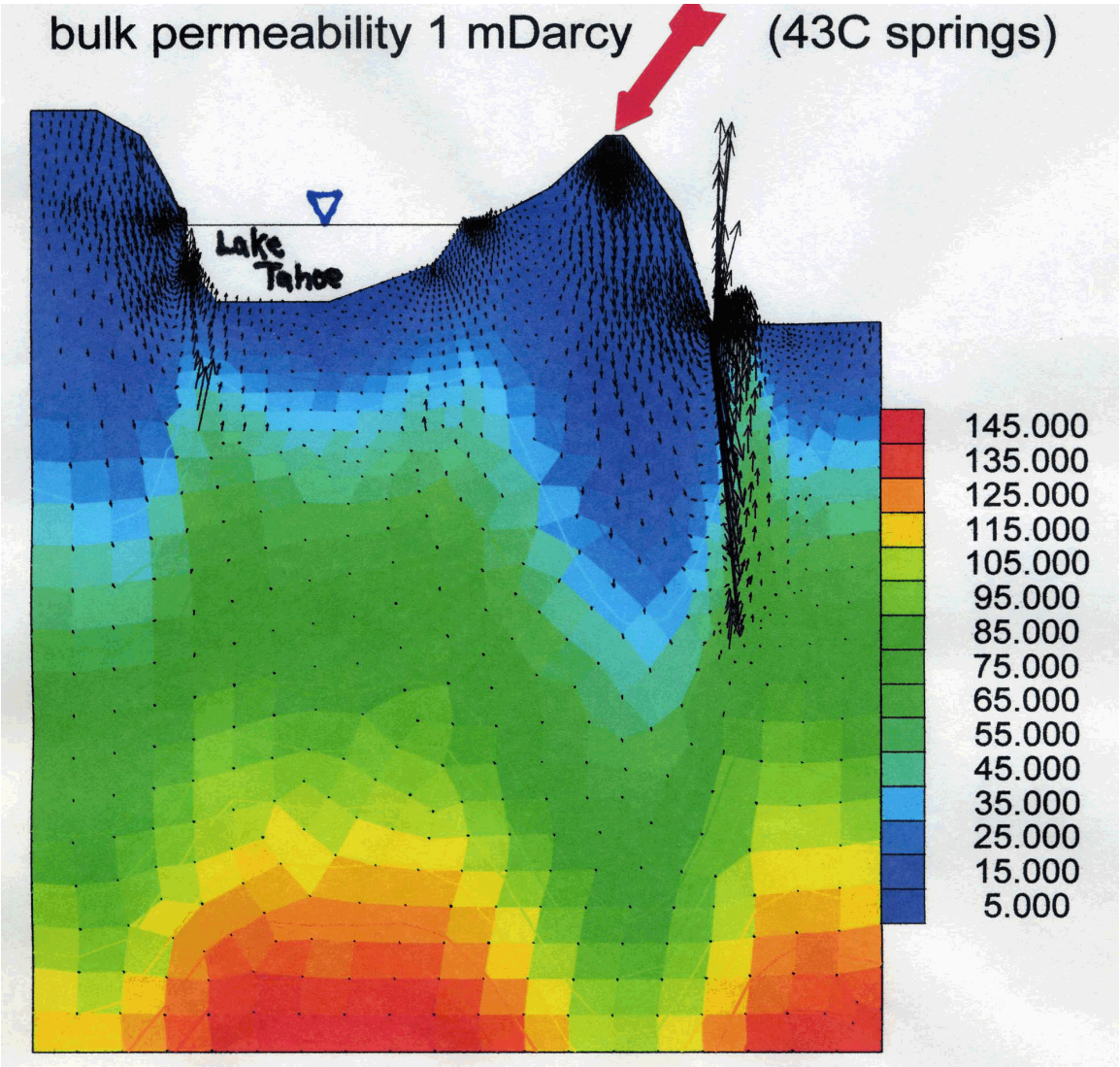

Figure 10-2a. Finite element numerical model of steady-state combined heat and groundwater flow in 2D cross-section of montane region. Upper domain boundary approximates topography at 39°N latitude from the Sierra Crest across the Tahoe Basin and Carson Range to the Carson River. Domain is 5 km depth x 36 km length. Deep sediment layers (not shown) of anisotropic permeability (Kx>>Kz) are modeled beneath Lake Tahoe and the Carson Valley. In bedrock; input uniform permeability 1 mD to ~2 km depth, below which permeability gradually decreases as described for figure 10-1a. Thermal parameters as described for figure 10-1a. Lower boundary is no-flow for groundwater, and steady Q = 66 mW/m^2 (Tahoe Basin heat flow). Side boundaries are no-flow for both heat and groundwater. Top boundary is steady Ts of ~5C at peaks, increasing at lapse 6C/km with decreasing elevation (exception: thermal springs area; set dT/dz=0 at surface). Water table set at top boundary (constant head set to surface elevation). Model computed recharge rate to depth is ~5 cm/yr near peaks; gradually decreases with elevation to hinge points (not shown) below which upper surface discharges groundwater (Lake Tahoe and Carson Valley). Model output temperatures indicated by color coding throughout domain; arrows show direction and relative magnitude (arrow length) of model computed groundwater flow. Large arrow at peak surface shows location of simulated monitoring well for figure 10-2b.

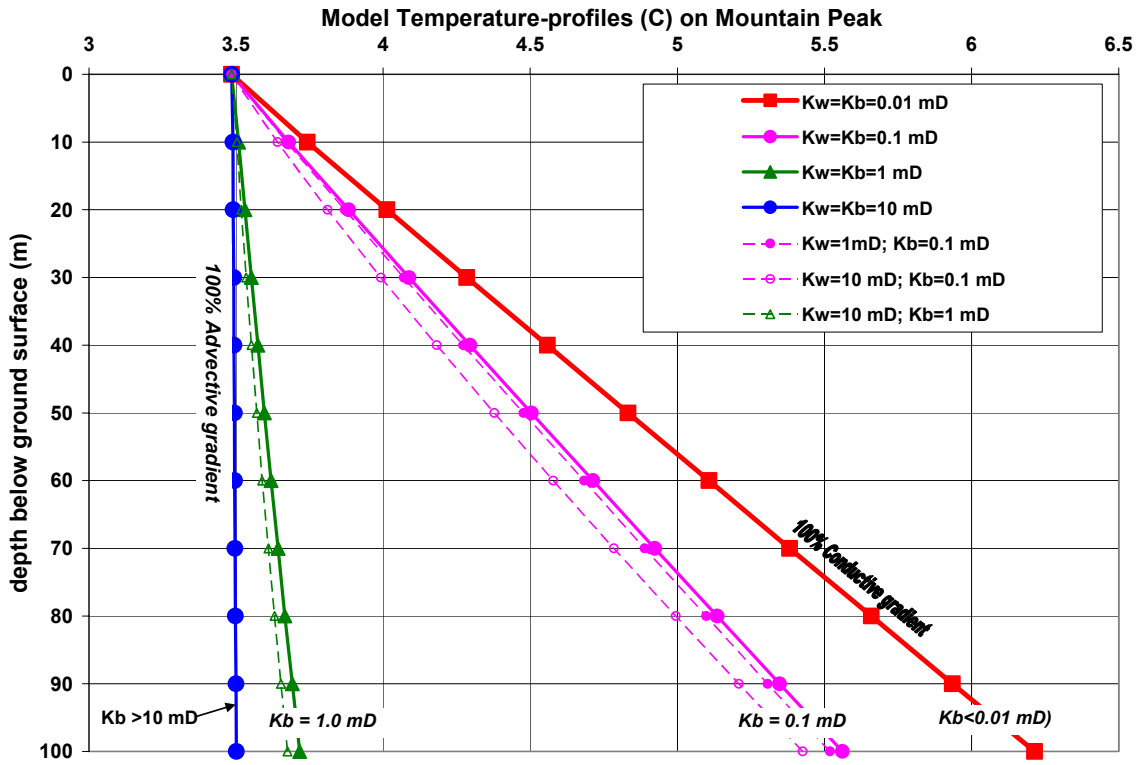

Figure 10-2b. Model output T-profiles at mountain peak location in figure 10-2a, for various combinations of shallow (weathered) and deep bedrock (nonweathered bulk) permeabilities. A 100m thick layer of weathered bedrock is placed on the peak surface (not shown in figure 10-2a), which is modeled to have either the same (as in figure 10-2a) or higher permeability than the underlying bulk bedrock. T-profiles shown in solid lines each for shallow permeability Kw set equal to deep bedrock permeability Kb (i.e. negligible weathering enhancement of permeability). Note that the T-profile shape within the weathered layer is not sensitive to the permeability of the weathered layer, but is highly sensitive to the permeability of the underlying bulk bedrock; particularly in the range 0.1 to 1 mD, over which heat flow transitions from conduction-dominated to advection-dominated.

Results from this and related simulations of regional-scale mountain-block flow include:
(a) At the regional scale, groundwater recharged at high elevation in the mountain block flows downward to great depth and then laterally beneath neighboring valley areas, where it discharges upward. Both heat and groundwater discharge from deep bedrock tend to be focused near the base of mountain front areas, such as breaks in slope that are often present near the toe of mountain-fronts.
(b) There is a window of intermediate permeability of deep bedrock for which groundwater recharging to depth in high elevation mountain block areas and discharging from deep under the mountain-block is substantially warmed, and can result in thermal spring discharge (see Smith et al, 1989). At lower permeabilities, deep groundwater flow is very slow and conductive heat flow is dominant. At higher permeabilities, the deep groundwater flow rate is so large that geothermal heat flow is 'washed out' and diluted; insufficient in quantity to warm the large volumetric rate of groundwater discharge. This permeability window depends on topographic relief and the depth of attenuation of

permeability, but in montane regions typically overlaps (partially) the worldwide range 0.1-50 mDarcy for bulk crystalline rock at areal and larger scales. Upward groundwater flow rates as slow as ~ 1 cm/yr are associated with substantial enhancement of heat flow from depth, and can significantly increase shallow T gradients near valley discharge areas.
(c) T-profiles near peak elevation mountain-block bedrock recharge areas are insensitive to shallow lateral groundwater flow, but are sensitive to the rate of groundwater recharge to depth in the bedrock. T-profiles measured near peak areas can be sensitive indicators of the magnitude of bedrock flow to depths far below the bottom of the well.

10.3 Distance attenuation of mountain-block discharge: At the regional scale, the numerical model simulations for uniform deep permeability at areal and larger scales described above show that groundwater discharge upward from depth in bedrock tends to decrease semi-exponentially with distance away from the mountain-front and into the valley:

$F_z(x) \sim F_z(0)*\exp^{-(x/c)}$ = deep groundwater discharge flux at location x
where x = distance into valley from base of mountain-front
c = characterstic decay length for deep groundwater discharge flux
(function of geometry of flow system)

The value of $F_z(0)$ is determined by integration of $F_z(x)$ over the entire valley width (all x), and equating this to the recharge rate (volume/time) in the contributing area of the mountain block.

For the topographic relief typical of many Tahoe watersheds, c ~ 2500 ft, such that at a location in the valley that is 1 mile distant from the base of the mountain-front, deep groundwater discharge is only ~10% the rate of that at the base of the mountain-front. Such an exponential discharge pattern is reported in the literature for groundwater discharge from sloping areas to areas of flat head (McBride and Pfannkuch, 1975). The presence of faults can substantially interrupt this pattern (see section 11.2).

Note: this exponential discharge pattern is not evident in figures 10-1a or 10-2a above, due to the absence of a break in slope in the domain for figure 10-1a (which is not flat except at the right boundary of the domain), and to the presence of ~1.6 km thick sediments (with anisotropic permeability) in the valley area of figure 10-2a. These deep sediments alter the pattern of bedrock discharge from depth (also the model grid element size used is large and obscures details of the spatial groundwater discharge pattern).

11: Discussion

Mountain-front and mountain-block recharge to valley basin-fill sedimentary aquifers in the Tahoe Basin region is supported by results of the thermal investigations presented in this report. In the Clear Ck area, such recharge is also supported by independent hydraulic investigations performed by the USGS (sections 8.4,5). In the South Tahoe area, such recharge is also supported by stable isotope data (see section 9.4 and appendix 8), and by areal groundwater flow models calibrated on hydraulic data (Bergsohn et al, 2007). Recently, peer-reviewed reports of investigations of groundwater recharge mechanisms in valley aquifers in or near montane regions have also found that mountain-front and/or mountain-block recharge can be significant recharge source for nearby valley aquifers (see review appendix 1).

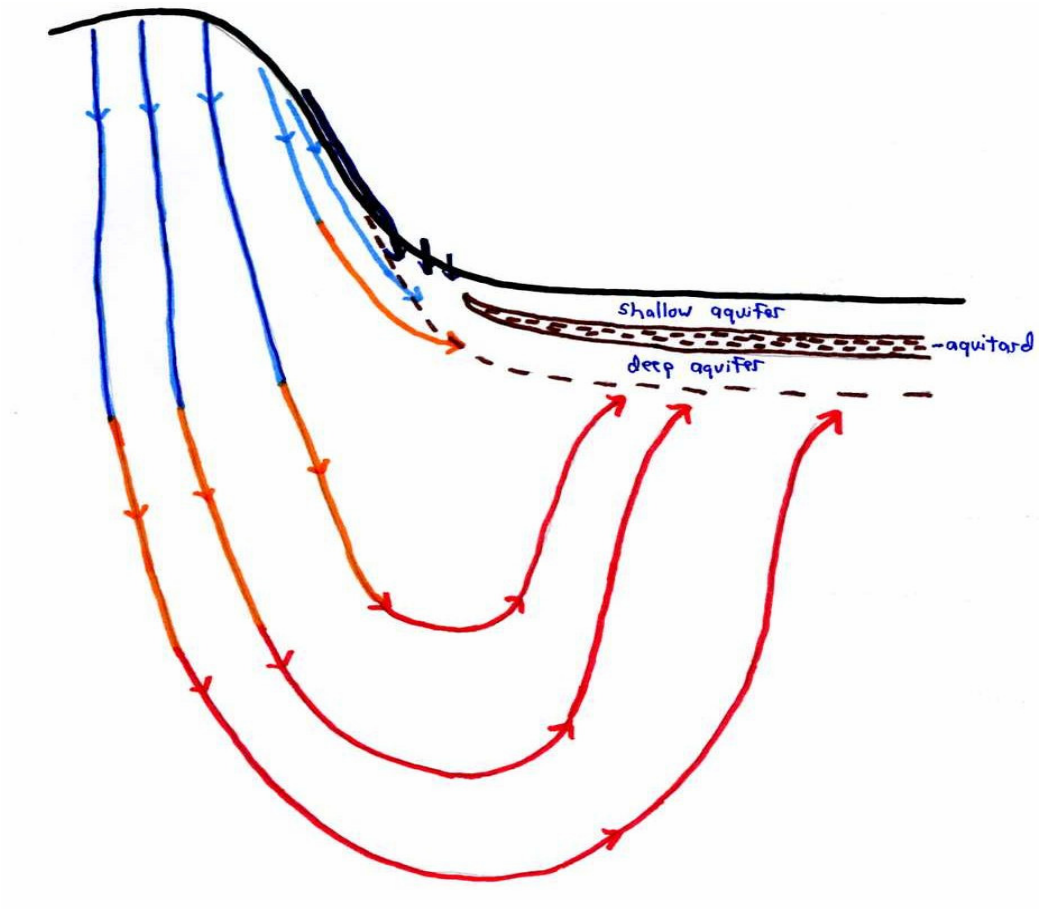

Figure 11-1. Conceptual sketch of mountain-front and mountain-block groundwater recharge of valley sedimentary aquifer system. Mountain-block recharge infiltrates at high elevation mountain-block areas and flows downward, often to great depth, before discharging warmed groundwater upward into valley aquifers. Mountain-front recharge can infiltrate high up on the mountain-slope or lower down on the mountain-front (see section 11.1), and recharge the lateral edges (i.e. mountain-front boundaries) of valley aquifers with cold (nonwarmed) to slightly warmed groundwater. The resulting T of water in shallow and deep valley aquifers is dependent on the relative volumetric contribution of each recharge source (and also on ambient conductive heat flow from depth and on valley mean annual ground surface T).

11.1 Mountain-front recharge: Mountain-front recharge refers to recharge into the lateral edges of montane valley basin-fill aquifers; i.e. the portion of valley aquifer recharge that occurs near the mountain-front. Potential sources of mountain front recharge to valley aquifers include:

(1) precipitation derived infiltration at mountain front
(2) surface flow derived infiltration at mountain front:
    --streams and rills flowing down across or along the mountain front
    --sheet flow over exposed hardrock slopes during snowmelt and rainfall events
(3) cool shallow groundwater flow down mountain slope, in:
    --soils and sediments
    --alluvial fans
    --talus slopes (e.g. west slope of Christmas Valley)
    --shallow bedrock, where fractured and/or decomposed
(4) warmer deeper flow down mountain slope, in deep fractured bedrock

Many of the sources of flow listed above are ephemeral (notably rainfall, overland sheet flow, ephemeral rills and streams). Much of shallow groundwater flow in mountain-front areas likely has significant seasonal variation, however mountain-slope bedrock flow likely has a significant perennial component. Perennial streams may be the only seasonably stable source for mountain-front recharge. Availability of mountain-front recharge combined from all sources could be significantly seasonally variable in some areas of valley aquifers, and have little seasonal variation in other areas.

Near the edges of many valley aquifers, fine sediment layers may pinch out, enabling vertical recharge to depth in the sediments. Water recharged at the mountain-front can then flow laterally into the valley basin-fill aquifer system. Over half of the Tahoe valley wells profiled exhibit marked T inversions, some to depths of nearly 200 ft or more, indicating the presence of rapid cool lateral flow in the sediments, consistent with a mountain-front recharge source (section 8.7).

11.2 Mountain-block recharge: Mountain-block recharge refers to recharge at the bottom of valley basin-fill aquifers due to discharge of water upward from the underlying bedrock. The bedrock itself is recharged from high elevation mountain-block areas. Depth to water was measured in 3 granitic bedrock wells at high elevation (see section 8.6). The data shows a high elevation water table in these high-elevation recharge areas, with little seasonal variation in head relative to the total head drop between mountain upland areas and the valleys. Therefor the total head drop between Tahoe mountain-block recharge areas and valley discharge areas can often be accurately approximated as seasonally invariant. Multi-annual droughts or shifts to a dryer climate could potentially significantly affect high elevation water tables on longer time scales.

Permeability of deep granitic bedrock worldwide at the regional (>1 km) scale ranges from 0.00026 to 0.13 ft/day (see appendix 1). Well pump test data and well temperature data for two deep granitic bedrock wells (Echo Pass and Heavenly Gondola) yield permeability values that fall near the low (Echo Pass) and high (Heavenly Gondola) ends of this worldwide range (see section 8.6), demonstrating substantial areal variation in permeability of deep granitic bedrock in Tahoe area mountains. Flow modeling indicates that this permeability range supports high elevation deep bedrock recharge of

>0.01 ft/yr at the areal scale (the high end of the permeability range can accommodate nearly all of available annual precipitation), which could discharge up under valley floor areas. The surface area of the valley floor in many Tahoe watersheds is comparable to the surface area of upgradient mountain-block areas, such that mean areal discharge flux into the valley aquifers is comparable to the mean areal recharge flux at high elevation in the mountain block (>0.01 ft/yr). Areas such as Christmas Valley are exceptions; this deep narrow valley is bounded by a large area of high-elevation mountain blocks; such that the likely contributing area of recharge in the mountain blocks is >5-fold that of the valley floor discharge area. Therefore, mean areal mountain-block discharge from under the floor of Christmas Valley is likely >0.05 ft/yr.

Discharge of deep groundwater flow up into valley floor areas is likely highly nonuniform across the valley floor. Flow modeling indicates that at the regional scale, such discharge from deep bedrock with spatially uniform permeability (at areal and larger scale) is likely to be most pronounced near the base of mountain front areas, such as near breaks in slope that may be present at the toe of the mountain-front, and also indicates that the discharge rate tends to decrease semi-exponentially with distance away from the mountain-front toward the valley axis (see section 10.3). For relief typical of Tahoe Basin watersheds, the semi-exponential decline rate is such that the groundwater discharge flux at the valley floor at a distance of 1 mile from the mountain-front is likely to be, on average, about 10% of the discharge flux at the mountain front.

Furthermore, discharge areas are likely to be associated with fault zones (references appendix 1). Fault zones generally have highly heterogenous permeability at all length scales. Fault discharge is likely to be focused in some segments of the fault zone, with negligible or no discharge from neighboring segments of the same fault zone.

Several T-profiles in Tahoe valley areas show upward heat flow that is substantially enhanced over that of conduction of regional ambient geothermal heat flow from depth (see section 8.7). This enhanced heat flow is caused by a source of advective heat flow at depth beneath the bottom of these wells. The advective heat flow source could be groundwater flow upward from depth in the bedrock. An upward Darcy discharge rate from depth of >~0.04 ft/yr (mean over an area of valley floor) is sufficient to produce the observed large gradient T-profiles. Observed T-profiles are consistent with upward flow of groundwater in the area deep below the bottom of some wells, but not others. Mountain-block sourced groundwater recharge is likely significant in some (but not all) areas of Tahoe valley basin-fill.

12: Summary and Conclusions

We have performed additional analysis and modeling of previously collected data consisting of temperature (T) profile measurements in dozens of wells and boreholes in the Tahoe Basin region. We have also performed thorough analysis and modeling of previously collected long-term soil T monitoring data from a large number of sites in the South Tahoe area. The relationship of soil T to site surface characteristics and radiative exposure conditions has been determined. Overall, results indicate that T-profile data together with reliable estimates of surface T can help to constrain groundwater flow models, enabling more accurate and reliable portrayal of actual groundwater flow patterns, including sources of groundwater recharge.

The T-profiles are especially valuable in helping to better define recharge sources and rates. This includes water table recharge (downward into top of bedrock or sedimentary aquifers), recharge from the mountain-front (into sides of valley aquifers), and mountain-block discharge (upward into bottom of valley area sedimentary aquifers; originating from high-elevation mountain-block recharge). In the South Tahoe area, thermal evidence for mountain-front and mountain-block recharge is consistent with isotope and hydraulic results.

12.1 Previous results: This investigation was initiated as part of a prior project with the South Tahoe PUD (Bergsohn, 2007). The findings summarized below were part of this prior project, but have been strengthened by the additional analyses performed for the current investigation.

Measured T-profiles in many wells reflect the presence of vertical intra-borehole flow; with higher sensitivity threshold than many standard well flowmeters.

Modeling results and T-profiles suggest a particularly powerful application of thermal analysis in high relief areas: the shape of the T-profile near the borehole bottom is sensitive to small (and large) rates of groundwater flow present at depths far below the bottom of the borehole. For example, T-profiles in wells in basin-fill that terminate near the bedrock surface are sensitive to groundwater flow deep within the bedrock. This sensitivity is particularly pertinent in hardrock areas of thin or absent sedimentary cover, since the magnitude and depth of flow into bedrock is generally very difficult and/or expensive to determine using hydraulic or other geophysical approaches.

Our modeling results have shown that T-profile measurements can be particularly useful in defining vertical groundwater flow rates, and also help to define the depth to which substantial groundwater flow occurs, and whether substantial groundwater flow is present at depths below the bottom of wells and boreholes probed.

Subsurface T inversions are present in many Tahoe valley localities, and may be attributable in part to warming of mean annual soil T (Ts), but are mainly due to a specific pattern of rapid, relatively shallow groundwater flow from cooler recharge areas (e.g. mountain-front recharge).

12.2 New results: A novel ‘black-box’ approach to the thermal energy balance on mountain-front recharge was presented. This approach is conceptually simple and is proposed to be a quick, robust approach for bracketing the magnitude of mountain-front recharge into adjacent valley aquifers, given T-profile measurements in one of more

valley well(s) penetrating into the aquifer. This 'black box' energy balance approach is one of the highlights of the publication draft (appendix 9).

As documented in the literature for other regions and found by us in the Tahoe Basin, mean annual surface T (Ts) can vary laterally by as much as ~5C within a small area, depending mainly on radiation exposure, albedo, moisture and plant cover environments. Results showed that these variables are more important in determining Ts than is site elevation over the 1400 ft range in elevation of our field investigation.

Given the estimated normal conductive geothermal gradient in South Tahoe sediments (~1.25 C/100 ft); the range in shallow subsurface T over short lateral distances (due to heterogeneity in Ts) can be as large as the typical change in T over ~400 ft of sediment depth. For example, groundwater flowing laterally from under a cool forested area to under a warm meadow area will be warmed from the surface downward as it flows under the meadow area. Accurate knowledge of the spatial variability of Ts is required for specification of the top surface thermal boundary conditions in modeling of heat and groundwater flow in a given area or locality. This enables separation of the effects of spatial T differences caused by groundwater advection from spatial T differences produced by areal differences in Ts. Significant spatial variation in Ts is present in many areas, particularly montane areas where slope, aspect, and type of vegetative cover (forest, brush, meadow, etc) often changes substantially over small distances. The often significant spatial variability in Ts has generally been neglected in the literature of heat & groundwater flow, presumably owing largely to lack of sufficient data for estimation of Ts variations.

Results for soil T (monthly and annual) can be generalized for much of the rest of the Sierra Nevada, and should be useful as indicators of the magnitude of inter-site differences in mean summer T and Ts in other montane areas. With the main factors responsible for shallow subsurface T quantified accurately, Ts maps can be generated for montane regions. In addition to its use in thermal tracing of groundwater flow, accurate knowledge of soil T areal heterogeneity is useful in a wide variety of ecological and environmental investigations.

Results for Mt. Pluto provide an example of significant permeability to depth within a volcanic formation, determined using borehole T measurements and heat flow analyses. Results at Clear Ck illustrate good agreement in the rate of groundwater flux upward from depth in granitic bedrock determined independently using either thermal or hydraulic data. The estimated groundwater mass balance is consistent with the subsurface thermal energy balance in the Clear Ck alluvial fan, providing additional support for the estimated groundwater mass balance.

12.3 Recommended Additional Investigations: In this report, we have mainly performed semi-quantitative analyses using simplified analytic models of heat and groundwater flow developed by us and others. The peer-reviewed literature and agency (e.g. USGS) reports include a variety of heat and groundwater flow modeling investigations. However, additional conceptual numerical modeling of coupled heat and groundwater flow is needed, in part to evaluate the robustness and range of applicability of analytic models that have been developed for simple flow geometries and boundary conditions.

Rigorous and thorough end-member modeling analyses addressing some common problems in interpretation of field data (encountered in thermal tracing investigations) have not been documented in the peer-reviewed literature. The examples below are proposed to be of high practical value to address:

(a) Determine the radius of influence of discrete fracture flow (pipe-1D and sheet-2D) recharge and discharge, on the subsurface T-field. This is of particular importance in evaluation of observed T-profiles in hardrock areas; to address questions such as: Is groundwater flow in a fault several hundred feet distant from a well expected to have a significant influence on the well T-profile? How close to a well does fracture flow need to occur in order to significantly influence the well T-profile? Results by Sorey (1978) for thermal springs discharge indicate that the subsurface T field is significantly influenced to lateral distances ~1X-2X the depth of rapid vertical flow; however investigations are needed that specifically focus on the effects of highly localized groundwater recharge on the areal subsurface T field.
(b) Perform a rigorous analysis, including coupled heat and groundwater flow modeling, of the effect of areal heterogeneity in Ts on deeper subsurface T, in the presence and absence of groundwater flow. Start with a simple case of a valley area of relatively flat topography, with lateral groundwater flow from under a forested area of low Ts to under a meadow area of higher Ts (and vice-versa). By performing such investigations, the influence of the distribution of surface T on deeper subsurface T can be quantified under various rates and patterns of groundwater flow. Such analyses enable the effects of areal Ts heterogeneity on T-profiles to be distinguished from the effects of groundwater flow patterns on T-profiles.

Results of such general conceptual studies should provide valuable interpretative tools for heat flow tracing of groundwater flow, particularly for case study investigations.

References

Anderson, M.P. (2005) Heat as a Ground Water Tracer. Groundwater, Vol. 43, No. 6, pp. 951-968, Nov.-Dec. 2005.

Anderson, Michael (2006) Climate Change Impacts on Flood Management. *Chapter 6 in* Progress on Incorporating Climate Change into Planning and Management of California's Water Resources: CA DWR Technical Memorandum Report, July 2006.

Armin, Richard A., and John, David A. (1983) Geologic Map of the Freel Peak 15-Minute Quadrangle, California and Nevada. USGS Miscellaneous Investigations Series, Map I-1424.

Barnett et al (2008) Human-Induced Changes in the Hydrology of the Western United States. Science, 319, 1080 DOI: 10.1126/science 1152538

Bergsohn, Ivo, Fogg, Graham, LaBolle, Eric, Trask, Jim, and Roll, Laura (2007) Development of Groundwater Resources in the Presence of Contaminant Plumes, South Lake Tahoe, CA. Final Project Report (July 2007) *for* Local Groundwater Management Assistance Act of 2000, Grant Agreement No. 4600003173. Prepared For CA Dept. of Water Resources, Division of Planning and Local Assistance, Sacramento CA.

Birkeland, Peter W. (1963) Pleistocene Volcanism and Deformation of the Truckee Area, North of Lake Tahoe, California. Geological Society of America Bulletin, v. 74, pp1453-1464, December 1963.

Birkeland, Peter W. (1964) Pleistocene Glaciation of the Northern Sierra Nevada, North of Lake Tahoe, California. Journal of Geology 72(6):10-25.

Blum, J.L. (1979) Geologic and gravimeteric investigation of the South Lake Tahoe groundwater basin, California. unpublished M.S. thesis, University of California, Davis, 96 pp.

Bonham, H.F., and Burnett, J.L. (1976) South Lake Tahoe Folio Geologic Map. Nevada Bureau of Mines and Geology, Environmental Series, Lake Tahoe area.

Boughton, C.J., T.G. Rowe, et al (1997) Stream and ground water monitoring program, Lake Tahoe Basin, Nevada and California. USGS Fact Sheet, Carson City, Nevada.

Brace, W.F. (1980) Permeability of Crystalline and Argillaceous Rocks. Int. J. Rock Mech. Min. Sci. & Geomech. Abstr., Vol. 17, pp 241-251.

Brace, W.F. (1984) Permeability of Crystalline Rocks: New In Situ Measurements. Journal of Geophysical Research, Vol. 89, No. B6, pp 4327-4330, June 10, 1984.

Bredehoeft, J.D., and Papadopulos, I.S. (1965) Rates of Vertical Groundwater Movement Estimated from the Earth's Thermal Profile. Water Resources Research, Vol. 1, No. 2, pp 325-328.

Burnett, J.L. (1968) Geology of the Lake Tahoe Basin. Geologic Studies in the Lake Tahoe Area, California and Nevada, Annual Field Trip Guidebook of the Geological Society of Sacramento, pp. 1-13.

Burnett, John L. (1971) Geology of the Lake Tahoe Basin. California Geology, July 1971.

Carslaw, H.S. and Jaeger,J.C. (1959) Conduction of Heat in Solids. Oxford University Press, USA.

Cermak, Vladimir (1989) Heat Flow in a Sedimentary Basin in Czechoslovakia: Evaluation of Data with Special Attention to Hydrogeology. Hydrogeological Regimes and Their Subsurface Thermal Effects, Beck et al (eds), Geophysical Monograph 47, Volume 2, AGU and IUGG, pp 75-80.

Clauser, Christof (1992) Permeability of Crystalline Rocks. EOS Transactions, American Geophysical Union, Vol. 73, No. 21, pp. 233-240, May 26, 1992.

Crippen, J. R., and Pavelka, B. R. (1970) The Lake Tahoe Basin, California-Nevada. U.S. Geological Survey Water-Supply Paper No. 1972.

Davis, S.N., and Turk, J.L.(1964) Optimum Depth of Wells in Crystalline Rocks. Groundwater, Vol. 2, pp. 6-12.

Dettinger, Michael D., and Cayan, Daniel R. (1995) Large-Scale Atmospheric Forcing of Recent Trends toward Early Snowmelt Runoff in California. Journal of Climate, Volume 8, pp. 606-623.

Dettinger, Mike (2002) Responses of Sierra Nevada Resources to future climate changes. Sierra Nevada Science Symposium (University of CA and U.S. Forest Service), Kings Beach, CA, October 7-10, 2002.

Drury, M.J., Jessop, A.M., and Lewis, T.J. (1984) The detection of groundwater flow by precise temperature measurements in boreholes. Geothermics, vol. 13, No. 3, pp. 163-174.

Henyey, T. L., and Lee, T. C. (1976) Heat Flow in Lake Tahoe, California-Nevada, and the Sierra Nevada-Basin and Range transition. Geolgical Society of America Bulletin, v. 87, pp. 1179-1187, August 1976.

Huang, Shaopeng, Pollack, Henry N. and Shen, Po-Yu (2000) Temperature trends over the past five centuries reconstructed from borehole temperatures. Nature, Vol 403, pp 756-758, 17 February 2000.

Lachenbruch, Arthur H. (1968) Rapid Estimation of the Topographic Disturbance to Superficial Thermal Gradients. Reviews of Geophysics, Vol 6, No 3, pp 365-400, August 1968.

Lachenbruch, Arthur H. (1969) The Effect of Two-dimensional Topography on Superficial Thermal Gradients. USGS Bulletin 1203-E.

Lind, Rick A., and Goodridge, James D. (1978) Lake Tahoe Water Balance. California Dept. of Water Resources.

Loomis, Alden A. (1981) Geology of the Fallen Leaf Lake 15-minute Quadrangle, El Dorado County, CA. California Division of Mines and Geology, Map Sheet 32.

Lu, Ning, and Ge, Shemin (1996) Effect of horizontal heat and fluid flow on the vertical temperature distribution in a semiconfining layer. Water Resources Research, Vol. 32, No. 5, pp. 1449-1453, May 1996.

Marjanovic, Prvoslav (1989). Mathematical Modeling of Eutrophication Processes in Lake Tahoe: Water Budget, Nutrient Budget, and Model Development. Dissertation, Ecology, UC Davis.

Markiewicz, Richard D. (1992) Geophysical Investigations: Lake Tahoe Basin Technical Assistance to the States, Nevada and California. U. S. Dept. of Interior, Bureau of Reclamation, D-3611.

Maurer, Douglas K. and Berger, David L. (1997) Subsurface Flow and Water Yield from Watersheds Tributary to Eagle Valley Hydrographic Area, West-Central Nevada. USGS Water Resources Investigations Report 97-4191, Carson City, NV.

Maurer, Douglas K, and Thodal, Carl E. (2000) Quantity and Chemical Quality of Recharge, and Updated Water Budgets, for the Basin-Fill Aquifer in Eagle Valley, Western Nevada. USGS Water-Resources Investigations Report 99-4289.

McBride, M.S., and Pfannkuch, H.O. (1975) The Distribution of Seepage within Lakebeds. Jour. Research USGS, Vol. 3, No. 5, Sept.-Oct. 1975, p. 505-512.

Ramey, H.J. (1962) Wellbore Heat Transmission. Journal of Petroleum Technology, Vol. 14, pp. 427-435.

Reiter, Marshall (2001) Using precision temperature logs to estimate horizontal and vertical groundwater flow components. Water Resources Research, Vol. 37, No. 3, pp. 663-674, March 2001.

Ronan, A.D., D.E. Prudic, C.E. Thodal, and J. Constantz (1998) Field study and simulation of diurnal temperature effects on infiltration and variably saturated flow beneath an ephemeral stream.Water Resour. Res. 34:2197–2153.

Schon, J.H. (1996) Seismic Exploration, Volume 18: Physical Properties of Rocks: Fundamentals and Principles of Petrophysics. Elsevier Science Inc., New York.

Schweickert, R.A., Lahren, M.M., Karlin, R.E., and Howle, J.F. (2000) Preliminary map of Pleistocene to Holocene faults in the Lake Tahoe Basin, California and Nevada. Nevada Bureau of Mines and Geology, Open-File Report, Report: 2000-4, 4 pp.

Singhai, B.B.S., and Gupta, R.P. (1999) Applied Hydrogeology of Fractured Rocks. Kluwer Academic Publishers, Dordrecht, Netherlands.

Smith, Leslie, Forster, Craig, and Woodbury, Allen (1989) Numerical Simulation Techniques for Modeling Advectively-Disturbed Thermal Regimes. Hydrogeological Regimes and Their Subsurface Thermal Effects, Beck et al (eds), Geophysical Monograph 47, Volume 2, AGU and IUGG, pp 1-5.

Sorey, M.L., (1978) Numerical Modeling of Liquid Geothermal Systems. USGS Professional Paper1044-D.

SWRCB (2005) Voluntary Domestic Well Assessment Project, El Dorado County Data Summary Report (DRAFT). State Water Resources Control Board, Groundwater Ambient Monitoring and Assessment Program, September, 2005.

Taniguchi, Makato, Shimada, Jun, Tanaka, Tadashi, Kayane, Isamu, Sakura, Yasuo, Shimano, Yasuo, Dapaah-Siakwan, S., and Kawashima, Shinichi (1999a) Disturbances of temperature-depth profiles due to surface climate change and subsurface water flow: 1. An effect of linear increase in surface temperature caused by global warming and urbanization in the Tokyo metropolitan area, Japan. Water Resources Research, Vol. 35, No. 5, pp. 1507-1517, May 1999.

Taniguchi, Makoto, Williamson, David R., and Peck, Adrian J. (1999b) Disturbances of temperature-depth profiles due to surface climate change and subsurface water flow: 2. An effect of step increase in surface temperature caused by forest clearing in southwest Western Australia. Water Resources Research, Vol. 35, No. 5, pp. 1519-1529, May 1999.

Thodal, Carl E. (1995) Hydrogeologic Setting and Ground-Water Quality of Areas Tributary to Lake Tahoe in Douglas County and Carson City, Nevada, Through 1987. U.S. Geological Survey Water Resources Investigations Report 94-4079.

Thodal, Carl E. (1997) Hydrogeology of Lake Tahoe Basin, California and Nevada, and Results of a Ground-Water Quality Monitoring Network, Water Years 1990-92. U.S. Geological Survey Water-Resources Investigations Report 97-4072.

Trask, James C, and Fogg, Graham E (2000) Recharge Source Identification for Brockway Hot Springs. *In* Hydrology of the Tahoe Basin: Field Trip Guidebook, Prudic, David E, Glancy, Patrick R and Fogg, Graham E (eds.), GSA Annual Meeting, Reno NV, Field Trip 19, November 17-18, 2000.

Trask, James C (2007) Resolving Hydrologic Water Balances through Novel Error Analysis, with Focus on Inter-annual and long-term Variability in the Tahoe Basin. PhD dissertation, Hydrologic Sciences Program (LAWR), University of CA at Davis.

Voss, Clifford I. (1984) A Finite Elelment Simulation Model for Saturated-Unsaturated Fluid-Density-Dependent Groundwater Flow with Energy Transport or Chemically-Reactive Single-Species Solute Transport. USGS Water-Resources Investigations Report 84-4369.

Wise, W.S., and Sylvester, A.G. (2004a) Geologic Map of the Truckee 7.5' Quadrangle, California. Scale 1:24,000, unpublished.

Wise, W.S., and Sylvester, A.G. (2004b) Geologic Map of the Tahoe City 7.5' Quadrangle, California. Scale 1:24,000, unpublished.

Woodbury, Allan D., Narod, B., Chandra, B., and Bennest, J.R. (1991) Temperature measurements in geotechnical studies using low-noise, high-resolution digital techniques. Can. Geotech. J., Vol. 28, pp. 639-649.